PhD degree in Molecular Medicine
European School of Molecular Medicine (SEMM)

University of Milan and University of Naples "Federico II"

Faculty of Medicine

Settore disciplinare: MED/04

UNRAVELLING THE ROLE OF THE HISTONE DEMETHYLASE JARID1B IN MACROPHAGES

Samuele Notarbartolo

IFOM-IEO Campus, Milan

Matricola n. R07389

Supervisor: Dr. Gioacchino Natoli

IFOM-IEO Campus, Milan

Added co-Supervisor: Dr. Giuseppe Testa

IFOM-IEO Campus, Milan

Anno accademico 2009-2010

INDEX

LIST OF ABBREVIATIONS

2OG	2-oxoglutarate
5'-TOP	5'-terminal oligopyrimidine
α-KG	alpha-ketoglutarate
Ala	alanine
AP-1	activator protein 1
ARID	A/T rich interactive domain
BM	Bone marrow
BMDM	Bone marrow-derived macrophages
bp	base pair
BSA	Bovine serum albumin
Ccl	chemokine (C-C motif) ligand
cDNA	complementary DNA
ChIP	chromatin immunoprecipitation
ChIP-seq	ChIP-sequencing
CREB1	cAMP-responsive-element-binding protein 1
CsA	cyclosporin A
CTD	carboxy-terminal domain
C-terminal	carboxy-terminal
Ctrl	control
Cxcl	chemokine (C-X-C motif) ligand
Cys	cysteine
ddH_2O	double-distilled water
dNTP	deoxynucleotide tri-phosphate
ES cell	embryonic stem cell
FBS	Fetal bovine serum
F.C.	Fold change
FDR	False discovery rate
FFL	feed forward loop
GO	Gene Ontology
H2AK119	lysine 119 on histone 2A
H3	histone 3
H3K4	lysine 4 on histone 3
H3K9	lysine 9 on histone 3
H3K27	lysine 27 in histone 3
H3K36	lysine 36 on histone 3
H3K79	lysine 79 on histone 3
H3S10	serine 10 on histone 3
H4K20	lysine 20 on histone 4

HA	hemagglutinin
HDAC	histone deacetylase
Het	heterozygous
Hif1α	hypoxia inducible factor 1, alpha subunit
HMT	histone methyltransferase
HSC	hematopoietic stem cell
IFNγ	interferon gamma
IκBα	NF-κB inhibitor alpha
IKK	inhibitor of kappaB kinase
Il	interleukin
IP	immunoprecipitation
IRF	IFN-regulatory factors
Jmj	Jumonji
kb	kilobase
KD	knock-down
KDM	lysine-specific demethylase
KO	knock-out
LPS	lipopolysaccharide
Luc	(firefly) luciferase
LXR	Liver X Receptor
LXRE	LXR responsive element
MBP	maltose binding protein
-me1	monomethylated lysine residue
-me2	dimethylated lysine residue
-me3	trimethylated lysine residue
MEF	mouse embryonic fibroblast
MEKK1	MAPK/ERK kinase kinase 1
M-MuLV	Moloney Murine Leukemia Virus
mRNA	messenger RNA
NFAT	nuclear factor of activated T-cells
NF-κB	nuclear factor of kappa light polypeptide gene enhancer in B-cells
N-teminal	amino-terminal
o.n.	over night
QPCR	quantitative PCR
PBS	phosphate buffered saline
PCR	Polymerase chain reaction
PHD	plant homeodomain
Phe	phenylalanine
PWM	Position-specific weight matrix
PolII	polymerase II
PPAR	peroxisome proliferator-activated receptor
PRC2	Polycomb repressive complex 2
RNAi	RNA interference

rpm	revolutions per minute
rRNA	ribosomal RNA
RT	room temperature
RXR	retinoid X receptor
SAM	S-adenosyl-methionine
SDS	Sodium Dodecyl Sulphate
Ser	serine
shRNA	short hairpin RNA
siRNA	short interfering RNA
snoRNA	small nucleolar RNA
STAT	signal transducer and activator of transcription
Surn	supernatant
TBP	TATA binding protein
TF	transcription factor
TLR4	toll-like receptor 4
Trp	tryptophan
TSS	transcription start site
Tyr	tyrosine
UTR	Untranslated Region
VDR	vitamin D receptor
WB	Western blot
WCE	whole-cell extract
WT	wild-type
XLMR	X-linked mental retardation

FIGURE INDEX

TABLE INDEX

ABSTRACT

Inflammation is a fundamental response to the loss of cellular and tissue homeostasis with many important physiological roles, including host defence, tissue remodelling and repair, and the regulation of metabolism. Macrophages are not only crucial mediators of the inflammatory response, but they are also able to integrate lipid metabolism and inflammatory signalling. After an inflammatory stimulus, the expression of several hundred genes is either induced or repressed in macrophages. This complex transcriptional response consists of multiple transcriptional modules that encode different functional programmes and that are controlled by dedicated transcription factors.

Post-translational modifications of histones are important determinants of transcriptional activity, and it has become evident that many chromatin modifications are extremely dynamic also in response to environmental stimuli. Among these, trimethylation of H3K4 is well conserved during evolution, and is usually associated with the 5' ends of actively transcribed or "poised" genes.

Although in the last decades the signalling pathways leading to the activation of an inflammatory response have been very well characterized, the knowledge about the tuning of this complex transcriptional network is still limited.

Using a candidate approach we demonstrated that Jarid1b is transcriptionally up-regulated with a slow kinetics by LPS stimulation under the control of the transcription factor Hif1α.

Jarid1b is a member of the JARID1 family of H3K4 demethylases, and it has been proposed to act as transcriptional repressor, with a putative role in cell proliferation.

Depletion experiments in primary macrophages suggested that Jarid1b is necessary for the activation of the master regulator of cholesterol metabolism, LXR, and the expression of its target genes, likely through the control of cellular oxysterols pools.

We also generated Jarid1b knock-out mice, and performed global expression analysis in Jarid1b-deficient macrophages. The obtained data together with genomic binding analyses showed a very limited transcriptional regulatory function for Jarid1b in this cellular system. We also collected preliminary data on a possible role for Jarid1b, independent of its reported histone demethylase enzymatic activity, in regulating RNA methylation levels.

INTRODUCTION

1. Inflammation

Inflammation is a fundamental response to the loss of cellular and tissue homeostasis with many important physiological roles, including host defence, tissue remodelling and repair, and the regulation of metabolism (37). Already in the first century Celsus described the initial cardinal signs of inflammation: rubor (redness), calor (heat), tumor (swelling) and dolor (pain). In fact, inflammation is a complex process that requires its functional components to be co-ordinately controlled in some situations and independently in others. This means that multiple control mechanisms must operate at different levels, going from the alteration of the composition of immune cells in tissues, to the regulation of signalling pathways and the control of gene expression in individual cells (58).

Cell-specific mechanisms regulate the recruitment and activation of different cell types: for example, during the early phases of an inflammatory response, the release of some chemokines (like Cxcl1, Cxcl5 and Cxcl8) by activated tissue-resident macrophages serves to recruit neutrophils to the damaged tissue (116) (105) (101); following the extravasation and tissue infiltration, neutrophils sequentially release preformed granule proteins which, in turn, promote the recruitment and activation of inflammatory monocytes (50).

Signal-specific mechanisms operate at the level of signalling pathways: for example, the binding of bacterial endotoxin (lipopolysaccharide, LPS) to TLR4 triggers a signalling cascade that causes the translocation of the key transcription factor nuclear factor-kappaB (NF-κB) to the nucleus and the transcriptional activation of inflammatory genes. In outline, receptor engagement results in IκB kinase (IKK) activation, and the activated IKK complex phosphorylates IκBα on Ser32 and Ser36, leading to its polyubiquitination; the ubiquitinated IκBα is degraded via the 26S proteasome, thereby inducing nuclear

translocation of p65:p50 as well as other less abundant Rel/NF-kB hetero- and homo-dimers (44) (Figure 1).

Finally, gene-specific mechanisms operate at the level of individual genes and gene subsets: for instance, interleukin-10 (IL-10) and many nuclear receptors regulate the transcription of specific subsets of inflammatory genes, providing functional specificity in an inflammatory response.

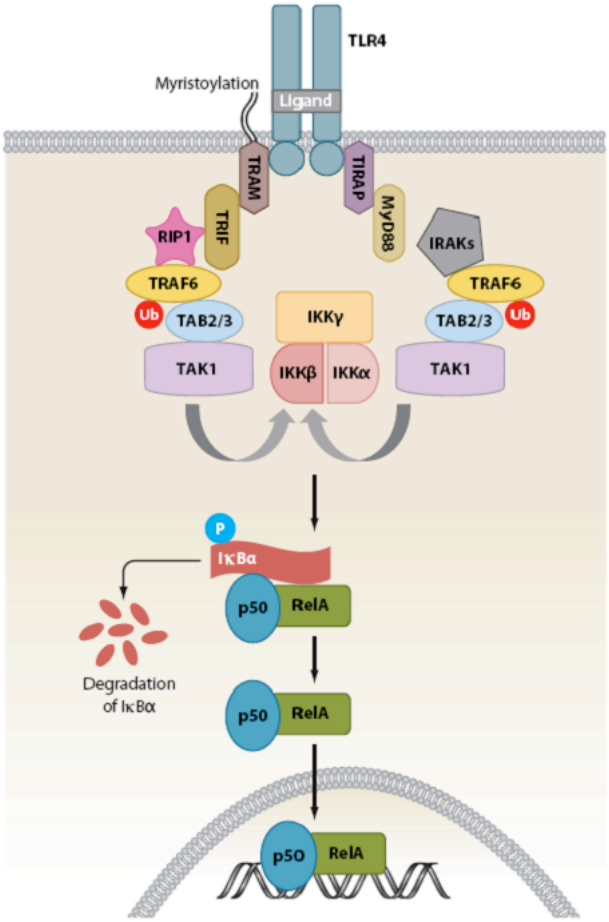

Figure 1 - Activation of the classical NF-κB pathway by TLR4.
Ligand binding by TLRs results in the recruitment of receptor-specific adapters and induces activation of NF-κB. Reproduced from (107).

Normal inflammation is a self-limiting process eventually leading to restoration of homeostasis, but deregulation of any of the factors involved may lead to excessive and/or sustained responses that may cause disease.

Macrophages are crucial mediators of the inflammatory response, since they are main players in the innate immune response as well as important regulators of the adaptive

immunity. Furthermore macrophages integrate lipid metabolism and inflammatory signalling, and the disruption of this equilibrium is associated with different diseases, like atherosclerosis, obesity, type 2 diabetes and fatty liver disease (37).

1.1 A complex transcriptional response underlies inflammation

After an inflammatory stimulus, the expression of several hundred genes is either induced or repressed in macrophages (73, 74). This complex transcriptional response consists of multiple gene sets, or transcriptional modules, that encode different functional programmes and that are often controlled by dedicated transcription factors. This feature enables autonomous control of individual transcriptional modules, because the transcriptional regulators that control their expression can be differentially regulated by positive and negative signals.

One of the clearest example of module-specific transcriptional regulation is provided by LPS tolerance. LPS tolerance is a state of hypo-responsiveness to LPS (and other microbial stimuli) that is induced during conditions of sustained inflammation to limit inflammation-associated pathology. LPS-tolerant cells are refractory to the induction of expression of inflammatory cytokines, such as tumour necrosis factor alpha and interleukin-6. Importantly, however, LPS-triggered signalling in these cells can still induce the expression of genes that encode anti-inflammatory cytokines as well as antimicrobial peptides. The differential inducibility of these classes of genes is associated with distinct patterns of chromatin remodelling (24). This indicates that the transcriptional regulation of LPS tolerance enables the inhibition of some functional programmes (like those encoding inflammatory cytokines) while inducing other programmes (for example, tissue repair), which could be advantageous when a host has to deal with a persistent infection (23).

1.2 Inflammation is a tightly regulated process

The LPS-induced transcriptional response is collectively regulated by transcription factors, chromatin modifications and transcriptional co-regulators.

The transcription factors that control the inflammatory response can be divided into three categories on the basis of their mode of activation and function.

The first category consists of transcription factors that are constitutively expressed by many cell types and are activated by signal-dependent post-translational modifications. In most cases, these transcription factors are retained in the cytoplasm in the basal state and their signal-dependent activation involves their nuclear translocation. This class comprises proteins that are known to have important roles in inflammation, such as NF-κB, IFN-regulatory factors (IRFs) and cAMP-responsive-element-binding protein 1 (CREB1). The genes that are induced most rapidly by LPS stimulation (including primary response genes and some secondary genes) are usually regulated by these transcription factors (58).

The second class of transcription factors are synthesized *de novo* after LPS stimulation. They regulate subsequent waves of gene expression after primary response genes and their activity is often subject to positive feedback control. For example, C/EBPδ is induced by LPS and it acts as an amplifier of NF-κB response discriminating between transient and persistent TLR4 signals. C/EBPδ is also recruited to its own promoter in a TLR4-dependent way, indicating a mechanism of autoregulation (52).

The third category of transcription factors consists of lineage-specific transcriptional regulators, whose expression is turned on during macrophage differentiation. This class of transcription factors includes PU.1 and C/EBPβ, as well as RUNX1 and IRF8 (25) (108). These proteins turn on constitutively expressed genes in macrophages, remodel chromatin at inducible genes and silence genes that are associated with alternative cell fates. In mature macrophages, these transcription factors mediate cell type-specific response to inflammatory signals and other stimuli, presumably by conferring a permissive chromatin state on macrophage-specific inducible genes. For example, in mature mouse macrophages

PU.1 has been recently shown to mark about 45,000 genomic regions and systematically associate with enhancers (H3K4me1^{hi}/H3K4me3^{lo} regions), suggesting that it controls the whole complement of regulatory regions in macrophages (28). Moreover PU.1 associates not only with the virtual totality of enhancers but also with about 80% of active TSSs, suggesting that a single master regulator of differentiation and cell identity may be able to supervise nearly all genomic regions controlling transcriptional regulation in macrophages (62).

Recent studies have highlighted an important role for chromatin in the control of inflammatory gene expression (8). Several histone modifications have been shown to differentially regulate subsets of LPS-induced genes. One of the first studies in this area indicated that phosphorylation of histone 3 at serine 10 (H3S10) might have a gene-specific role in NF-κB recruitment. After LPS stimulation, the genes encoding Il-6, Il-12p40 and Ccl2, but not Tnf and Ccl3, undergo H3S10 phosphorylation at their promoters. This phosphorylation event depends on the mitogen-activated protein kinase p38, and specific inhibition of p38 activity blocks H3S10 phosphorylation, NF-κB recruitment and gene induction (83).

Even more interesting are the inhibitory histone modifications that mark subsets of inducible genes. Ubiquitination of H2A at lysine119 (H2AK119) is one of such modification that inhibits the basal expression level of some LPS-inducible genes - like *Ccl5*, *Cxcl10* and *Cxcl2*, but not *Cxcl1* - in macrophages. LPS stimulation triggers the gene-specific recruitment of the deubiquitylating enzyme 2A-HUB, whose activity is necessary for H2AK119 deubiquitination and hence gene induction (118). Another subset of LPS-inducible genes undergoes signal-dependent demethylation of trimethylated H3K27 as prerequisite for induction. The enzyme responsible for this activity, Jmjd3, is itself transcriptionally up-regulated after LPS stimulation, and its shRNA-mediated knockdown inhibits demethylation and the induction of *Bmp2* expression (18).

It is important to point out that repressive histone modifications, such as H2AK119 ubiquitination and H3K27 trimethylation, are additional regulatory checkpoints of inducible gene expression. Stimulus-dependent induction of genes bearing these modifications requires recruitment of the appropriate chromatin-modifying enzyme, thus restricting both the types of biological signals able to activate them and the classes of genes that are induced.

Co-regulators are transcriptional regulators that, unlike transcription factors, lack DNA-binding specificity and must be recruited to their target genes through other mechanisms. Schematically, they can carry either positive or negative transcriptional regulatory activity. Some co-activators have histone-modifying activities and/or can remodel chromatin at target genes to promote gene induction, while others lack intrinsic enzymatic activity and might promote the assembly of a trans-activating complex.

Among co-repressors, NCoR and SMRT multi-protein complexes have emerged as important regulators of inflammatory gene expression. These complexes contain histone deacetylases (HDACs) activity, and their stimulus-dependent displacement from the promoters of inflammatory genes, a phenomenon known as derepression, is a prerequisite for the inducible expression of target genes. For example, NCoR is directed to many inflammatory genes, in part by the transcription factor Jun, and its clearance is triggered by signal-induced exchange of Jun homodimers for transcriptional active Jun-Fos heterodimers (29). Interestingly, some inflammatory genes are regulated by both NCoR and SMRT co-repressor complexes, thus amplifying the number of possible regulatory signals (29).

1.3 Resolution of inflammation

The induction of an inflammatory response is essential for host defence during infection, but its resolution at the right time is also important to limit the detrimental effects of

inflammation, particularly when it is inappropriately sustained or increased. This is the reason why acute inflammation also leads to the up-regulation of many negative regulators of inflammation.

There are two types of transcriptional negative regulators: basal and inducible repressors. Basal repressors are constitutively expressed and are important for the maintenance of a low basal level of transcription at many inflammatory genes. For example, p50 homodimers can function as transcriptional repressors that can be exchanged for transcriptionally active p65:p50 heterodimers as a result of LPS-induced signalling (102). On the contrary, inducible repressors are normally not expressed or expressed only at low levels, but are transcriptionally induced after an inflammatory stimulus, indicating that they are part of a negative feedback mechanism that limits the inflammatory response. Usually inducible repressors block the expression of secondary response genes, whereas basal repressors inhibit the expression of primary response genes associated with CpG islands, which otherwise would present high basal activity (58).

Limiting the patho-physiological consequences of excessive inflammation is crucial, as indirectly demonstrated by the existence of several pathways and mechanisms specifically dedicated to negative control of inflammatory gene expression, including anti-inflammatory cytokines, such as IL-10 and TGFβ, nuclear hormone receptors and cAMP.

Nuclear receptors are the major class of negative transcriptional regulators of inflammation. They include glucocorticoid receptors, liver X receptors (LXRs), peroxisome proliferator-activated receptors (PPARs) and vitamin D receptor (VDR). These proteins integrate the control of inflammation with various important physiological functions, and metabolism in particular.

Nuclear receptors are thought to inhibit inflammation by at least two distinct mechanisms. Activated nuclear receptors can directly induce anti-inflammatory gene expression programmes: for example, PPARδ activation results in disassociation of the Bcl-6 co-repressor from the *Ccl2* promoter, thereby enabling recruitment of Bcl-6 to mediate

transcriptional inhibition (48). Alternatively, activated nuclear receptors can be recruited to some inflammatory genes where they inhibit the clearance of the co-repressors NCoR and SMRT, a process known as trans-repression (30).

The multitude of mechanisms by which nuclear receptors can inhibit inflammatory gene expression underscores the importance of transcriptional control of inflammation by metabolism and other physiological processes.

2. Inflammation and metabolism

The integration of metabolism and immunity (or of nutrient- and pathogen-sensing pathways) can be traced back to an evolutionary need for survival, which resulted in the co-development of the signalling pathways controlling these two processes and of the organ systems where these processes take place (37). In fact, the initiation and maintenance of an immune response is a metabolically costly endeavour and cannot operate efficiently under conditions of negative energy balance (19). For example, fever is associated with a 7-13% increase in caloric energy consumption per 1°C increase in body temperature (80), and in humans sepsis can increase the metabolic rate by 30-60%.

It is clear that starvation and malnutrition can impair immune function, but even more interestingly a energy surplus, which is typical of individuals who are obese or suffer from metabolic syndrome, can also impair immune response and induce chronic inflammation. It is important to point out that this response does not resemble classic inflammation and perhaps could be considered as an aberrant form of immune response that is triggered by nutrients and has been referred to as meta-inflammation or para-inflammation (37).

Therefore a balanced energy flux and the maintenance of metabolic homeostasis are required for the proper functioning of the immune system. These processes may have been optimized through the close coordination and co-evolution of metabolic and immune responses. Evidence supporting such an evolutionary history can be found in lower

organisms as *Drosophila melanogaster*, in which metabolic and immune functions are controlled by the same organ, the fat body (47). This structure incorporates the mammalian homologues of the liver and the hematopoietic and immune systems; this site is also recognized as the equivalent of mammalian adipose tissue, sharing similar developmental and functional pathways (Figure 2). It is interesting to note that also in higher organisms both adipose tissue and the liver have an architectural organization in which metabolic cells (adipocytes or hepatocytes) are in close proximity to immune cells (Kupffer cells or macrophages) and both have an immediate access to a vast network of blood vessels (37).

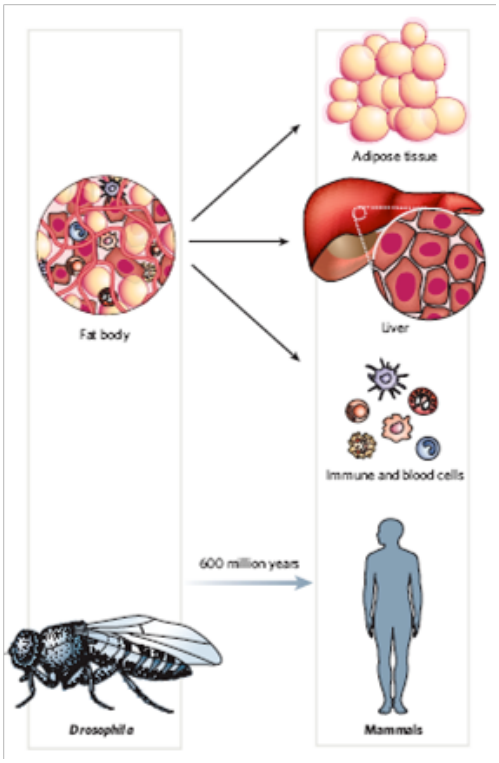

Figure 2 - Evolution of adipose tissue, the liver and the haematopoietic system into distinct organs in mammals.
The adipose tissue, liver and haematopoietic system are all organized in one functional unit in *Drosophila melanogaster*, known as the 'fat body'. This developmental heritage may underlie the highly overlapping biological repertoire of these organs, their effects on metabolic and immune cells, and the close link between immune and metabolic response systems. Reproduced from (37).

Cells that are involved in metabolic and immune responses also show evidence of coordination and co-evolution. More specifically, macrophages and adipocytes are closely related and share many functions: for example, they both secrete cytokines and can be activated by pathogen-associated components, such as LPS. Indeed, pre-adipocytes have been shown to trans-differentiate into macrophages, and transcriptional profiling has

suggested that macrophages and pre-adipocytes show related gene regulatory networks (14). Moreover, there is an extensive transcriptional and functional overlap between fully differentiate adipocytes and macrophages that have massively accumulated lipids in atherosclerotic plaques (foam cells), particularly in terms of metabolic genes (38).

2.1 Integration of inflammation and lipid metabolism in macrophages: the nuclear receptor pathways

Macrophages are important players in the integration of lipid metabolism and inflammatory signalling. This is achieved mainly through the activation of nuclear receptor pathways.

Nuclear receptors have a highly conserved structure comprising an amino-terminal domain that contains a ligand-independent activation function, a zinc-finger-type DNA-binding domain, a carboxy-terminal ligand-binding domain, and a ligand-dependent transcriptional activation function.

One class of nuclear receptors comprises metabolite-activated transcription factors that form obligate heterodimers with the retinoid X receptor (RXR). In the absence of ligand, most RXR heterodimers are bound to DNA in association with co-repressors, histone deacetylases and chromatin-modifying factors to maintain active repression of target genes (33). Ligand binding initiates a conformational change in the receptor, the exchange of co-repressors for co-activators, and the initiation of target-gene transcription, a phenomenon known as de-repression (Figure 3).

Several RXR heterodimers can activate and repress gene expression in a signal- and gene-specific manner. In particular LXRs and PPARs have emerged as important regulators of metabolic and inflammatory signalling, both in metabolic disease and immunity (13).

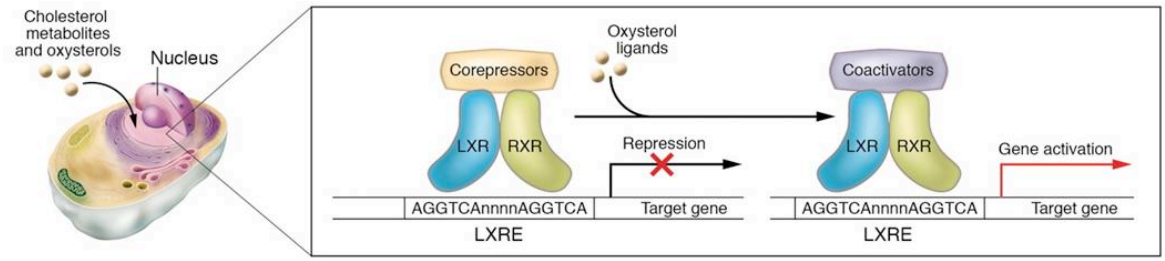

Figure 3 - Nuclear receptor "derepression".
Within the nucleus, LXR/RXR heterodimers are bound to LXREs in the promoters of target genes and in complex with co-repressors (e.g., SMRT, NCoR). In response to the binding of oxysterol ligands, the co-repressor complexes are exchanged for co-activator complexes, and target gene expression is induced. Reproduced from (117).

The PPAR family is composed of three proteins: PPARα, PPARγ and PPARδ. The three PPARs have different tissue distributions and seem to have distinct, albeit partially overlapping, biological functions. They have been shown to modulate various cell functions, including adipocyte differentiation, fatty acid oxidation and glucose metabolism. But it has also been demonstrated that PPARs repress in a signal specific manner genes activated by inflammatory transcription factors such as NF-κB, NFAT, AP-1 and STATs (32).

It has been difficult to identify a unifying mechanism of repression by activated PPARs; it is possible that there are mechanisms specific to signals, PPAR type or isoform, and even to individual gene promoters. The mechanism underlying the transcriptional repressive function of PPARγ in macrophages has been recently characterized by Glass and colleagues (67). Besides the de-repression mechanism previously described, PPARγ is able to inhibit inflammatory gene expression in a signal-specific manner. This process is termed trans-repression because inhibition occurs independently of the binding of PPARγ-RXR heterodimers to PPAR responsive elements in target-gene promoter. In the basal state, inflammatory genes (like *Nos2* and *Ccl2*) are repressed by a protein complex containing histone deacetylases, transducin-β-like proteins and either NCoR or SMRT. These protein complexes bind the promoters of inflammatory genes preventing the acetylation of histones and the binding of co-activator complexes. The binding of LPS to TLR4 initiates a signalling cascade that results in the ubiquitination and subsequent degradation of the co-

repressor complex by the 19S proteasome. In the model proposed by Glass and coll., ligand activation of PPARγ results in a conformational change allowing the SUMOylation of PPARγ in the ligand binding domain at lysine 365, mediated by the E2 ligase UBC9 and the E3 ligase PIAS1. Sumoylated PPARγ binds the NCoR-HDAC-containing co-repressor complex and blocks its degradation by the proteasome, thereby preserving the repressed state (67).

Liver X Receptors α and β (LXRα and β), also known as NR1H3 and NR1H2 respectively, are ligand-dependent nuclear receptors that play a central role in the transcriptional control of cholesterol metabolism and transport. Physiological LXRs ligands are oxysterols, oxidized derivatives of cholesterol obtained either from oxidation of exogenous cholesterol (like 22-hydroxycholesterol and 27-hydroxycholesterol) or as side products of intracellular cholesterol biosynthesis (24,25-epoxycholesterol).

An important distinction between the two LXR isoforms is represented by their tissue distribution: LXRα is highly expressed in the liver and at lower levels in macrophages, adrenal glands, intestine, adipose tissue and lung, whereas LXRβ is ubiquitously expressed (117).

LXRs regulate the expression of genes involved in cholesterol metabolism in a tissue-specific manner. For example, LXR activation in rodent liver up-regulates the expression of Cyp7a1, a member of the cytochrome p450 family of enzymes and the rate-limiting enzyme of the classical pathway of bile-acid synthesis. The inability of *Lxra*$^{-/-}$ mice to induce hepatic *Cyp7a1* expression results in a diminished ability to metabolize cholesterol to bile acids, and in the accumulation of cholesteryl esters (70) (Figure 4). LXRβ is also expressed in liver, but *Lxrb*$^{-/-}$ mice do not display an obvious hepatic phenotype even when challenged with a high cholesterol diet, suggesting that LXRα is likely the dominant isoform in this tissue.

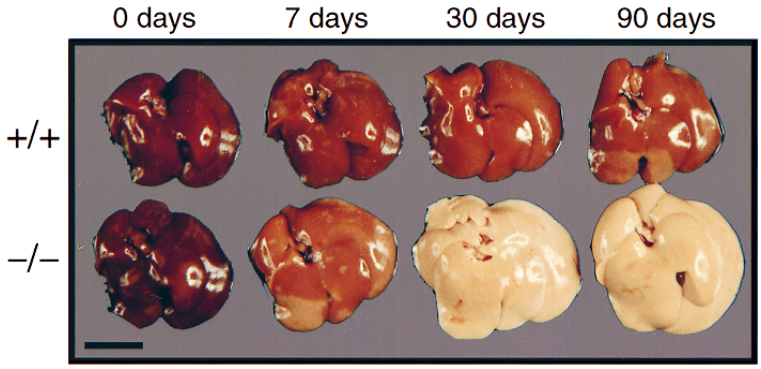

Figure 4 - Morphology of livers from LXRα KO vs. WT mice on high-cholesterol diet.
Gross morphology of livers from female LXRα null (-/-) and wild-type (+/+) mice fed with chow supplemented with 2% cholesterol for 0, 7, 30, or 90 days. The development of fatty livers in the LXRα (-/-) mice is evident after 7 days on the high-cholesterol diet. Reproduced from (70).

In peripheral cells such as macrophages, LXRs control the expression of a set of genes involved in the return of peripheral cholesterol to the liver, a process known as reverse cholesterol transport. In response to cholesterol loading, LXRs induce the expression of the cholesterol-efflux transporters Abca1 and Abcg1, the lipoprotein remodelling enzyme Pltp, and apolipoproteins of the ApoC subfamily and ApoE (13).

In addition to these functions, LXRs modulate immune and inflammatory responses in macrophages (117). Tontonoz and coll. used cDNA microarrays to examine the role of LXR activation on LPS-induced genes expression: they treated peritoneal macrophages from wild-type, *Nr1h3*$^{-/-}$, *Nr1h2*$^{-/-}$ and *Nr1h3*$^{-/-}$*Nr1h2*$^{-/-}$ mice with an LXR agonist (GW3965) 18 hours before the LPS treatment. Microarray data showed that the LPS-triggered up-regulation of several inflammatory genes, like *Nos2*, *Cox2*, *Il-6* and *Il-1b*, is dampened by LXRs activation, and this effect is dependent on the expression of LXRs, since it is reverted in LXR knock-out mice (43). This and other studies have shown that the cholesterol efflux pathway and the innate immune response are reciprocally modulated in activated macrophages (Figure 5), and if on the one hand LXR can be either activated or repressed by different inflammatory stimuli (12), on the other its activation negatively regulates inflammatory gene expression via trans-repression (43).

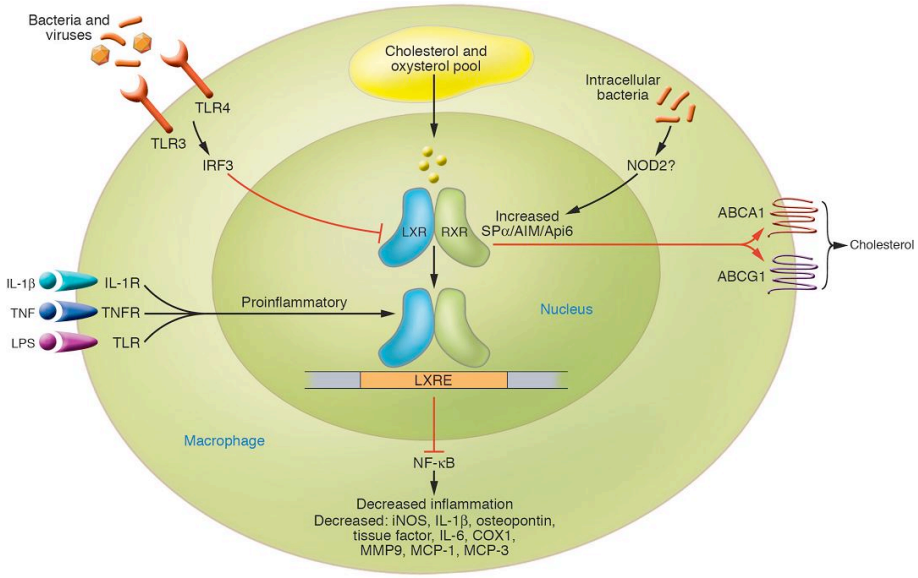

Figure 5 - Integration of lipid metabolic and inflammatory signalling in macrophages by LXRs. Activation of the TLR3/4 receptors blocks LXR-dependent gene transcription and cholesterol efflux from macrophages via an IRF3-dependent pathway. On the other hand, ligand-mediated activation of LXRs inhibits NF-κB-dependent induction of inflammatory gene expression. Intracellular bacteria induce LXRα expression, and promote macrophage survival, mainly through induction of Cd5l (also known as AIM or SPα). Reproduced from (117).

Although the mechanisms underlying signal-specific trans-repression remain incompletely understood, it is now clear that LXR activation inhibits inflammatory response in part blocking NF-κB signalling (63) via an N-CoR- and sumoylation-dependent process (30), with a mechanism similar to the one discussed above for PPARγ. In this case, ligand binding to LXRs results in SUMOylation by SUMO2 and SUMO3 (rather than SUMO1) and depends on HDAC4 activity for the preservation of the co-repressor complex during inflammatory signalling.

Although LXR is able to negatively regulate inflammatory gene expression, it has been found that the loss of LXR function compromised innate immunity. Mice lacking LXRs are more susceptible to challenge with the Gram-positive intracellular pathogen *Listeria monocytogenes* (42). In particular, loss of LXRα correlates with increased pathogen-induced macrophage apoptosis due, at least in part, to reduced activation of the anti-apoptotic gene *Cd5l* (*Aim/Spα*) by LXRα.

3. Modelling transcriptional networks: the feed-forward loop

Studying a complex transcriptional regulatory network, like the inflammatory response, is a very difficult task due to the great number of components that interact in the pathway. However, it is becoming increasingly clear that these complex networks are made up of a small set of recurring regulation patterns, called network motifs (59).

Network motifs can be thought of as recurring circuits of interactions from which the networks are built. The idea is that each motif can carry out specific information-processing functions.

Two important types of transcription networks are the sensory networks that respond to signals such as stresses and nutrients, and developmental networks, that guide differentiation events (2). The main characteristic of sensory transcriptional networks is that they have to respond rapidly and make reversible decisions.

One of the simplest and best conserved motif found in sensory networks is represented by the *feed-forward loop* (FFL), that consist of three genes: a regulator (X) which controls the expression of a downstream gene encoding for another regulator Y, and a final target Z, which is jointly regulated by X and Y. Because each of the three regulatory interactions in the FFL can lead either to activation or repression, there are 8 possible structural types of FFL (2) (Figure 6).

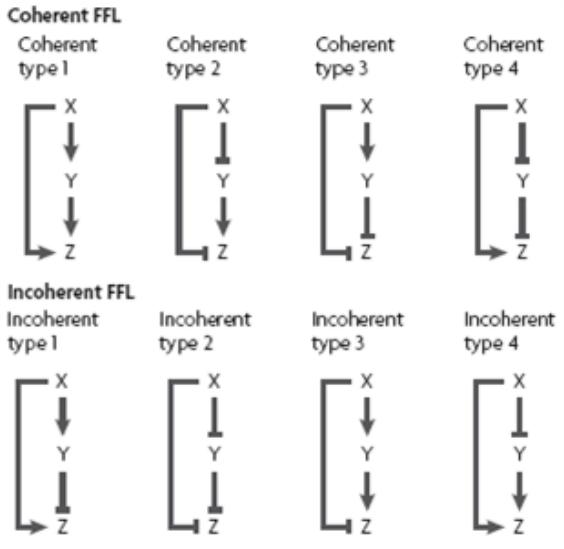

Figure 6 – Feed-forward loops (FFLs).

The eight types of feed-forward are shown. In coherent FFLs, the sign of the direct path from transcription factor X to output Z is the same as the overall sign of the indirect path through transcription factor Y. Incoherent FFLs have opposite signs for the two paths. Reproduced from (2).

In the best studied transcriptional networks (*E. coli* and yeast), two of the eight FFL types occur more frequently than the other six types (56). These common types are the coherent type-1 FFL and the incoherent type-1 FFL.

Interestingly these two FFL types have been also characterized in transcriptional inflammatory response networks: for example, Akira and coll. demonstrated that NF-κB activation induces the transcription of the ankyrin-repeat-containing nuclear protein IκBζ and the cytokine Il-6, and the expression of IκBζ is indispensable for the expression of a subset of genes activated in TLR/IL-1R signalling pathways, including *Il-6* (113). This scheme clearly resemble a coherent type-1 FFL. A typical incoherent type-1 FFL is instead represented by NF-κB and twist: the mammalian twist proteins, twist-1 and -2, are induced by p65 (a member of the NF-κB family of transcription factors), and their expression results in the repression of cytokines, like TNFα and Il-1β (96).

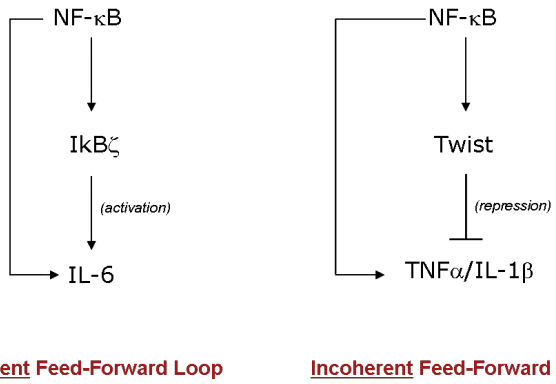

Figure 7 - Two examples of characterized feed-forward loop (FFL) involved in the inflammatory response.
On the left (coherent FFL), NF-κB and its target gene IκBζ cooperate in the activation of *interleukin-6* (*Il6*); in the incoherent FFL, NF-κB induces the expression of both cytokines and twist proteins, but the latest ones counteract NF-κB activity on *Tnf* and *Il1b*.

4. Chromatin organization and modifications

In eukaryotic cells, DNA is packaged with histones into a nucleoprotein complex known as chromatin.

Already in the early 1960s, evidence was reported that histones were modified at the post-translational level by acetylation and methylation, which may play a role in control of transcription (1). Methylation was shown to occur on the ε-amino group of lysine (61) and the guanidine group of arginine (66). However, the enzymes responsible for these reactions were unknown until the first histone methyltransferase was identified in year 2000 (75).

Histone methylation is now recognized as an important modification linked to both transcriptional activation and repression. Six lysine residues, including H3K4, -9, -27, -36 and -79 as well as H4K20, have been studied extensively and linked to chromatin and transcriptional regulation. Lysine can be mono-, di-, and tri-methylated (3), while arginine can be both monomethylated and symmetrically or asymmetrically dimethylated (5).

The numerous lysine and arginine residues on the histone tails, together with the various methylation levels that can be generated at each of these sites, provide a tremendous regulatory potential for chromatin modifications (94). In general, methylation on H3K4, H3K36 and H3K79 is associated with actively transcribed genes, whereas H3K9, H3K27 and H4K20 methylation usually marks silenced genes (57).

Recent studies have highlighted a significant role for chromatin in the control of inflammatory gene expression (8) and several histone modifications have been shown to differentially regulate subsets of LPS-induced genes (83) (114). For example, previous work in our lab demonstrated that the H3K4me3 mark is increased at hundreds of genes after inflammatory stimuli (17). We also identified the JmjC containing protein Jmjd3 as a H3K27 demethylase transcriptionally up-regulated after LPS stimulation, whose shRNA-mediated depletion inhibits the demethylation and the induction of *Bmp2* expression (18).

4.1 Methylation of lysine 4 on histone 3

Methylation of H3K4 has been linked to transcriptional activation in a variety of eukaryotic species. Recent genomic analyses of histone modifications demonstrated a

general correlation between different H3K4 methylation states, their genomic distribution, and gene expression levels (85) (86) (7) (72). The general consensus is that H3K4 trimethylation is associated with the 5' regions of active genes and its levels positively correlate with transcription rates, active polymerase II occupancy, and histone acetylation (85) (86) (7) (72).

In contrast, patterns of H3K4me2 differ significantly between yeast and vertebrate chromatin: in *S. cerevisiae*, dimethylated H3K4 appears to spread throughout genes, peaking toward the middle of coding region, and is associated with transcriptionally "poised" genes as well as active state, with monomethylation most abundant at 3' ends of genes (85) (72). Conversely, in vertebrates the majority of H3K4 dimethylation co-localizes with H3K4 trimethylation in discrete zones about 5-20 nucleosomes in length proximally to highly transcribed genes (7). Interestingly, a subset of dimethylated sites is devoid of trimethylation; these isolated H3K4 dimethylated regions do not correlate with transcription start sites, and their presence is highly dependent on the cell type tested, suggesting that they may have a role in determining lineage-specific chromatin state over genomic regulatory elements (7).

The first H3K4 methyltransferase to be identified was *S. cerevisiae* Set1, the only enzyme responsible for H3K4 methylation in yeast (10). In mammals, the complexity of methyl "writers" is greater, and at least ten known or predicted H3K4 methyltransferases have been identified (82): the six members of the MLL-family, SET7/9, SMYD3, ASH1 and Meisetz. The majority of these enzymes contain a SET domain, which catalyzes the addition of methyl groups to the lysine residue. The multiplicity of methyltransferases in vertebrate genomes likely results from their functional specialization either through differential expression patterns, recruitment to different target genes, or methylation of distinct non-histone substrates. For instance, the distinguishable phenotypes of deletions or truncations in *Mll1*, *Mll2*, and *Mll3* genes in mice suggest that MLL proteins are not

redundant in their function but instead are specialized to deal with the regulatory complexity of vertebrate development (82).

Like most histone-modifying enzymes, the MLL-family of methyltransferases exist in multi-protein complexes. MLL-family complexes share three common subunits: WDR5, RbBP5 and ASH2, and all these components are required for H3K4 methylation by MLL1 in vitro and in vivo (21) (Figure 8). In particular, WDR5 plays a critical scaffolding role and appears to "present" the H3K4 side chain for further methylation within HMT complexes, in a way that is somewhat analogous to the adaptor subunits E3 of ubiquitin ligases, which can recognize post-translational modifications on the substrate and bring it into close proximity of the E2 enzyme to promote ubiquitination.

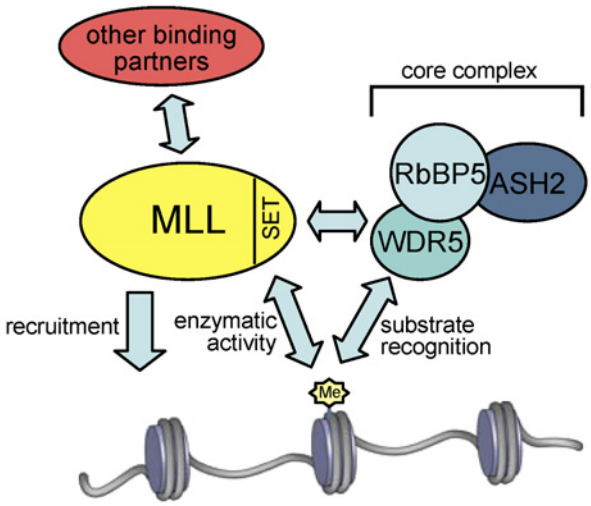

Figure 8 - Schematic representation of the interactions between MLL complex components.
MLL-family HMTs associate with the core complex containing RbBP5, WDR5, and ASH2. The core complex cooperates with the catalytic SET domain to methylate H3K4. WDR5 plays a role in substrate recognition and presentation, with preferential, but not exclusive, binding to the H3K4me2 substrate. Reproduced from (82).

In *S. cerevisiae*, Set1 is recruited to chromatin by the phosphorylated form of RNA polymerase II carboxy-terminal domain and the Paf1 elongation complex, and its H3K4 methyltranferase activity is dependent on H2B monoubiquitination.

This general mechanism is conserved from yeast to humans, but the greater number of H3K4 methyl writers in higher organisms is accompanied by the appearance of new mechanisms of recruitment. H3K4 methyltransferases may be recruited: a) directly or

indirectly, by sequence specific DNA binding factors, b) directly associate with basal transcriptional machinery, c) associate with chromatin through histone modification readers, d) or be recruited by RNA (Figure 9). Ruthenburg and coll. propose that the initial recruitment is gene specific, mediated by specific transcription factors and/or RNAs, and is sensitive to the signalling cues within the cell, whereas further stabilization of the complex on chromatin and stimulation of its catalytic activity occur through interactions with basal transcription machinery and by the association with acetylated and methylated histones (82). Recently, Thomson and coll. showed a distinct mechanism of HMT recruitment demonstrating that Cfp1, a component of the Setd1 methyltransferase complex, can be recruited to non-methylated CpG clusters, also independently of RNA PolII binding (104).

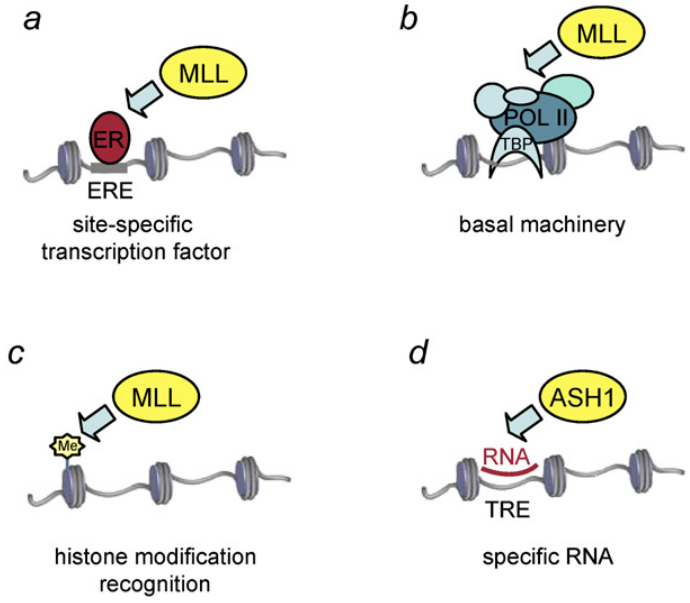

Figure 9 - Mechanisms of H3K4 methyltransferases recruitment to target genes.
The existing literature suggests that H3K4 methyltransferases are recruited to and/or stabilized on chromatin by a combination of mechanisms involving association with site-specific transcription factors *(a)*, basal transcription machinery *(b)*, histone modification recognition *(c)*, and specific RNAs *(d)*. Reproduced from (82).

But what is the biological role of H3K4 methylation?

Recent evidence suggests that histone methylation acts through the recruitment of downstream effector proteins, which in turn, execute specific independent functions on the chromatin template (92) (110).

A variety of domains are able to bind methylated lysine on histone 3 tail, with different degrees of preferences for distinct methylated species (mono- vs. di- vs. tri-). H3K4 effector modules may be classified in two superfamilies: the royal superfamily, including chromodomains and tudor domains (e.g. the chromodomain of CHD1 and the tudor domain of Jmjd2a), and the PHD-finger superfamily (e.g the PHD fingers of BPTF and ING proteins). The most striking mechanistic commonality among all methyl-lysine effectors that have been structurally characterized is the presence of an aromatic cage that mediates di- and trimethyl lysine recognition (82).

It is noteworthy that many of the known methyl readers reside within protein complexes associated with enzymatic activities operating on the chromatin template: ATP-dependent chromatin remodelling, histone acetylation and deacetylation, as well as demethylation. Thus, H3K4 methylation is directly coupled to further chromatin modification mechanisms necessary to execute specific biological functions. For example, the association of methylated H3K4 with ING3-5 and yeast Yng1 containing acetyltranferase complexes is consistent with the role of H3K4 methylation in transcriptional activation (92) (100). Histone acetylation directly promotes a more accessible chromatin structure and can recruit bromodomain-containing transcriptional regulators. Crosstalk between H3K4 methylation and acetylation is evidenced by a high correlation of hyper-acetylation and H3K4 methylation patterns in genomic location analyses (7) (72) (100).

In contrast, it is surprising that H3K4 trimethylated tail can also serve as a binding platform for recruitment of histone deacetylases complexes, leading to active gene repression, as reported by Shi and co-workers (92).

4.2 H3K4 methylation is a dynamic chromatin mark

Many of the covalent modifications on the histone tails are enzymatically reversible: for example, phosphorylation and acetylation are reversed by phosphatases and deacetylases

respectively, to provide the cell with a mechanism to respond quickly to changes through a rapid alteration in its gene expression programs.

However in the last 30 years, unlike phosphorylation and acetylation, histone methylation was considered static and enzymatically irreversible. This dogma was based on early studies that demonstrated comparable turnover rates of bulk histones and the methyl groups on histone lysine and arginine residues in mammalian cells (11) (103). Interestingly, in the same period, a separate study identified a low level of histone methyl group faster turnover (~2% per hour) (9); the same research group also identified an enzymatic activity in rat kidney extract that appeared to mediate the demethylation, but the enzyme was never identified (65). More recently, Seward and co-workers showed, in budding yeast, that H3K4me3 and H3K4me2 were greatly reduced relative to total H3 within 2 hours after the depletion of *Set1* (90), demonstrating that these two chromatin marks are highly dynamic and that the demethylation of H3K4 is normally countered by ongoing methylation via Set1p (it is important to bear in mind that this observation has been done in yeast, whose cell cycle is much faster than the one of mammalian cells, thus making difficult to directly translate these data to higher eukaryotes).

Only a few years ago a landmark study led to the discovery of the first histone demethylase, LSD1 (lysine-specific demethylase 1) (93), thus changing our view of histone methylation regulation and leading to the identification of numerous histone demethylases.

LSD1 is a flavin adenine dinucleotide (FAD)-dependent amine oxidase that is able to specifically demethylate lysine 4 on histone 3, but not other methylated arginine or lysine residues (93). Interestingly, the demethylation reaction carried by LSD1 requires the presence of a protonated nitrogen in the substrate, thus limiting the substrates to mono- or dimethylated peptides, and raising the question of whether trimethylated lysine is reversible by other classes of enzymes able to perform different oxidative mechanisms.

Jumonji C (JmjC) domain-containing proteins were the first new group of proteins suggested, and then demonstrated, to function as histone demethylases (106). The JmjC domain was later found in more than 100 proteins from bacteria to eukaryotes. In mammals JmjC proteins are divided in several sub-families, showing different substrate specificity (Figure 10).

JmjC proteins derive their name from their homology to a region in the mouse Jumonji (Jmj) protein, mutations in which result in a cruciform-shaped neural tube (Jumonji, indeed, is the Japanese word for cruciform) (98). They belong to the superfamily of 2-oxoglutarate (2OG) oxygenases, which require Fe(II) as a cofactor, utilize oxygen and, almost always, 2-oxoglutarate as co-substrates, and produce succinate and carbon dioxide as by-products.

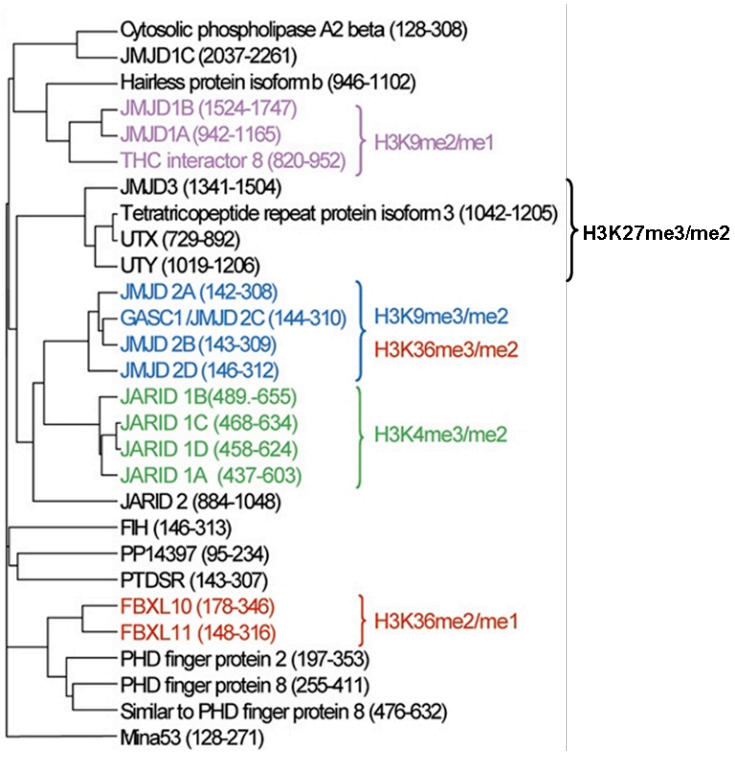

Figure 10 - Phylogenetic analysis of the human JmjC family.
The reported specificities of the different JmjC sub-families are indicated. Modified from (15).

The range of different types of reactions that the 2OG oxygenases are able to catalyze is among the most diverse of any enzyme family. In plants and microorganisms 2OG oxygenases catalyze hydroxylations as well as other oxidative reactions involving

desaturation, ring closure, epimerization and chlorination (53). In contrast, in animals the range of identified chemistry catalyzed by this class of enzymes is limited to hydroxylation and demethylation initiated by hydroxylation (53). 2OG oxygenases are involved in a wide range of biological roles, from metabolism (27) to hypoxic signalling (64) and DNA repair (89), and most of them have been still little or not at all characterized.

In JmjC domain-containing proteins the JmjC domain is characterized by the presence of the 2-hystidine-1-carboxylate facial triad (Figure 11A), a non-heme iron binding motif which requires iron to activate molecular oxygen and to generate oxidizing intermediates that are then used in oxidative reactions (e.g. hydroxylation) (Figure 11B).

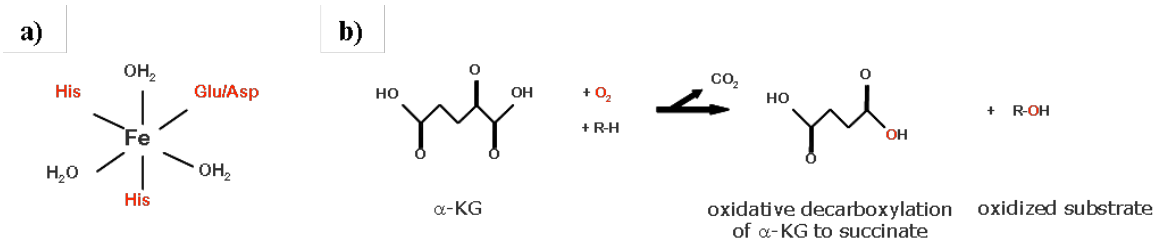

Figure 11 – JmjC containing proteins catalyze oxidative reactions.
A) The 2-His-1-carboxylate facial triad. *B)* The oxidative reaction catalyzed by the family of α-oxoacid dependent enzymes.

When this reaction occurs on a methylated lysine residue on histones, the iron-driven oxidation produces an unstable hydroxymethyl-lysine intermediate; the hydroxymethyl group is then released as formaldehyde and an unmethylated lysine residue is left (Figure 12) (indeed the release of formaldehyde is one of the methods for the *de novo* identifications of demethylating enzymes).

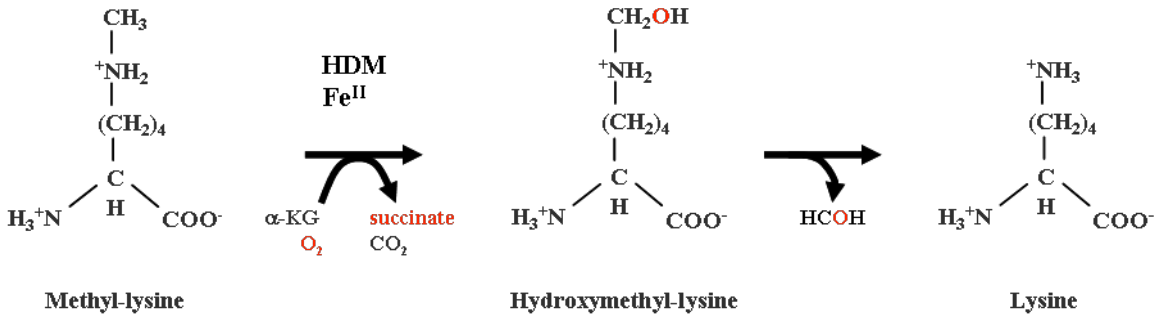

Figure 12 – JmjC-driven demethylation reaction on a methylated lysine residue.

Unlike LSD1, the JmjC domain demethylases do not require protonated nitrogen in the substrate; thus, they are capable of demethylating not only mono- and dimethylated but also trimethylated lysine residues.

The degree of lysine methylation on nucleosomes and their relative locations throughout the genome are associated with potentially different functional outcomes. For instance, the presence of H3K4me3 at the 5' end of a gene, but not H3K4me2, is usually (but not exclusively) associated to active transcription (90) or to genes poised to be transcribed.

It is likely that both methyltransferases and demethylases play a role in balancing methylation dynamics. Moreover, it is possible to speculate that demethylases may provide a mechanism for fine tuning histone methylation levels. For example, the trimethyl demethylases JMJD2A and JMJD2C predominantly convert H3K9me3 to H3K9me2, while JMJD2D reduces H3K9me3 to H3K9me1 (109), indicating that these related demethylases help in generating differential methylation states at the same lysine residue. The current model is that differentially methylated lysines may serve as platforms for different chromatin modifying enzymes and therefore may have different functional outcomes (94).

4.3 The JARID1 family

Mammalian cells encode four JmjC proteins that are able to demethylate lysine 4 on histone 3 (15) (45) (90) (41) (49); these proteins are collectively referred as the JARID1 family: Jarid1a (Rbp2), Jarid1b (Plu-1), Jarid1c (SMCX) and Jarid1d (SMCY) [Recently the family has been renamed as KDM5 – lysine-specific demethylase 5 – , accordingly to the reported enzymatic activity, and by consequence the family members are indicated as Kdm5a, -b, -c and –d]. On the contrary, lower eukaryotes *D. melanogaster*, *C. elegans* and

S. cerevisiae, each have a single ortholog, named little imaginal discs (lid), rbr-2 and Jhd2p, respectively.

In addition to the JmjC domain JARID1 proteins contains a conserved N-terminal motif, JmjN, whose presence is strictly correlated with the JmjC domain and is indispensable for the enzymatic activity of these proteins (97) (115). Other conserved motifs shared by the members of the JARID1 family include an ARID (A/T rich interaction domain) domain, implicated in DNA binding, a single C_5HC_2 zinc finger, and two or three PHD fingers (plant homeobox domain), involved in mediating protein-protein interactions and binding to methylated lysine residues (87). It is interesting to notice that while the ARID and C_5HC_2 zinc finger domains have been demonstrated to be important for Jarid1b and Jarid1d demethylase activity in vitro (115) (49), *S. cerevisiae* Jhd2p displays the same substrate preference even though it is approximately half the size of other JARID1 proteins and lacks all but the JmjN/JmjC domains and the first PHD finger (51).

While JARID1 proteins have been purified and their demethylase activity on lysine residues tested, there is very little data concerning the biological relevance of these enzymes.

Jarid1c and Jarid1d proteins are more similar to each other than either are to Jarid1a or Jarid1b, and they are encoded on X and Y chromosomes, respectively.

Jarid1c have been found to be one of the most frequently mutated genes in X-linked mental retardation (XLMR), a heterogeneous disease involving environmental and/or genetic factors, and characterized by mild to severe mental retardation (41). Interestingly, many of Jarid1c mutations identified in XLMR patients affect its demethylase efficiency and the reduction of this enzymatic activity roughly correlates with the severity of associated XLMR (97). The importance of Jarid1c in neuronal development has been then demonstrated in zebrafish and rodent primary neurons, where its depletion causes a significant reduction in dendritic length (41).

Little are the functional data regarding Jarid1d, but it is known that it binds and represses the developmentally important gene *engrailed2*, in association with Ring6a/MBLR, a polycomb-like Ring-finger-containing protein (49).

While Jarid1b has been reported as over-expressed in many tumour types, and in particular in breast cancer (see below), Jarid1a has been linked to development and differentiation. Christensen and coll. demonstrated that Jarid1a binds and represses HoxA genes (*Hoxa1*, *Hoxa5* and *Hoxa7*) in ES cells, and this binding is lost during differentiation in correlation with their transcriptional activation. Moreover, loss of Jarid1a binding to the *Hoxa1*, *Hoxa5* and *Hoxa7* promoters results in increased H3K4me3 levels, in agreement with Jarid1a H3K4 demethylase activity (15). On the contrary, Jarid1a is recruited together with the PRC2 complex to the promoters of *Fgf4* and *Otx2*, two genes whose expression is repressed during ES cells differentiation, suggesting that it contributes, together with the PRC2 complex, to maintain the silencing of specific target genes in ES cells, but can be also actively recruited to other target genes that need to be repressed during differentiation (69). In addition, a *C. elegans* mutant strain of the single JARID1-family gene, *rbr-2*, (or its RNAi-mediated depletion) exhibits a highly penetrant vulval phenotype with about 80% of the animals either having undeveloped vulvas or being multi-vulva (15).

The appearance of different JARID1 proteins in higher eukaryotes is likely due to a functional specialization of the different members of the family, still remaining the possibility of partial overlapping of target genes. Significantly, while mutations in *Drosophila lid* are homozygous lethal (31), Jarid1a$^{-/-}$ mice are viable and fertile, showing only a slight decrease in apoptosis of hematopoietic stem cells and an increase in the percentage of these cells in G0/G1 phase of cell cycle (45). The mild phenotype observed in these knock-out animals may be due to functional compensation by one of the three other JARID1 family proteins, whose expression has not yet been examined in Jarid1a mutants. Consistent with this possibility, while mutations in *Drosophila lid*, *C. elegans*

rbr-2, or *S. cerevisiae Jhd2p* result in increased global levels of trimethylated H3K4 (88) (15) (51), Jarid1a$^{-/-}$ MEFs did not show any global change in this chromatin mark (45).

Because trimethylated H3K4 is predominantly found surrounding the start site of transcriptionally active genes (7) (85) (86), the H3K4me3 demethylase activity of JARID1 proteins predicts that these proteins act as transcriptional repressors. Consistent with this model, chromatin immunoprecipitation (ChIP) analysis revealed that, as already mentioned, Jarid1a binds to the promoter region of homeobox genes *Hoxa1*, *a5* and *a7* and repress their transcription in ES cells (15). When ES cells are stimulated to differentiate, Jarid1a binding decreases upon gene activation, concomitant with an increase in trimethylated H3K4 levels surrounding the TSS. Similar ChIP analyses of Jarid1d reveal that it binds to the *engrailed2* gene. siRNA-mediated knock-down of Jarid1d in H1299 lung carcinoma cells results in derepression of *engrailed2* and enhanced recruitment of the basal transcription machinery and of the NURF chromatin remodelling complex, indicating that Jarid1d normally represses this gene (49).

Nevertheless different studies demonstrated also a transcription co-activator function for JARID1 proteins. For example in *Drosophila*, lid has been shown to enhance dMyc-mediated transcriptional activation. Lid H3K4me3 demethylase activity is in contrast with both gene transcriptional activation and the observation that Myc E-box binding is strongly dependent on the H3K4me3 levels of target genes promoter. A possible explanation is that lid enzymatic activity is negatively regulated by dMyc, which binds to lid catalytic domain (88), raising the hypothesis that lid is still able to recognize trimethylated H3K4 but is unable to catalyze its removal, thereby facilitating E-box binding by dMyc in this chromatin context.

Jarid1a has also been shown to either repress or activate the transcription of different target genes. While the loss of Jarid1a binding to target genes during differentiation correlates with an increase in both the transcription of some target genes and in the levels of

H3K4me2/me3, Jarid1a can also act as a co-activator and is required for the pRB effects on transcription of other genes, such as *BRD2* and *BRD8* (6).

4.4 Jarid1b/Kdm5b

Jarid1b was first discovered as a transcript down-regulated in a human mammary epithelial cell line transfected with HER2/c-erbB2, after treatment with the 4D5/HERCEPTIN antibody, which inhibits c-erbB2 signalling (16). Subsequent *in situ* hybridization and Northern blot analyses showed that *Jarid1b* is expressed in most breast cancers and breast cancer cell lines, regardless of the level of c-erbB2 (54).

In the following ten years different research groups showed that the expression level of *Jarid1b* is up-regulated in different cancer types, e.g. breast cancer (54) (4) (115), prostate cancer (112) and melanoma benign nevi (79) (78). Recently, Hayami and coll. extended the analysis of *Kdm5b* expression to other cancer types, reporting a significant up-regulation in most of the clinical cancer samples analyzed compared to their corresponding normal tissues: bladder cancer, non-small and small cell lung cancer, acute myeloid leukemia, chronic myelogenous leukemia, cervical cancer and renal cell carcinoma (34).

On the other hand, Jarid1b is reported to have a restricted expression pattern in normal adult tissues, with high levels in regenerative tissues, like testis and bone marrow (4) (55) (77), and low levels in placenta, ovary and mammary gland (4).

These observations generated much effort in trying to understand the physiological and pathological function of this protein.

The Jarid1b gene encodes for a 1544 amino acids nuclear protein characterized by a JmjC domain in combination with JmjN, BRIGHT/ARID, PHD and zinc-finger domains, which order is conserved among the members of the JARID family (Figure 13) (90). An additional Trp/Tyr/Phe/Cys domain is characteristic of this protein and called PLU-1 domain (99).

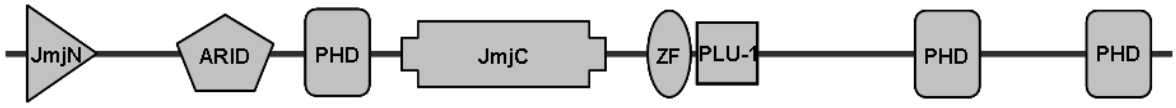

Figure 13 - Schematic representation of Jarid1b domains.

The JmjC domain is the catalytic centre responsible for the hydroxylation reaction leading to the reported H3K4 demethylase activity (90) (115). The contribution of the other domains to the demethylase activity has been tested through the generation of a series of deletion mutants and the analysis of the methylation level of H3K4me3 in the transfected cells (115) (112). The removal of the two C-terminal PHD domains does not affect the demethylase activity of Jarid1b, but the further deletion of the C-terminal C_5HC_2-zinc finger domain results in both the delocalization of the protein, which diffuses in nucleus and cytoplasm, and a complete loss of the demethylase activity. On the other hand the deletion of either the JmjN or the BRIGHT/ARID or the N-terminal PHD domains has no effects on Jarid1b nuclear localization but does result in loss of its demethylase activity (115). While the JmjN domain has been shown to be required for efficient enzyme function of other JmjC domain containing proteins (e.g. JMJD2A (22)), neither BRIGHT nor PHD domains are absolutely required for demethylase activity, suggesting that their deletion may alter the spatial arrangement between the JmjN and JmjC domain and thus inhibit proper folding of the functional enzyme.

As a H3K4 demethylase Jarid1b is supposed to be a transcriptional repressor. Indeed luciferase reporter assay demonstrated that increasing amount of Jarid1b leads to a correspondent reduction in luciferase expression (99). However, while Jarid1b has been shown to have limited co-repressive effects when co-transfected with the transcription factors *BF-1* and *PAX9* (99) (79), it has also been found to cooperate with the androgen receptor in transcriptional activation (112), suggesting that Jarid1b, similarly to Jarid1a, might have different context-dependent transcriptional regulatory properties.

Although the ability of Jarid1b of demethylating methylated H3K4 has been well established both *in vitro* and in cultured cell lines, very few and restricted to single genes are the *in vivo* data on the physiological activity of this protein.

Most of the data regarding Jarid1b biological function link this protein to cellular proliferation. Jarid1b depletion in MCF-7 cell line resulted in a slower growth rate when compared to the control, with a reduction in the S phase cell population accompanied by an increase in the G1 cell population, suggesting that Jarid1b positively regulate the cell cycle by facilitating the G1/S transition (115), maybe through the transcriptional repression of known or putative negative regulators of cell growth, such as *Cav1*, *Hoxa5* and *Brca1*. An independent study showed a significant growth suppression upon Jarid1b siRNA-mediated knock-down, characterized by an augmented fraction of cells in the sub-G1 phase (34). Following expression profiling of Jarid1b-depleted cells highlighted a ~50% reduction in E2F1 and E2F2 expression, supporting the idea that Jarid1b might have a role in facilitating the progression of the cell cycle, in particular between the G1 and S phases.

Interestingly, Jarid1b has been found down-regulated in malignant melanocytic tumours (77), with only 5-10% of the total population expressing high levels of Jarid1b. Recently, Roesch and coll. demonstrated that Jarid1b expression correlates with slow-cycling melanoma cells sub-population characterized by self-renewal capacity (78), raising the hypothesis that Jarid1b might have a role in long-term tumour maintenance rather than tumour initiation.

However, the finding that other JmjC proteins (e.g. JMJD1A) could be differentially regulated among slow- and normal-cycling cell sub-populations, together with the observation that long-term culture of sorted Jarid1b-positive cells give rise to a heterogeneous daughter population, consisting of Jarid1b-positive and -negative cells, and vice versa, raised the possibility that Jarid1b might simply be highly expressed in a subset of cells subjected to low oxygen concentration. In fact, it has been recently demonstrated that the expression of Jarid1b, as well as of Jmjd1a and other JmjC proteins, is up-

regulated in hypoxic conditions under the control of the transcription factor hypoxia-inducible factor 1α (Hif1α) (46) (111).

5. Thesis outline

Aiming at identifying new transcriptional co-regulators involved in the inflammatory response we analyzed global gene expression profiles of macrophages subject to inflammatory stimuli. Using a candidate approach we found the histone demethylase Jarid1b deserving of deeper studies, as a potential negative regulator of inflammation late phases.

In the first part of this thesis it will be presented the characterization of Jarid1b expression profile determined by different stimuli in macrophages, followed by the investigation directed at identifying the transcription factor responsible for Jarid1b up-regulation.

The second part will be dedicated to the study of the transcriptional network controlled by Jarid1b. This goal has been achieved by analyzing global gene expression alterations deriving from the perturbation of Jarid1b expression levels. In particular, I will expose how Jarid1b depletion affects a well-defined pathway (the LXR pathway), independently of the inflammatory stimulus and the consequent Jarid1b protein up-regulation.

Then they will be briefly described how we generated Jarid1b knock-out mice and the early phenotypic observations on the same mice.

Following, they will be presented some data on Jarid1b-KO macrophages aimed at corroborating the findings resulted from previous depletion experiments.

In the last part I will describe how genome-wide analyses (expression and genomic binding analyses) together with some observations on Jarid1b demethylase activity, demonstrated a limited role for Jarid1b in transcriptional regulation.

I will also present interesting preliminary results on the expression analysis of some small nucleolar RNA in Jarid1b-ablated cells that might associate Jarid1b function to RNA methylation/demethylation.

At the end of this thesis I will discuss about the significance of our findings and the possible explanations to the limited transcriptional role for Jarid1b deduced from the collected data, reasoning about different practicable approaches to answer to the several questions arising from this work and the recent literature.

MATERIALS AND METHODS

Cell culture procedures

All the cell lines used (Raw 264.7, J774, L929, Phoenix-ECO and 293T) were cultured in Dulbecco's Modified Eagle's Medium (DMEM) supplemented with 10% heat-inactivated Fetal Bovine Serum (FBS), 2 mM glutamine, 100 U/ml penicillin and 100 mg/ml streptomycin. Cells were incubated at 37°C in a 5% CO_2 humidified atmosphere.

Bone marrow-derived macrophages in vitro differentiation

Bone marrow (BM) cells were isolated from either Fvb/Hsd or Jarid1b-knock-out (C57BL/6-129P2) mice. Red blood cells were lysed by osmotic shock (1 min in 2 ml NaCl 0.2% followed by addition of the same volume of NaCl 1.6% to reconstitute the physiological osmotic pressure). BM cells were then washed twice in cold PBS, resuspended in BM medium (DMEM supplemented with 30% L929-conditioned medium, 20% FBS, 2 mM glutamine, 100 U/ml penicillin 100 mg/ml streptomycin, 0.5% sodium pyruvate, 0.1% β-mercaptoethanol) and plated $1x10^6$ cells in 5 ml of BM-Medium per 100 mm petri dish. Differentiating cells were fed with 2 ml of fresh BM medium every 2 days and harvested at day 7-8 of differentiation (or as otherwise stated).

Retroviral Constructs and Production of Retroviruses

All shRNA constructs were prepared in the MSCV-based pLMP retroviral vector (20). The sequences of the two shRNAs used in the experiments are:

KD1:TGCTGTTGACAGTGAGCGACCAGTACATCTCAATTCTTTATAGTGAAGCC ACAGATGTATAAAGAATTGAGATGTACTGGGTGCCTACTGCCTCGG;

KD2:TGCTGTTGACAGTGAGCGCGCTTTCTTCAGGGAATCTAAATAGTGAAGCC ACAGATGTATTTAGATTCCCTGAAGAAAGCATGCCTACTGCCTCGG.

Phoenix-ECO packaging cells were co-transfected with 1 μg pCLECO and 5 μg of either LMP empty vector or the same vector carrying the Jarid1b-directed shRNA sequences, using the Lipofectamine and Plus reagents (Invitrogen) accordingly to manufacturer's protocols. Supernatants from transfected Phoenix-ECO were collected at 48 and 60 hours post-transfection and immediately used for infections.

Retroviral Transduction of Bone Marrow-Derived Macrophages

On day 0, bone marrow cells were isolated and $3x10^6$ cells/well were seeded on 6-well plates in BM medium. Spin infection was performed on days 1 and 2 for two consecutive days (2 infections per day). In details, cells were first spun at 2500 rpm for 5 min, the BM medium was removed, and the retroviral supernatants, supplemented with 8 μg/ml polybrene and 8 μl/ml of 1 M HEPES pH 7.5, were added. Spin infections continued for 1.5 hours at 2500 rpm room temperature (RT); after 4 hours the virus-containing medium was gently removed and replaced by fresh BM medium. Puromycin selection (3 μg/ml) started on day 3. Assays were carried out at days 7–8.

Antibodies and Reagents

The C-terminus (amino acids 1270-1544) of Jarid1b was cloned in a pMAL vector. The produced maltose binding protein (MBP)-fused peptide was used to raise a polyclonal antibody in rabbit. The serum obtained after four cycles of immunization was then affinity-purified by the Biochemistry unit at IFOM-IEO-Campus Facility, first against the MBP to eliminate those antibodies recognizing the fusion partner, and then with the same peptide used for the immunization. The C-terminus was chosen to guarantee the highest specificity of the antibody, being the least conserved region among the members of the JARID1 family. Moreover the high similarity with the human JARID1B protein allowed the recognition of the human homolog.

The following antibodies were used in western blot at the concentrations suggested by the supplier: H3 (ab1791), H3K4me3 (ab8580), H3K4me1 (ab8895), H3K9me3 (ab8898), H3K9me2 (ab1220), H3K36me3 (ab9050) and LXRα (ab41902) were from Abcam; H3K4me2 (07-030), H3K27me3 (07-449) and H3K27me2 (07-452) were from Millipore; H3K4me3 (39159) was from Active motif; Cyp27a1 (sc-14835) was from Santa Cruz Biotechnology.

The following antibodies were used for IP or ChIP: p65 (sc-372), c-Rel (C) (sc-71) and HA-probe (Y-11) (sc-805) were from Santa Cruz Biotechnology; Hif1α (NB100-134) was from Novus Biologicals; Jarid1b serum (ab50958) and LXRα (ab41902) were from Abcam.

LPS from E.Coli serotype 055:B5 (Sigma), was used at 10 or 100 ng/ml, while IFNγ (R&D) was always used at 50 ng/ml. Pravastatin sodium (P4498), Ro-48-8071 (R-2278), cyclosporin A (30024) and TO901317 (T-2320) were from Sigma-Aldrich; 24(S),25-epoxycholesterol (GR-231) was from Biomol International, and 22(R)-hydroxycholesterol (700058) was from Avanti Polar Lipids.

RNA extraction and cDNA synthesis

Total RNA was extracted using Trizol (Invitrogen) or RNeasy kit (Qiagen), according to manufacturer instruction. RNA was quantified by ND-1000 spectrophotometer (NanoDrop Technologies) and its quality was assessed by measuring A_{260}/A_{280} and A_{260}/A_{230} ratios. Complementary DNA (cDNA) was obtained by reverse transcription with the following protocol: RNA was denatured at 65°C for 10min and immediately placed on ice; 0.5 μg of denatured RNA were mixed with 1 μl 10x Reaction buffer, 2.5 μM random hexamers, 0.5 mM dNTP and 0.5 μl M-MuLV (Fynnzymes) reverse transcriptase, in a total volume of 10 μl. Enzymatic reactions were performed in a PCR machine: 10 min 25°C (annealing), 60 min 42°C (elongation) and 5 min 95°C (enzyme inactivation). Samples were then diluted in double-distilled water (ddH_2O) to a final volume of 100 μl.

Small RNA enriched RNA was extracted using the mirVana kit (Ambion) and cDNA was reverse transcribed as previously described with the addition of a mix of 1 μM *Gas5*-hosted snoRNAs specific primers.

Quantitative RT-PCR (QPCR)

Real time PCR was performed using the SYBR Green detection system on either a 7500 or a 7900HT Applied Biosystem machine. Briefly, 10 μl of SYBR Green Master Mix (2X) (Applied biosystems) were mixed with 0.1 μM gene-specific primers, 4 μl of cDNA and ddH_2O to a final volume of 20 μl. Accumulation of fluorescent products was monitored for 40 PCR cycles. Each PCR reaction generated only one specific amplicon, as revealed by the melting temperature profile of final products (dissociation curve). QPCR detection system was updated with the Fast SYBR Green Master Mix during the course of the presented work and the PCR cycle settings adjusted following manufacturer instruction. Error bars in QPCR graphs represent standard deviation of three biological independent replicates unless otherwise stated.

Chromatin Immunoprecicpitation (ChIP)

The purpose of ChIP assay is to determine whether a protein binds to a particular genomic region on chromatin. The principle underpinning this assay is that DNA-bound proteins can be cross-linked to the chromatin on which they are situated, usually by formaldehyde fixation. After cross-linking cells are lysed and the DNA is sheared into small fragments (200-500 bp) by sonication. Smaller is the size of DNA fragments more precise will be the identification of protein localization, with the limitation that the DNA fragment has to be long enough to be efficiently amplified by PCR. Then, the protein-DNA complexes can be immunoprecipitated using specific antibodies and, after cross-linking reversion, the DNA can be purified. The identity of immunoprecipitated DNA can be determined by PCR using

sequence specific primers; in alternative, the whole pool of DNA can be sequenced to have a global protein binding profile (ChIP-sequencing).

Preparation of ChIP extracts. Cells were fixed in PBS with formaldehyde 1%. Cross-linking was allowed to proceed 10 min RT and then stopped by addition of 125 mM Tris-HCl pH 7.6. Cells were washed three times with 15 ml PBS, collected in PBS using a silicon scraper, pooled in a 50 ml Falcon tube and spun at 1,500 rpm for 5 min. Pellets were washed again in 3 ml PBS, transferred to a 15 ml conical tube and spun at 1500 rpm for 5 min. Pelleted cells were resuspended in LB1 buffer (50 mM Hepes-KOH pH 7.5, 140 mM NaCl, 1 mM EDTA, 10% glycerol, 0.5% NP-40, 0.25% Triton X-100), kept 10 min on ice to lyse cell membranes and centrifuged at 2500 rpm for 5 min. Nuclei were washed in LB2 buffer (10 mM Tris-HCl pH 8.0, 200 mM NaCl, 1 mM EDTA, 0.5 mM EGTA) for 10 min at RT under gentle rocking to remove the detergents and then centrifuged at 2500 rpm for 5 min. Finally, pellets were resuspended in LB3 buffer (10 mM Tris-HCl pH 8.0, 100 mM NaCl, 1 mM EDTA, 0.5 mM EGTA, 0.1% Na-deoxycholate, 0.5% N-lauroylsarcosine). All the centrifugation steps were carried out at 4°C and all lysis buffers were supplemented with protease inhibitors: 1 mM PMSF, 10 μg/ml aprotinin and 10 μg/ml leupeptin.

Nuclei suspension was sonicated to share cross-linked DNA to 300-500 bp fragments (amplitude 30%, 30 sec, 5-7 cycles) and then centrifuged at max speed for 10 min to eliminate cell debris. DNA fragments size was checked by extracting DNA from a little aliquot (30 μl) and loading it on a 1.3% agarose gel. After reaching the desired DNA fragment size, 1% Triton X-100 was added to neutralize the SDS-like detergents. A 50 μl aliquot of cell lysate was saved as whole-cell extract (WCE) and used as ChIP input.

Pre-block and antibody binding to magnetic beads. 50 μl protein G dynabeads (Invitrogen) were washed three times with 1 ml block solution (PBS/BSA 0.5%), collected using a magnetic stand, resuspended in 250 μl block solution with 10 μg antibody and incubated on a rotating platform o.n. at 4°C. The day after, dynabeads were washed 3 times

with 1 ml block solution and resuspended in 100 µl block solution (ready-to-use beads). The amount of antibody and dynabeads was adjusted, according to the need, as following: p65 and c-Rel, 10 µg antibody with 50 µl beads; Hif1α, 25 µg with 100 µl beads; Jarid1b, 20 µg with 100 µl beads. Antibody against HA-probe was always used as mock ChIP, in the same conditions of the antibody of reference.

Chromatin immunoprecipitation. Ready-to-use beads were added to cell lysate and gently mixed on rotating platform o.n. at 4°C.

Wash, elution and cross-link reversal. The IP was transferred to a 1.5 ml pre-chilled tube, splitting the volume when necessary. Dynabeads were collected using a magnetic stand and the supernatant was removed. Dynabeads were washed 6 times with 1 ml Wash Buffer (50 mM Hepes-KOH pH 7.6, 500 mM LiCl, 1 mM EDTA, 1% NP-40, 0.7% Na-Deoxycholate) for 5 min on ice, and once with 1 ml TE/50 mM NaCl. All the washing steps were performed on ice. Beads were spun at 3000 rpm for 3 minutes at 4°C and the residual TE buffer was removed. IP DNA was eluted with 250 µl elution buffer (TE/SDS 2%) at 65°C for 15 min under shaking. Finally, dynabeads were spun at max speed for 1 min at RT, 240 µl of supernatant was transferred to a new tube and cross-linking was reversed by incubating IP DNA at 65°C o.n. The WCE aliquot reserved after sonication was thawed and mixed with 3 volumes of elution buffer. Cross-linking was reversed by incubating WCE DNA at 65°C o.n.

Purification of DNA. Extracted DNA was diluted five-fold with 600 µl PB buffer (Qiagen) and incubated 30 min at 37°C in a thermo-mixer. Both tubes were loaded on a single Qiaquick column, washed following manufacturer's protocol and eluted in 70 µl TE.

Protein extraction

Cells were washed twice with PBS, collected in 2 ml PBS using a silicon scraper, and centrifuged at 1500 rpm 5 min at 4°C. (All centrifugation steps were performed at 4°C and

protease inhibitors - 1 mM PMSF, 10 μg/ml aprotinin and 10 μg/ml leupeptin - were added to all the lysis buffers).

Total protein extracts. Pellets were resuspended in 250 mM NaCl lysis buffer (50 mM Tris-HCl, 250 mM NaCl, 5 mM EDTA, 0.5% NP-40) or in RIPA-modified buffer (50 mM Hepes-KOH pH 7.6, 500 mM LiCl, 1 mM EDTA, 1% NP-40, 0.7% Na-Deoxycholate) and lysed 10 min on ice. Cell lysates were sonicated twice for 15 sec, centrifuged 10 min at max speed to remove cell debris and supernatant was recovered as total protein extract.

Fractionated protein extract (cytosolic/nuclear protein extract). Pellets were resuspended in L1 buffer (50 mM Tris-HCl pH 8.0, 2 mM EDTA, 0.1% NP-40, 10% glycerol) lysed 5 min on ice, to break the cell membrane maintaining the nuclear envelope intact, and centrifuged 2500 rpm 5 min. Supernatant was recovered as cytosolic protein extract and nuclei enriched pellet was further lysed as previously described (total protein extract).

Sub-nuclear fractions protein extract. Pellets were resuspended in solution 1 (100 mM Pipes, 1 mM EGTA, 1 mM $MgCl_2$) plus 0.5% Triton X-100 for 2 min RT and centrifuged 900 g 5 min. Supernatant represented the cytosolic protein fraction. Nuclei in the pellet were washed once in solution 1 and spun as before. Pellets were resuspended in solution 2 (10 mM Pipes, 100 mM KCl, 300 mM sucrose, 3 mM Mg Cl_2, 1 mM EGTA), digested with 200 μg/ml DNAseI 45 min at 33°C and centrifuged 1500 g 10 min. Supernatant of this centrifugation represented the DNAse released protein fraction. Pellets were resuspended again in solution 2 and 0.25 M ammonium sulfate was added dropwise. Lysates were centrifuged at 2000 g 5 min. Supernatant of this centrifugation represented the histone protein fraction. Pellets were resuspended in solution 2 and 2.5 M NaCl was added dropwise. Lysates were centrifuged at 4000 g 5 min. Supernatant of this centrifugation represented the outer nuclear matrix protein fraction. Pellets, representing the inner nuclear matrix protein fraction were resuspended in laemmli buffer.

Mitochondrial enriched protein extract. After washing with PBS, cells were collected in Isolation buffer (10 mM Tris-HCl, 250 mM saccarose, 0.5 mM EGTA) and centrifuged at 600 g 5 min. Pellets were resuspended in Isolation buffer, cells broken in a Potter homogenizer (40-50 strokes) and centrifuged at 600 g 10 min. Supernatant was recovered and centrifuged at 7000 g 10 min. The pellet from this centrifugation step represent the mitochondrial enriched fraction.

Protein co-immunoprecipitation (co-IP)

For exogenously expressed Jarid1b/LXRα/RXRα co-IP, 293T cell were co-transfected with 1 μg pCDNA3-Flag-LXRα, 1 μg pSG5-RXRα and 4 μg myc-JARID1B. Cells were lysed in IP buffer (50 mM Tris-HCl, 150 mM NaCl, 5 mM EDTA, 10% glycerol, 0.5% NP-40) and total protein extracts quantified. 3 mg of protein extract were used for each IP. Protein extracts were pre-cleared twice with 50 μl protein A beads (blocked with PBS/BSA 2%), the first time for 2 hours and then o.n., on a rotating platform at 4°C. Flag immunoprecipitation was performed with 50 μl anti-Flag M2 agarose conjugated beads (Sigma-Aldrich) for 4 hours on a rotating platform at 4°C. Beads were washed 5 times with 500 μl IP buffer and once with 1 ml PBS, and immunoprecicpitated proteins were recovered with laemmli buffer 5 min at 95°C.

For Jarid1b/LXRα co-IP on endogenous proteins, BMDM were stimulated with LPS (100 ng/ml) + IFNγ (50 ng/ml) for 8 hours and nuclear proteins were extracted in IP buffer. Protein extracts were quantified and 2 mg nuclear extract were used for each IP. Samples were pre-cleared with 50 μl protein A beads (blocked with PBS/BSA 2%) 2 hours on a rotating platform. Immunoprecipitation was performed at 4°C o.n. with the following antibodies: 1) 8 μg Jarid1b non cross-linked, 2) and 3) 25 μl Jarid1b cross-linked beads, 4) 10 μl Jarid1b serum, 5) 8 μg HA-probe, 6) 4 μg LXRα. The day after, IPs were collected with 50 μl protein A beads (excluded those with cross-linked antibodies) and washed three

times with 500 μl IP buffer. Immunoprecipitated proteins were recovered from beads with 25 μl laemmli buffer and loaded on a 10% polyacrylamide gel.

Luciferase reporter assay

For the LXRα luciferase assay, 293T cells were co-transfected with 400 ng of luciferase reporter construct (hABCA1-Luc), 100 ng pCDNA3-LXRα, 100 ng pSG5-RXRα and increasing amount of pCDNA3-Jarid1b (50, 100 and 500 ng). For the MEKK1-AP-1 luciferase assay, 293T cells were co-transfected with 400 ng of luciferase reporter construct (AP-1-Luc), 100 ng pCDNA3-MEKK1, and increasing amount of pCDNA3-Jarid1b (50, 100 and 500 ng). Empty pCDNA3 vector was used to make the transfection homogeneous, meaning that each sample was transfected with the same total amount of DNA.

Cells were collected 48 hours post-transfection, washed twice with PBS and lysed with 600 μl Reporter lysis buffer (Promega) 10 min on ice. Cell lysates were sonicated once for 12 sec and centrifuged 10 min at max speed. Supernatant was recovered and quantified. 5 μg protein lysate/sample were mixed with lysis buffer to reach 20 μl final volume. Samples were loaded on a 96 well white plate, luciferase substrate (100 μl) was added and luminescence was read with a luminometer.

Microarray Analyses

BM cells from Fvb/Hsd mice were infected with the control LMP vector or with the vector expressing the Jarid1b-specific shRNAs (KD1 and KD2). After differentiation into macrophages, cells were stimulated with 100 ng/ml LPS + 50 ng/ml IFN-γ for 8 and 12 hours.

BM cells were isolated from heterozygous and Jarid1b-KO mice (RRO123 strain), differentiated in macrophages and stimulated with 10 ng/ml LPS for 0, 8 and 24 hours.

RNA was, in both cases, extracted using the RNeasy kit (Qiagen).

Quality analysis of total RNA, cRNA synthesis, hybridization, and data extraction were performed by the Microarray Core Facility at IFOM-IEO campus. Affymetrix platform arrays were used for gene expression screening. Results were captured and analyzed using GeneChip analysis software (Affymetrix, Inc.).

Jarid1b knock-out mice

Knock-out embryonic stem (ES) cell lines were produced by BayGenomics, as part of the International Gene Trap Consortium, through gene trapping, a method of randomly generating ES cells with well-characterized insertional mutations. The mutation is generated by inserting a gene trap vector construct into an intronic or coding region of genomic DNA.

The gene trap vector construct is constituted by a splicing acceptor site (SA), causing the vector sequence to be spliced into the mRNA, a selection/reporter cassette (β-geo, containing the *lacZ* reporter gene encoding β-galactosidase, and the neomycin resistance) used to identify the cells where the vector has successfully interrupted a gene, and a polyadenilation signal at the 3' end that causes the mRNA to be truncated and non-functional (Figure 14). Thus, when this construct lands within a gene, the exon preceding the gene trap is spliced onto the gene trap vector, and the transcription from the trapped gene results in a truncated transcript fused to a selectable marker that is then translated into a tagged protein.

We chose two different ES cell lines (129P2/OlaHsd mouse strain), named RRO123 and RRR598, bearing the trap construct within *Jarid1b* second intron.

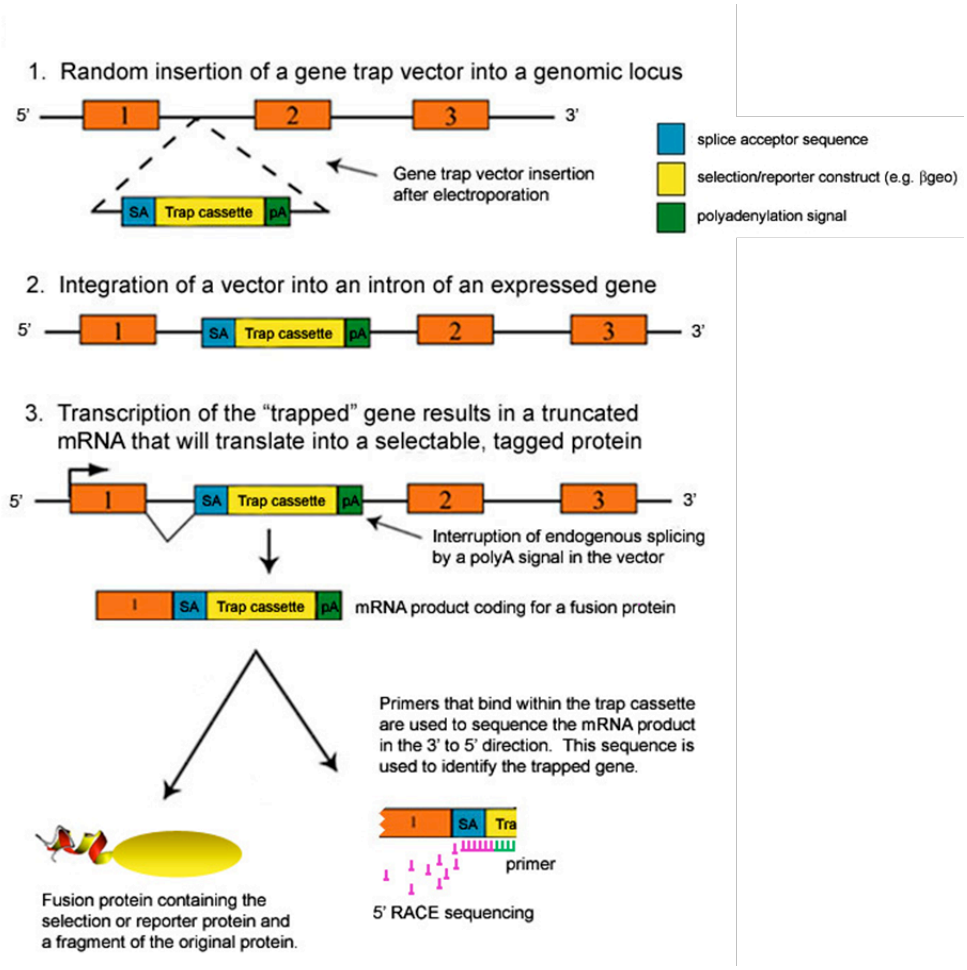

Figure 14 - Gene trap strategy.
Integration of a gene trap vector into an intron of an expressed gene results in a truncated mRNA that will translate in a selectable tagged protein. Reproduced from http://www.genetrap.org/tutorials/overview.html.

RESULTS

Although in the last decades inflammation has been extensively studied and the signalling pathways leading to the activation of an inflammatory response have been very well characterized, the knowledge about the tuning of this complex transcriptional network and in particular about the transcriptional control of inflammation resolution is still limited.

To identify new potential transcriptional co-regulators involved in the inflammatory response, we generated a global gene expression profile of mouse bone marrow-derived macrophages (BMDM) stimulated with inflammatory stimuli at different time points. Then we created a list of candidate genes, selected among those up-regulated at least two fold after stimulus and that possessed a known or suspected transcriptional activity, based on either a Gene Ontology or a manual selection (Figure 15B).

A

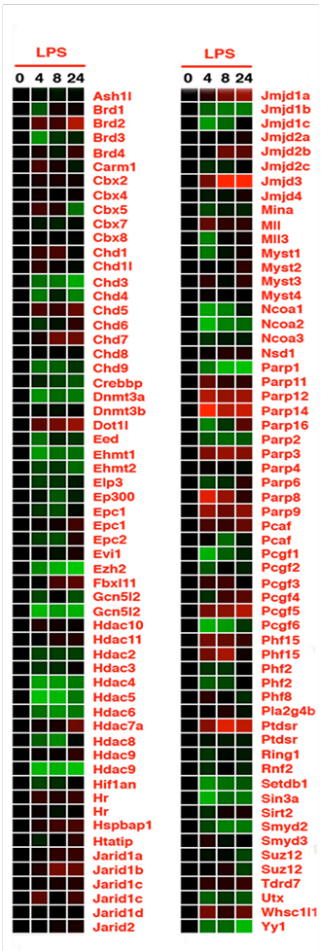

B

Gene Ontology selected	Manually selected
Ankib1	Abtb2
Copeb	Brd2
Eaf1	Dot1l
Jarid1b	Jmjd1a
Lass6	Jmjd3
Lmo4	Parp3
Mllt6	Parp8
Rest	Parp9
Rnf14	Parp12
Sap30	Parp14
Sertad1	Pcgf5
Sertad2	Phf15
Thrap1	Ptdsr
	Rhobtb1
	Zbtb7a

Figure 15 - Putative transcriptional co-regulators involved in the inflammatory response.

A) Expression profile of different genes bearing potential transcriptional regulatory activity in response to LPS stimulation; many JmjC domain-containing proteins appeared to be modulated by inflammatory stimuli. *B)* A list of Gene Ontolgy (GO) or manually selected genes, potentially or known to be involved in transcriptional regulation, whose expression was up-regulated more than two-fold after LPS stimulation.

As shown in Figure 15A, many are the JmjC domain containing proteins that were either activated or repressed when macrophages were challenged with LPS. Since recent studies and our previous work have shown that chromatin remodelling proteins and histone modifiers may modulate the expression of genes involved in the inflammatory response (17) (18), we focused our attention on the H3K4 demethylase Jarid1b. As a H3K4 demethylase, in fact, Jarid1b is a putative transcriptional repressor, and appearing to be up-regulated at late time points (8 and 24 hours) in microarray data it bore the potentiality to be involved in the regulation of inflammation resolution.

1. Jarid1b expression is up-regulated in LPS stimulated macrophages

We first validated the microarray data by quantitative PCR (QPCR) analysis and demonstrated that *Jarid1b* expression was strongly up-regulated in primary macrophages upon inflammatory stimuli, and this up-regulation happened with slow kinetics (Figure 16A).

At that time there was not any good commercial antibody for the detection of Jarid1b, so we generated a polyclonal antibody directed against the Jarid1b C-terminus, in order to confirm the expression data at the protein level. We chose Jarid1b C-terminus to guarantee the maximum specificity of the antibody, since this is the least conserved region among the members of the JARID1 family. Moreover, mouse and human Jarid1b C-terminal region are extremely conserved; indeed the antibody generated cross-reacted with human Jarid1b, at least when over-expressed, thus providing a powerful tool for the study of this protein in different organisms. The rabbit polyclonal anti-serum obtained after four cycles of immunization was then purified on an affinity column.

Western blot analysis confirmed the slow kinetics of Jarid1b protein induction in BMDM and highlighted its exclusive nuclear localization (Figure 16B), accordingly to what already published in literature (4) (115), and as expected for an enzyme exerting its activity on histones. The same up-regulation was observed in monocyte/macrophage cell lines (J774 and Raw 264.7), even though with a slower kinetics and an expression peak after 24 hours of LPS treatment (Figure 16C).

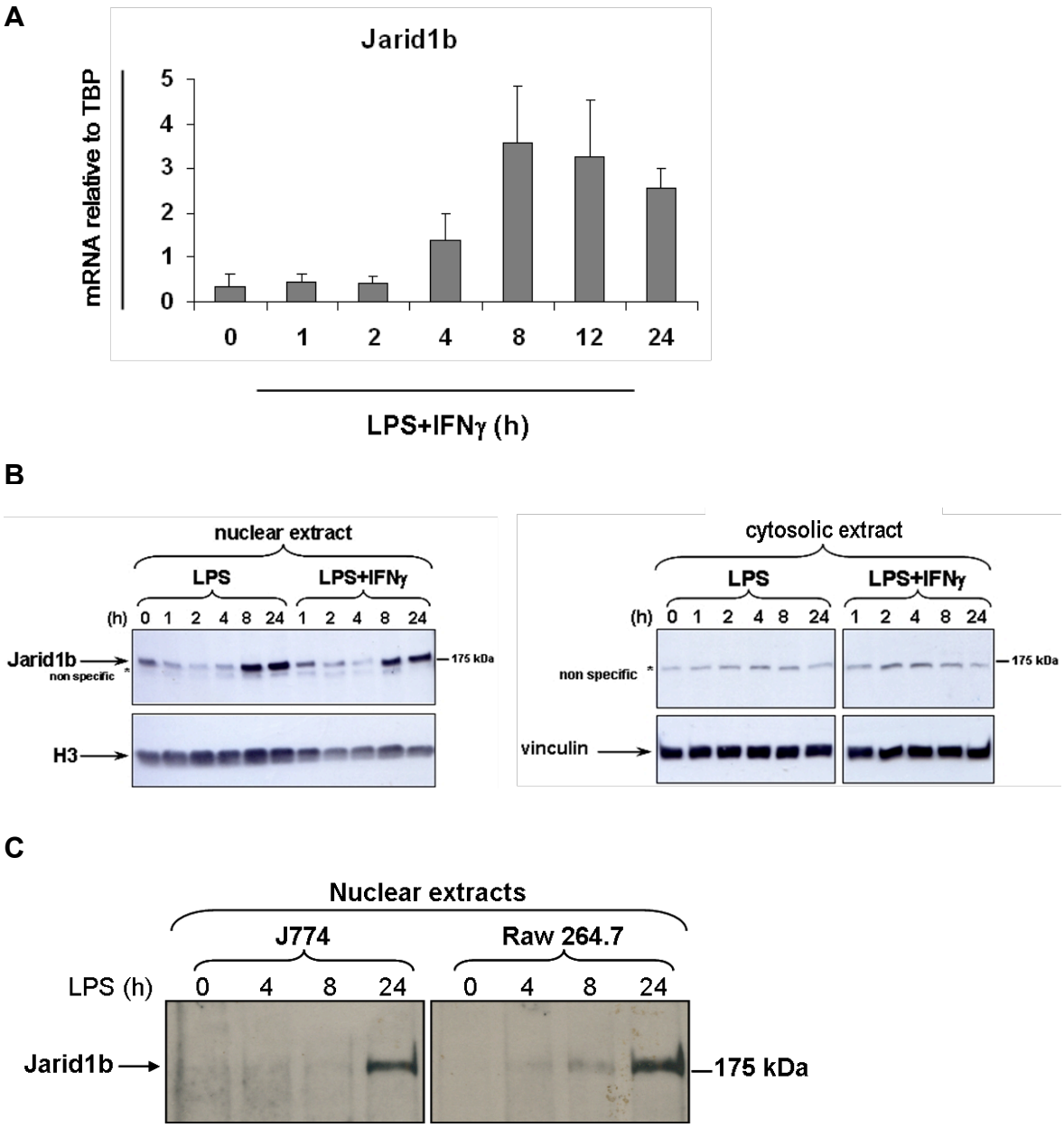

Figure 16 - Jarid1b expression is up-regulated in bone marrow-derived macrophages and macrophage cell lines upon inflammatory stimuli.
A) QPCR analysis confirmed the up-regulation of *Jarid1b* upon LPS+IFNγ treatment observed in microarray data. *B)* Western blot analysis corroborated mRNA data; nuclear (left) and cytosolic (right) protein extracts are shown. Histone 3 and vinculin are used to normalize nuclear and cytosolic protein extracts loading respectively. Asterisk (*) indicates a non-specific band. *C)* J774 and Raw 264.7 macrophage cell lines were treated with LPS for the indicated time points; WB on nuclear extracts shows Jarid1b strong up-regulation after 24 hours treatment.

Then we characterized the expression profile of *Jarid1b* in response to distinct inflammatory stimuli in order to understand the contribution of different inflammatory pathways to *Jarid1b* up-regulation: LPS and IFNγ (alone or in combination), and the conditioned medium of primary macrophages stimulated with LPS and IFNγ for 8 hours, corresponding to the time point of *Jarid1b* expression peak, were tested. We found that LPS alone, but not IFNγ, was sufficient to induce *Jarid1b* expression (Figure 17). A similar profile was obtained stimulating macrophages with the conditioned medium; the absence of an anticipated response excluded the hypothesis that the late expression kinetics reflected autocrine or paracrine signalling.

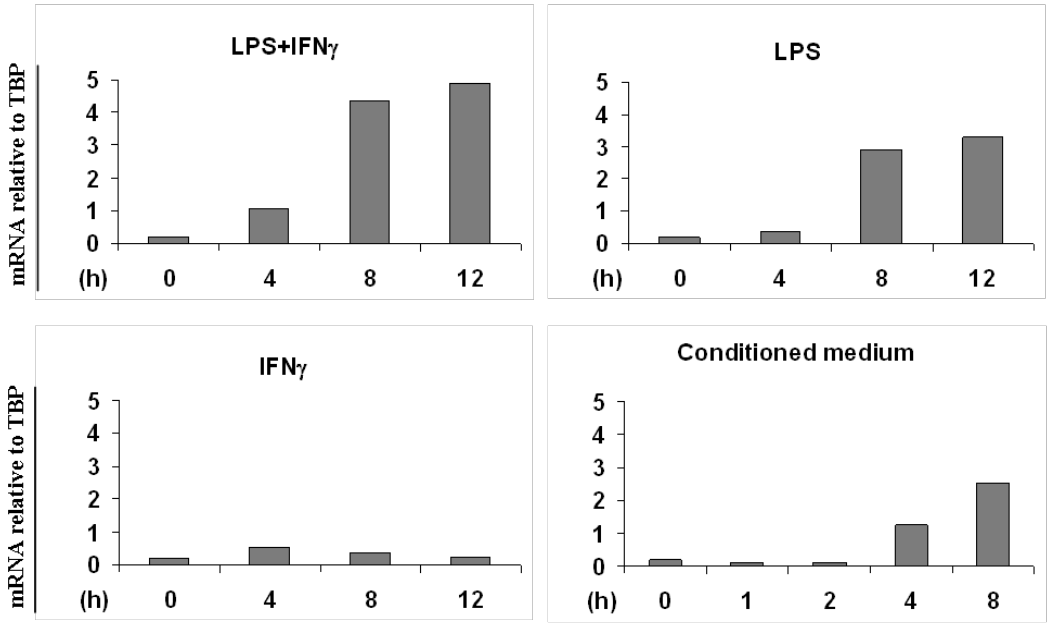

Figure 17 - LPS is sufficient to induce *Jarid1b* up-regulation.
QPCR analysis of *Jarid1b* expression in response to different inflammatory stimuli: while LPS treatment was sufficient to trigger the up-regulation of *Jarid1b*, IFNγ had only moderate cumulative effects. The stimulation with conditioned medium, obtained from the supernatant of macrophages stimulated with LPS and IFNγ for 8 hours, resulted in the same up-regulation profile triggered by LPS treatment, excluding the occurrence of autocrine or paracrine signalling.

We then extended the expression analysis to the other members of the JARID1 family in the same inflammatory-inducible context. Interestingly, *Jarid1b* was the only member of the JARID1 family responding to LPS stimulation (Figure 18), raising the hypothesis that Jarid1b might have acquired a functional specialization during evolution.

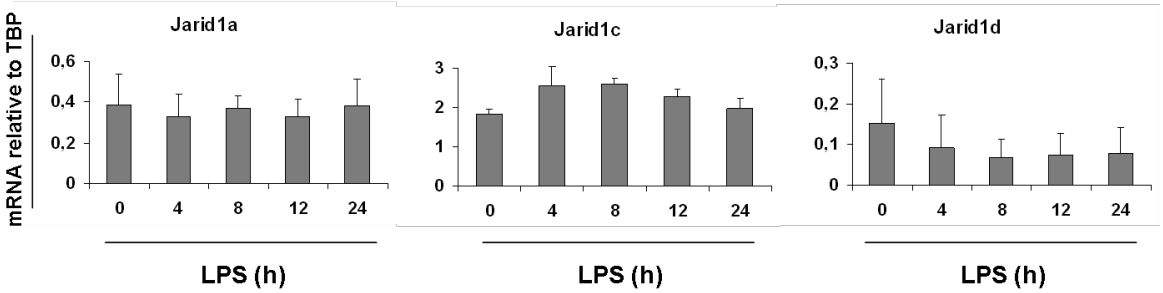

Figure 18 - JARID1 family members are not induced in response to inflammatory stimuli.
QPCR analysis revealed that JARID1 family members are not responsive to inflammatory stimuli. While *Jarid1a* had a completely flat expression profile after LPS stimulation, *Jarid1c* and *Jarid1d* were minimally (less than 2-fold) up-regulated and down-regulated respectively.

Once assessed the responsiveness of Jarid1b to LPS inflammatory stimulus, we decided to elucidate the transcriptional network architecture to which Jarid1b belongs. As recently reviewed by Alon (2), transcriptional networks can be rethought as a combination of interconnected simpler circuits, called motifs. One of the most common and best conserved motif is the feed-forward loop (FFL), which has already been characterized also in the inflammatory transcriptional response (see *Introduction*). Thus we organized our workflow according to the FFL structure, aiming at identifying the transcription factor/factors (TFs) driving Jarid1b up-regulation and the set of target genes whose expression is under the control of Jarid1b, with the final goal of characterizing Jarid1b biological function in macrophages.

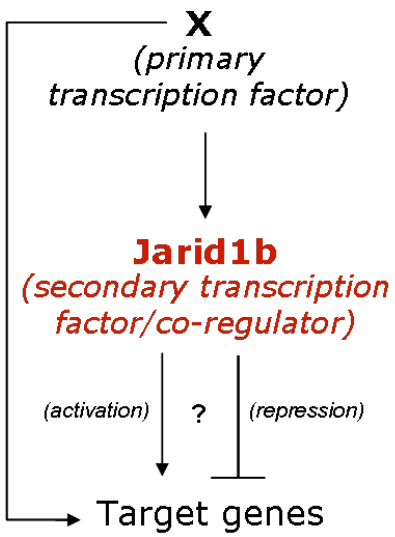

2. Jarid1b up-regulation is under the control of Hif1α

In order to identify the transcription factor responsible for the LPS-triggered Jarid1b up-regulation we searched for conserved binding sites for transcription factors possibly involved in the inflammatory response.

To achieve this goal we exploited the ConSite software, a web-based tool for finding cis-regulatory elements in genomic sequences. ConSite predictions are based on the integration of binding site prediction generated with high-quality transcription factor models and cross-species comparison filtering (phylogenetic footprinting) (84).

We compared mouse and human *Jarid1b* genomic sequences, starting from 5 kb upstream the TSS to the end of the gene, looking for conserved binding sites belonging to the NF-κB family; in particular, we queried for the following ConSite TFs profiles: c-Rel, NF-kappaB, p50, p65, Dorsal_1 and Dorsal_2. Setting a conservation cut-off of 80% and a TF score threshold of 80%, we obtained an output of 10 total putative binding sites; none of these binding sites was located in the gene promoter. After a further manual screening based on the similarity of the output sequences to the NF-κB consensus sequences derived from position-specific weight matrices (Figure 19), we selected three most likely binding sites. As summarized in Table 1, the first two NF-κB putative binding sites are located in the first intron and the third one in proximity to the 3' UTR.

			Position (relative to TSS)	
TF binding site	Name	Sequence	From	To
Hif1α	#1	CACGTGC	-4229	-4223
		CACGTGC	-4173	-4167
	#2	CACGTGC	-3788	-3782
		TACGTGC	-3779	-3773
	#3	GACGTGA	-230	-224
NF-kB/cRel	#4	GGGGACTTGC	809	818
	#5	GGGGACTTGC	2509	2518
	#6	TGGGTCTTTCT	70700	70710

Table 1 - Putative TFs binding sites on *Jarid1b*.
A total of 3 NF-κB and 3 Hif1α putative binding sites have been identified on *Jarid1b* gene, by ConSite and manual browsing respectively. On the right are indicated the binding sites positions relative to the transcription start site (TSS) (assembly July 2007 NCBI37/mm9).

Subsequent analyses with the Irf1 and Irf2 TFs profiles did not retrieve any additional binding site.

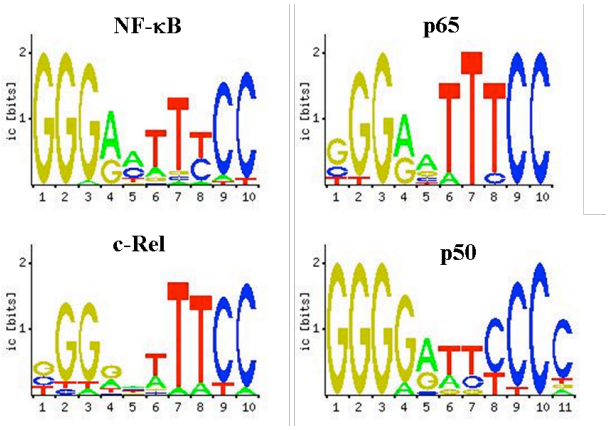

Figure 19 - Position-specific weight matrices (PWMs) of NF-κB family of transcription factors.
The consensus sequence based on the represented PWMs has been used for a manually curated selection of NF-κB binding sites on *Jarid1b*.

To verify the NF-κB binding to the identified DNA sequences, we performed chromatin immunoprecipitation (ChIP) of two NF-κB family members, p65/RelA and c-Rel. As expected, both p65 and c-Rel bound *Ccl5*, a well known NF-κB target gene; moreover, the binding was clearly LPS stimulus-dependent, as it was comparable to the negative control in non-stimulated cells and increased more than 5-fold after 8 hours of LPS treatment. On the contrary we could not detect any appreciable binding of either p65 or c-Rel to the putative NF-κB binding sites previously identified on *Jarid1b* (Figure 20 A and B). Even when a weak binding might be envisioned, as in the case of c-Rel to binding site #4, it was not responsive to LPS stimulus.

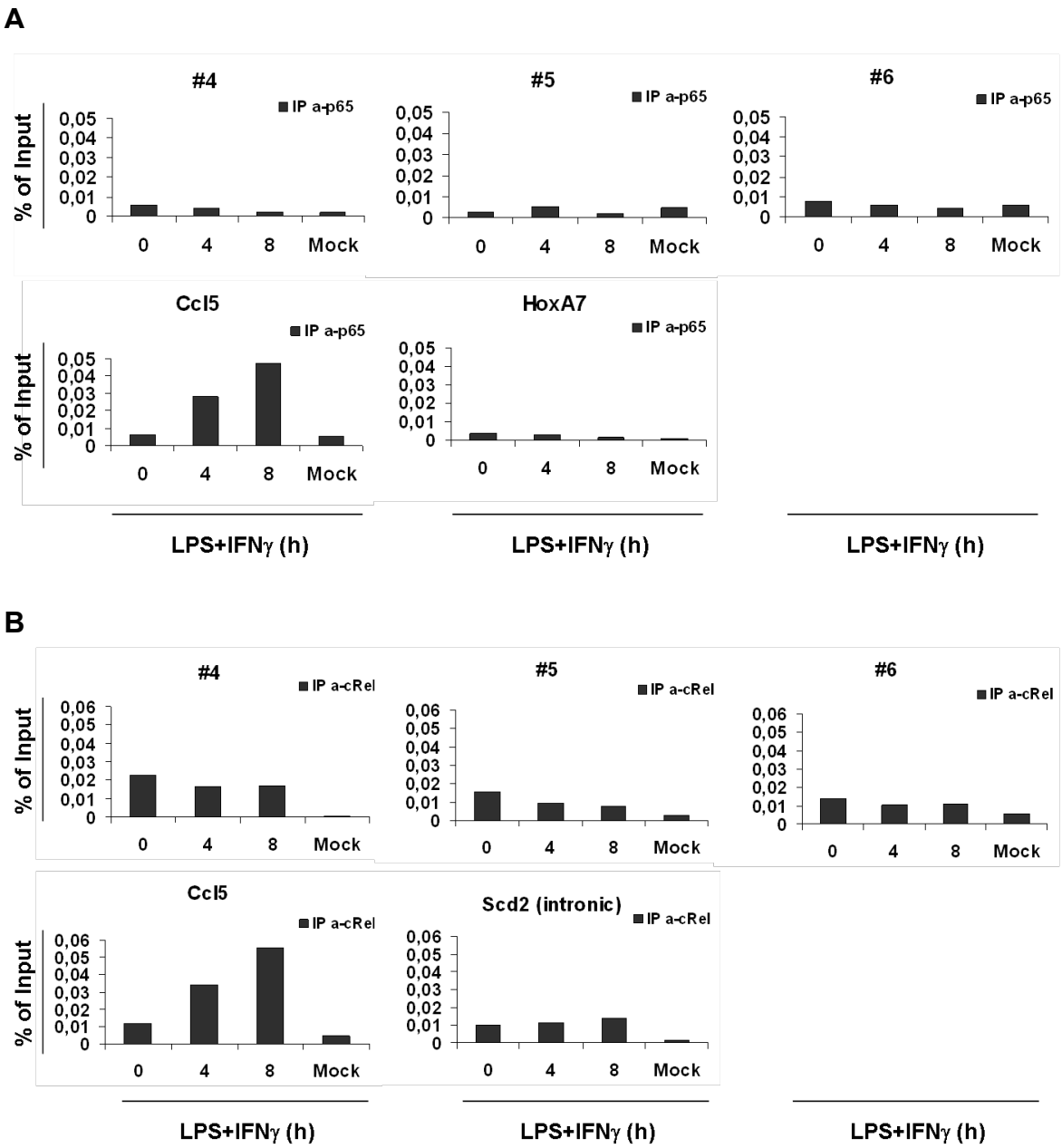

Figure 20 - Neither p65 nor c-Rel bind *Jarid1b* putative NF-κB binding sites.
ChIP analyses of p65 *(A)* and c-Rel *(B)* on primary macrophages revealed that neither p65 nor c-Rel bind to the *Jarid1b* putative NF-κB binding sites identified by ConSite algorithm. *Ccl5* and either *Hoxa7* or an intronic region of *Scd2* were used as positive and negative control genomic regions, respectively. Anti-HA ChIP was used as ChIP negative control (mock).

To exclude the possibility that NF-κB bound to *Jarid1b* on other unidentified genomic sites we functionally characterized the NF-κB activity on *Jarid1b* expression. To determine the requirement for NF-κB in *Jarid1b* induction, we took advantage of a mutant of IkBα (commonly indicated as IkBα-Super Repressor, IkBα-SR), which bears Ser>Ala mutations in the amino-terminal serines, whose phosphorylation normally triggers

stimulus-induced degradation. Since IkBα-SR cannot be degraded, it retains NF-κB into the cytoplasm preventing the induction of NF-κB target genes.

IkBα-SR was delivered to a macrophage cell line (J774) with an adenoviral vector. In conditions in which NF-κB activity was almost completely blocked, confirmed by the severely impaired induction of *Tnf* (a well characterized NF-κB target gene), *Jarid1b* induction was only partially inhibited (Figure 21), suggesting that NF-κB is not the sole transcription factor controlling *Jarid1b* up-regulation but it may contribute indirectly to *Jarid1b* induction.

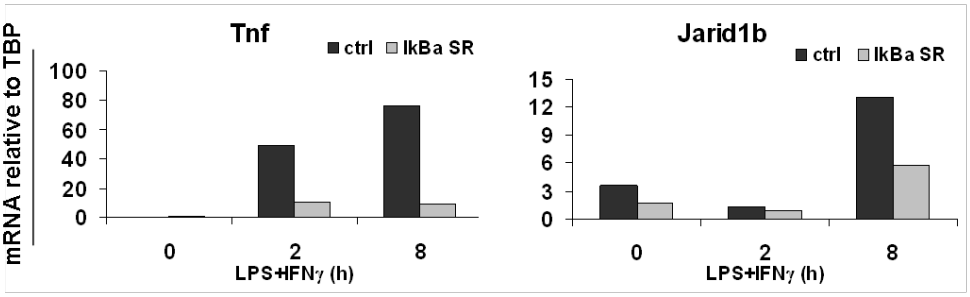

Figure 21 - NF-κB activity blockade partially inhibits LPS-triggered *Jarid1b* up-regulation.
J774 macrophages were infected with an adenoviral vector carrying either the IκBα-SR or GFP (ctrl) and then stimulated with inflammatory stimuli as indicated. The blockage of NF-κB activity, confirmed by the impaired up-regulation of *Tnf*, only partially impaired *Jarid1b* up-regulation. (Samples provided by Dr. Francesca De Santa, PhD).

Recent studies have demonstrated that human *JARID1B* expression is induced in hypoxic conditions under the control of hypoxia-inducible factor 1 (Hif1α) (46) (111); moreover Hif1α is transcriptionally up-regulated in response to inflammatory stimuli by NF-κB (76). These findings prompted us to explore the possibility that *Jarid1b* might be under the control of the same transcription factor in our macrophage cellular system.

Expression analysis revealed that *Jarid1b* is up-regulated in primary macrophages exposed to low oxygen concentration (Figure 22A), and this up-regulation reached almost identical levels to those triggered by LPS stimulation. We extended the expression analysis to the other members of JARID1 family and we found that their expression in hypoxic conditions was the same as in control cells (Figure 22B), as previously observed for the inflammatory stimulation.

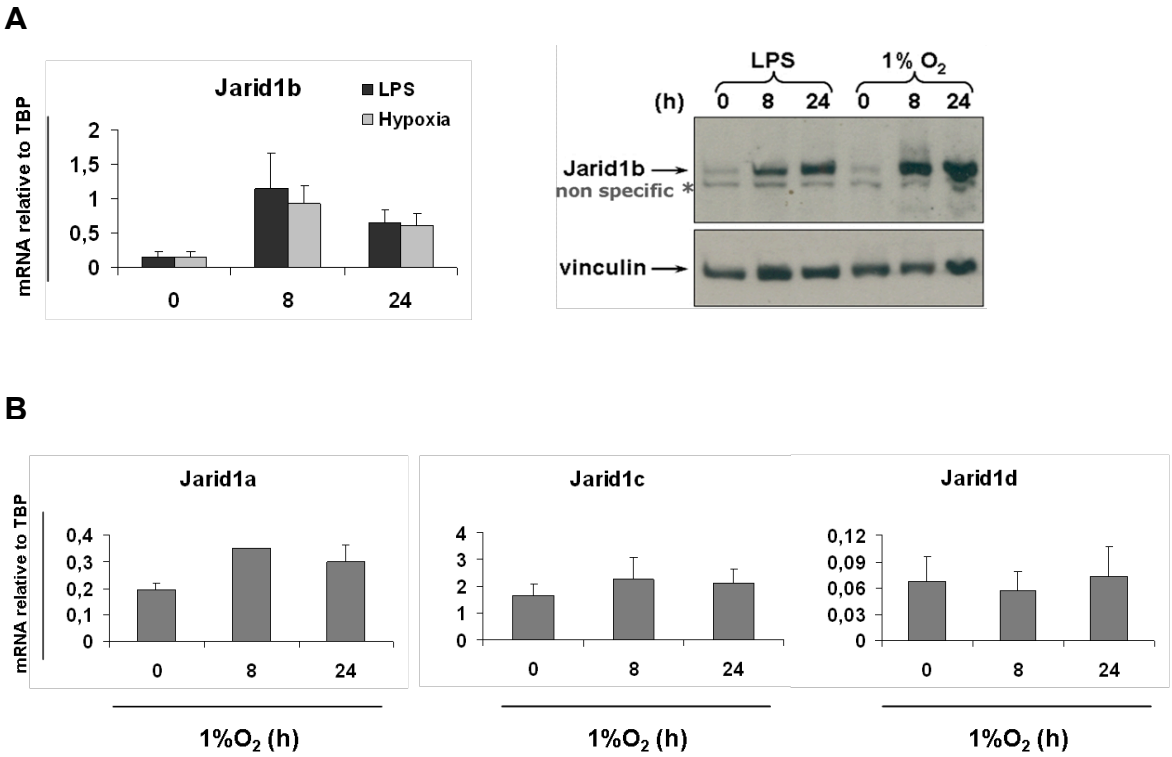

Figure 22 - *Jarid1b* is the only JARID1 family member whose expression is up-regulated in response to hypoxia.
BMDM were subjected to low oxygen concentration (1% O_2) for the indicated time points. *A) Jarid1b* is strongly up-regulated during hypoxia, reaching comparable levels to those triggered by LPS treatment; the up-regulation is documented at mRNA and protein levels. Asterisk (*) in WB represent a non-specific band. *B)* The other JARID1 family members show a flat expression profile under the same hypoxic conditions. Error bars represent standard deviation of 5 *(A)* or 3 *(B)* biological independent replicates.

To determine whether *Jarid1b* LPS-triggered up-regulation is driven by Hif1α, we first searched for Hif1α binding sites on *Jarid1b* promoter. We manually browsed the genomic region spanning from -5 kb to +5 kb of *Jarid1b* TSS and we found three putative Hif1α binding sites (Table 1), basing our search on a recently updated Hif1α binding site consensus sequence (111). Interestingly, binding sites #1 and #2 are clusters of two Hif1α binding sites separated by 50 bp and 3 bp, respectively.

Then to assess the binding of Hif1α to these DNA sequences we performed ChIP analysis. As shown in Figure 23A, Hif1α bound to *Jarid1b* on a region corresponding to the second putative binding site (#2), and this binding was clearly dependent on the inflammatory stimulus. We also verified the binding of two other transcription factors to exclude the possibility that the observed Hif1α binding was a result of a greater accessibility of the

considered chromatin region. Since we could not retrieve any binding of either p65 or c-Rel (Figure 23B) we can conclude that Hif1α binding was specific.

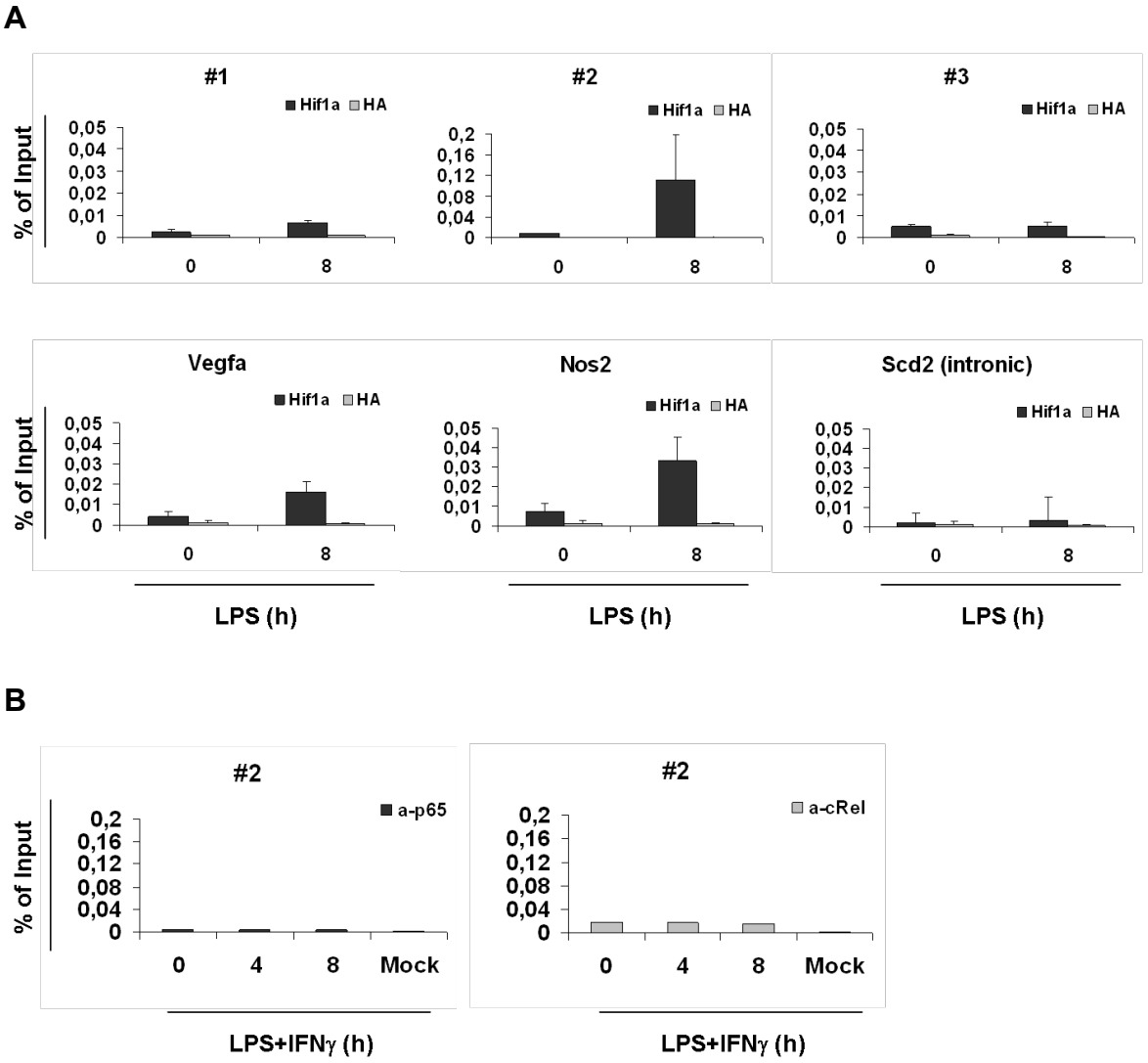

Figure 23 - Hif1α binds *Jarid1b* in a LPS stimulus dependent manner.
A) Hif1α bound to *Jarid1b* promoter only after LPS treatment, on a region comprising the identified Hif1α binding site #2. *Vegfa* and *Nos2* were used as putative positive controls, as they are Hif1α target genes in cells subjected to hypoxic conditions; an intronic region of *Scd2* was used as a negative control. Anti-HA ChIP was used as a mock. Error bars represent standard deviation of two biological independent replicates. *B)* Neither p65 nor c-Rel bound to the region #2, excluding the possibility that Hif1α binding was due to a greater accessibility of that region.

These data together demonstrate that Jarid1b is strongly up-regulated in primary macrophages in response to inflammatory stimulation (LPS), most likely under the control of the transcription factor Hif1α. Interestingly, Jarid1b is the only JARID1 family member whose expression is modulated in response to both inflammatory and hypoxic stimuli,

suggesting that it might have acquired a functional specialization during evolution to cope with such environmental stresses.

3. Jarid1b depletion impairs LXR target genes expression

In order to identify those genes whose expression is modulated by Jarid1b, we generated retroviral vectors expressing short hairpin RNAs (shRNAs) specifically targeting *Jarid1b*. We tested six different shRNAs and we chose the two most efficient ones (shRNA2 and shRNA3, renamed KD1 and KD2 afterwards) in reducing Jarid1b levels both at mRNA and protein levels (Figure 24) to perform a cDNA microarray analysis in which global gene expression of wild type macrophages, stimulated with LPS and IFNγ for 8 and 12 hours, was compared to that of Jarid1b-depleted macrophages. We used two distinct shRNAs to filter possible off-target effects.

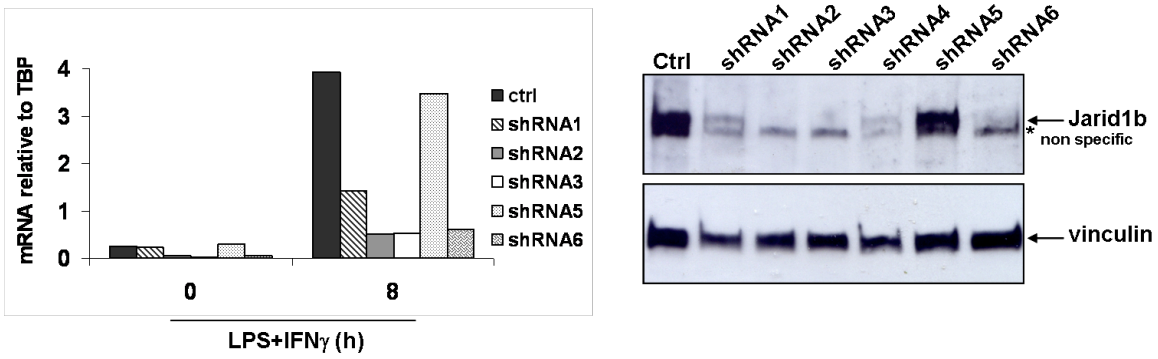

Figure 24 - Jarid1b depletion in bone marrow-derived macrophages.
BMDM were infected with a retroviral vector carrying the different shRNAs. The control (ctrl) was represented by the retroviral empty vector (LMP). Jarid1b mRNA (left) and protein (right) levels in infected macrophages were compared; the two most efficient shRNAs (shRNA2 and shRNA3) were chosen to perform further experiments and then indicated as KD1 and KD2. Jarid1b was depleted by 85-90% at mRNA level and no protein signal could be detected by western blot analysis. Asterisk (*) indicates a non-specific band.

Microarray data showed a very limited number of genes whose transcription was affected more than two-fold by Jarid1b depletion. Moreover, the genes whose expression was most consistently down-regulated in response to Jarid1b depletion are all well-defined targets of the nuclear receptor Liver X Receptor (LXR): *Abca1* and *Abcg1*, two ABC transporters that export cholesterol to lipid-poor ApoA-I and to HDL; *ApoE* and *Pltp* involved in the

constitution and remodelling of lipoproteins; the transcription factor *Srebp1c* and its target genes *Scd1* and *Scd2* that control the mono-unsaturated fatty acids synthesis pathway (Figure 25A).

We validated the microarray data by QPCR analysis and we observed that the transcription of LXR target genes was impaired also in unstimulated Jarid1b-depleted macrophages, meaning that the effect of Jarid1b depletion was independent of the inflammatory stimulus and the consequent protein up-regulation (Figure 25B).

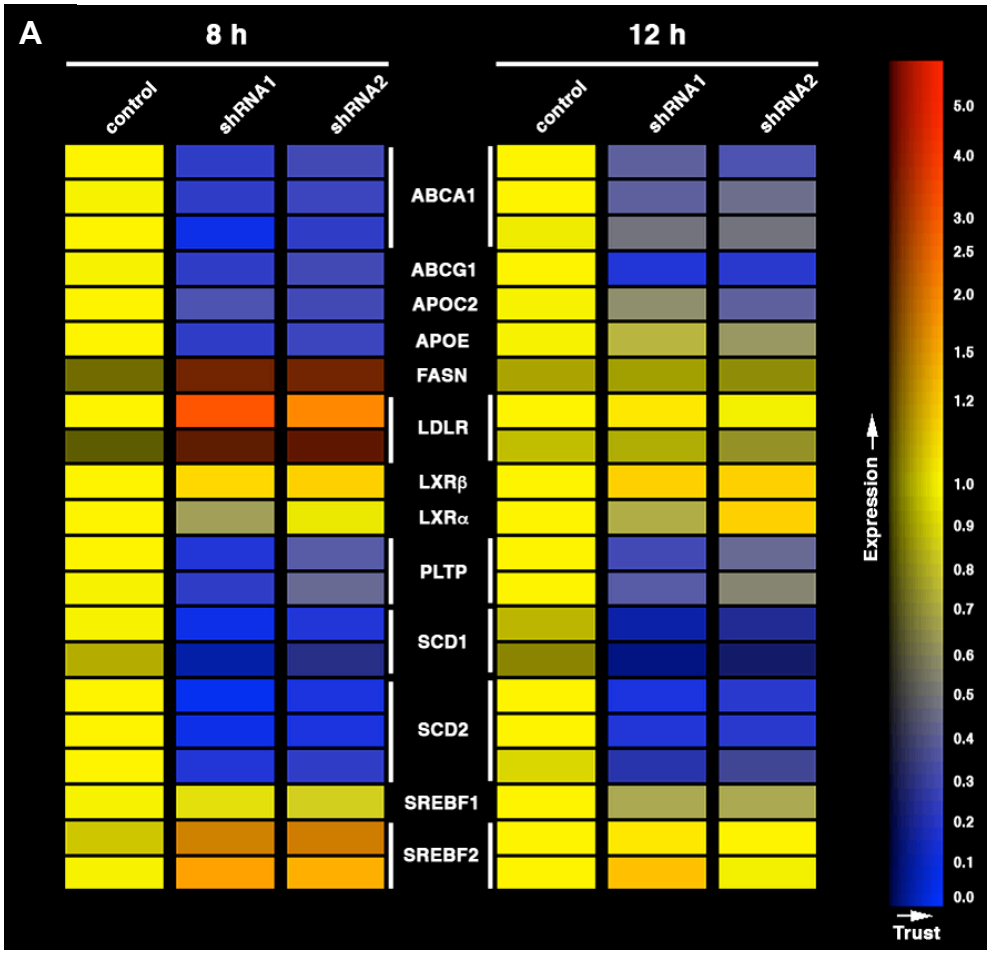

B

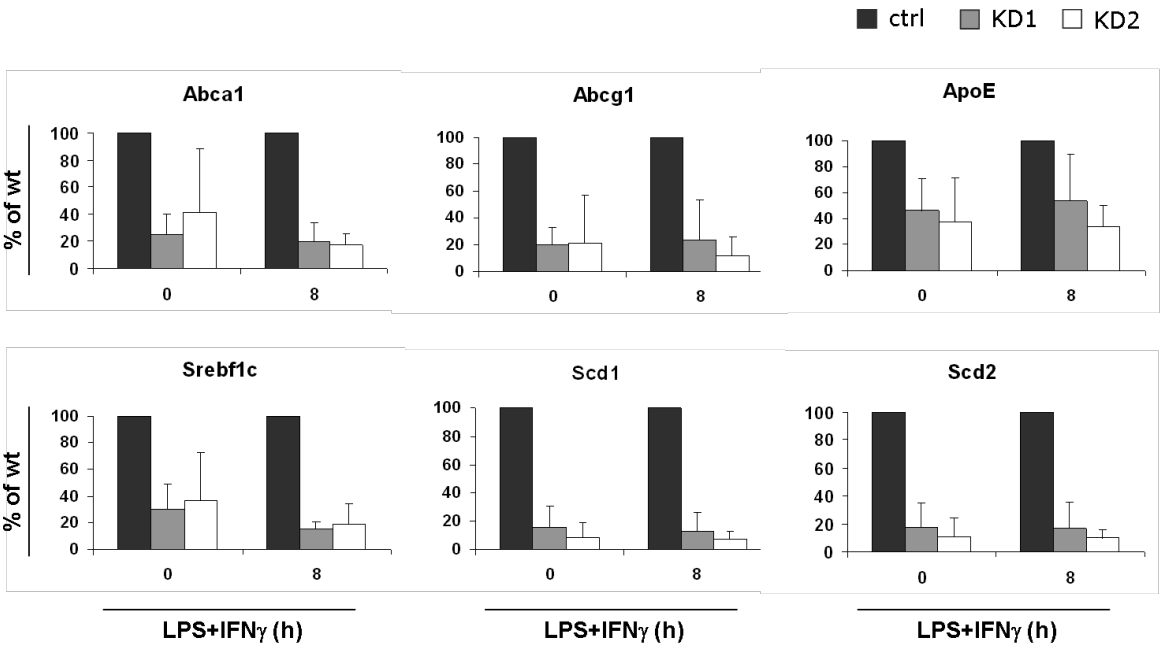

Figure 25 - Jari1b-depletion impairs LXR target genes expression.
A) Schematic representation of microarray data: listed are those genes showing a significant change (≥ two-fold) in the expression levels between wild type and Jarid1b-depleted macrophages (with both shRNAs). All the down-regulated genes are LXR targets. *B)* Validation of microarray data by QPCR analysis. Gene expression is represented as percentage of wild type levels. Error bars represent the 95% confidence interval of 3 (KD1) or 2 (KD2) independent experiments.

Interestingly, while the expression level of LXR targets genes was strongly reduced, LXRα and LXRβ mRNAs and proteins were not affected (Figure 26). Additionally, we observed that LXR target genes expression was strongly induced during macrophages terminal differentiation, and this up-regulation was heavily impaired in Jarid1b-depleted macrophages (Figure 27A). Such up-regulation was attributable to an enhanced LXR activity, since *LXRα* and *LXRβ* expression levels were unchanged (Figure 27B). LXR target genes impaired induction was not due to a delay in Jarid1b-depleted macrophages differentiation, as demonstrated by the expression analysis of three typical macrophage differentiation markers (Figure 27C).

Together these data suggest that Jarid1b might regulate LXR activity.

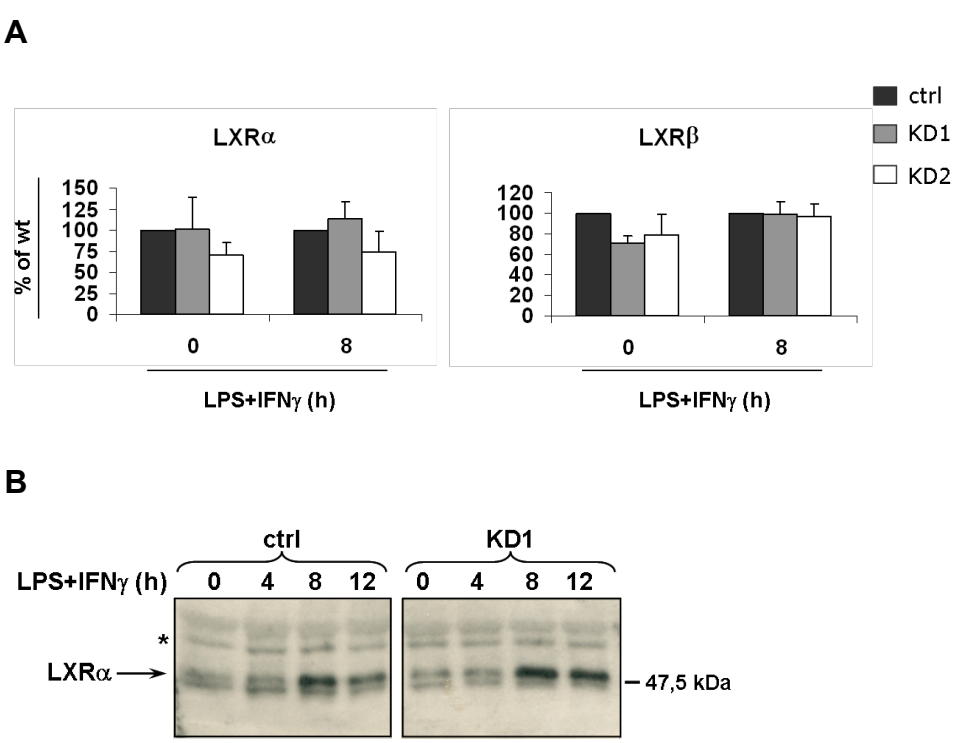

Figure 26 - Jarid1b depletion does not affect LXRs expression levels.
QPCR *(A)* and western blot *(B)* analyses show that *LXRα* and *LXRβ* expression levels were not impaired by Jarid1b depletion. Gene expression in *(A)* is represented as percentage of wild type levels; error bars represent the 95% confidence interval of 3 (KD1) or 2 (KD2) independent experiments. Asterisk (*) in *(B)* indicates a non-specific band.

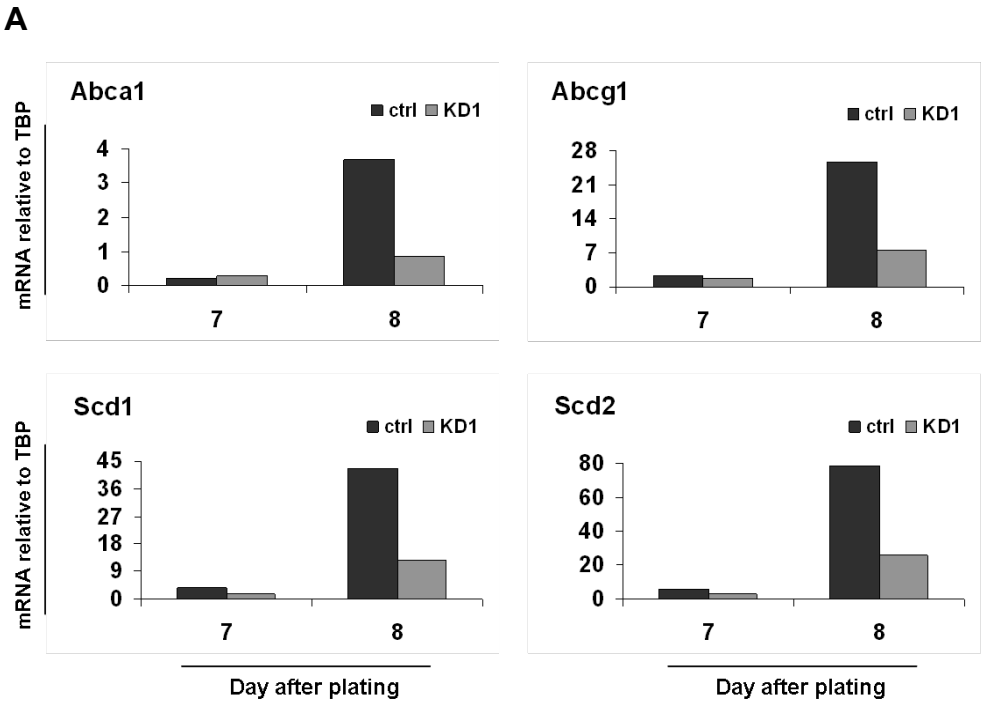

B

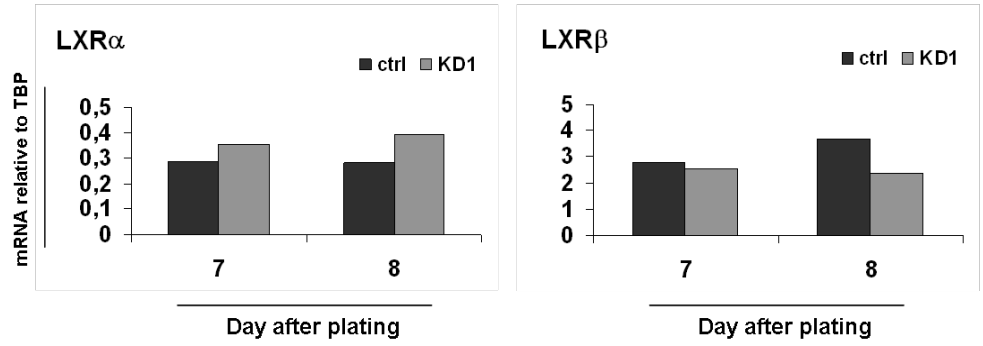

C

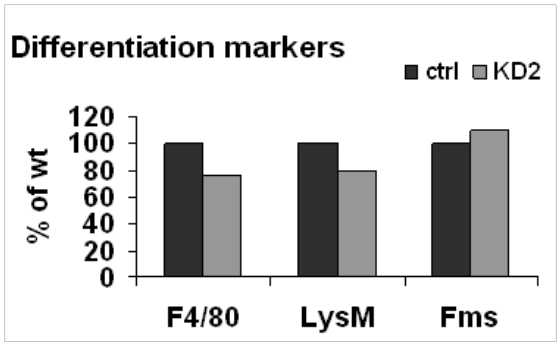

Figure 27 - Jarid1b depletion impairs LXR target genes induction during macrophages terminal differentiation.
A) QPCR analysis shows LXR target genes induction during macrophages terminal differentiation; this up-regulation was impaired by Jarid1b depletion. *B) LXRα* and *LXRβ* expression levels were unchanged during terminal differentiation, indicating that the induction of target genes was due to an enhanced activity. *C)* Expression analysis of macrophage differentiation markers demonstrated that Jarid1b-depleted macrophages differentiated normally, indicating that LXR target genes altered induction was not attributable to a delayed or impaired differentiation.

4. Jarid1b depletion impairs LXR activation

To further investigate a relationship between Jarid1b and LXR we explored three possible experimentally-testable scenarios: 1) the low LXR activity may be due to reduced intracellular cholesterol basal levels resulting in a response aiming at minimizing the cholesterol efflux; 2) Jarid1b may directly co-activate LXR; 3) Jarid1b depletion may reduce ligand (oxysterols) availability or production, thus resulting in low LXR activity.

To determine whether the impaired LXR target genes activation in Jarid1b-depleted macrophages was a cellular reaction to low cholesterol levels aimed at reducing the cholesterol efflux, we analyzed, in non stimulated macrophages, the expression profile of

some genes involved in the synthesis or the uptake of cholesterol, such as *Hmgcr*, the rate limiting enzyme of the cholesterol synthesis pathway, the receptor *Lldr*, that drives the uptake of low density lipoproteins, and *Srebf1* and *Srebf2*, the transcriptional regulators of these pathways (Figure 28A). We did not find any significant difference between wild type and Jarid1b-depleted macrophages (Figure 28B), indirectly suggesting that there was no difference in the basal cholesterol content of the two populations and excluding the first hypothesis.

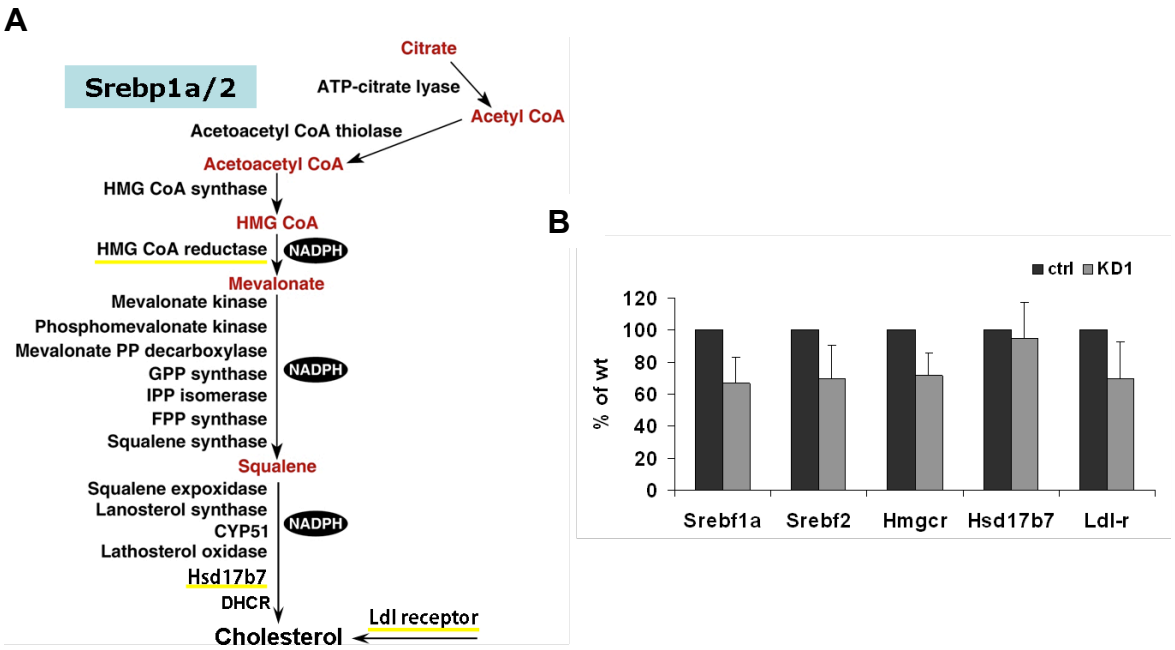

Figure 28 - Cholesterol-uptake and cholesterol-biosynthesis genes are not induced upon Jarid1b depletion.
A) Schematic representation of the intracellular cholesterol synthesis pathway, under the control of Srebp1a and Srebp2 transcription factors; adapted from (36). *B)* RT-QPCR analysis shows that there was not any significant change in cholesterol biosynthesis genes expression levels between wild type and Jarid1b-depleted macrophages. Gene expression is represented as percentage of wild type levels. Error bars represent the 95% confidence interval of three independent experiments.

Then we tested the ability of oxysterols to restore LXR target genes expression in Jarid1b-knock-down macrophages, in order to understand if LXR activity was compromised by the depletion of Jarid1b. The oxysterols, oxidized metabolites of cholesterol, are the natural ligand of LXR. Their binding to the LXR binding pocket causes a conformational change that facilitates the co-activator/co-repressor exchange, resulting in the transcription of target genes (117). Treating Jarid1b-depleted cells with either two different physiological

ligands (24,25-epoxycholesterol and 22(R)-hydroxycholesterol) or a chemical agonist (TO901317), we obtained a complete reconstitution of LXR target genes expression to the wild type levels (Figure 29A) without affecting *LXRα* and *LXRβ* transcriptional levels (Figure 29B), indicating that LXRs are fully functional even in the absence of Jarid1b.

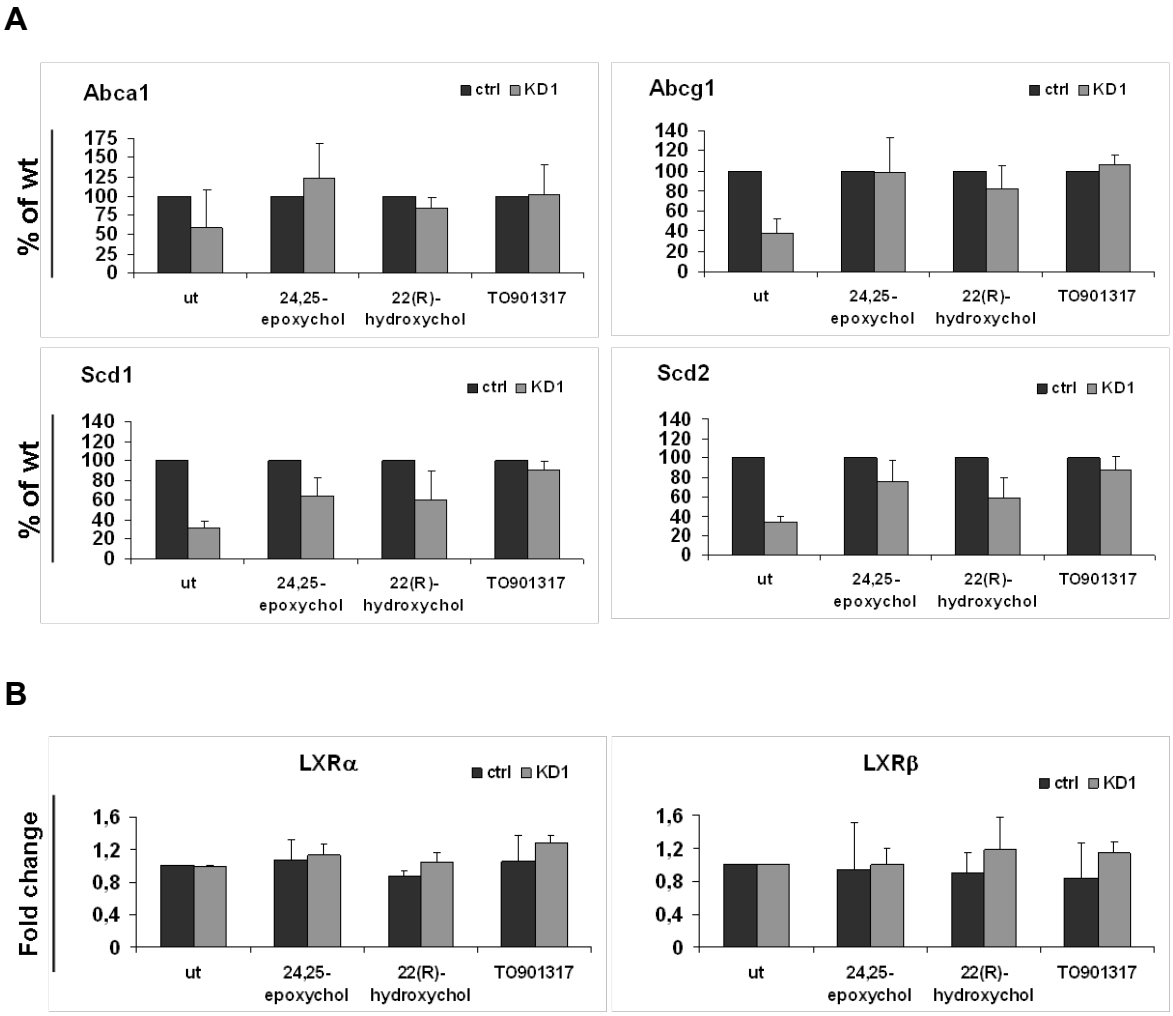

Figure 29 - LXR agonists treatment rescues LXR target genes expression in Jarid1b depleted macrophages.
A) Primary macrophages were treated with the LXR ligands 24,25-epoxycholesterol (1μM) and 22(R)-hydroxycholesterol (5μM) or the chemical agonist TO901317 (0,5μM) for 24 hours. These treatments rescued the wild type expression levels of all the genes tested. Error bars represent the 95% confidence interval of three independent experiments. *B)* LXR agonists treatment did not alter *LXRα* and *LXRβ* expression neither in wild-type nor in Jarid1b-depleted macrophages. Error bars represent the 95% confidence interval of two independent experiments.

In order to define whether Jarid1b was a direct co-activator of LXR, we sought the presence of physical interactions between Jarid1b and LXRα. When LXRα, its heterodimer partner RXRα, and Jarid1b were exogenously co-expressed in 293T cells they co-immunoprecopitated (

Figure 30A); however we could not detect any direct interaction between the endogenous proteins in macrophages (

Figure 30B), raising the doubt that the previously observed co-IP was an artefact due to the overabundant amount of expressed proteins.

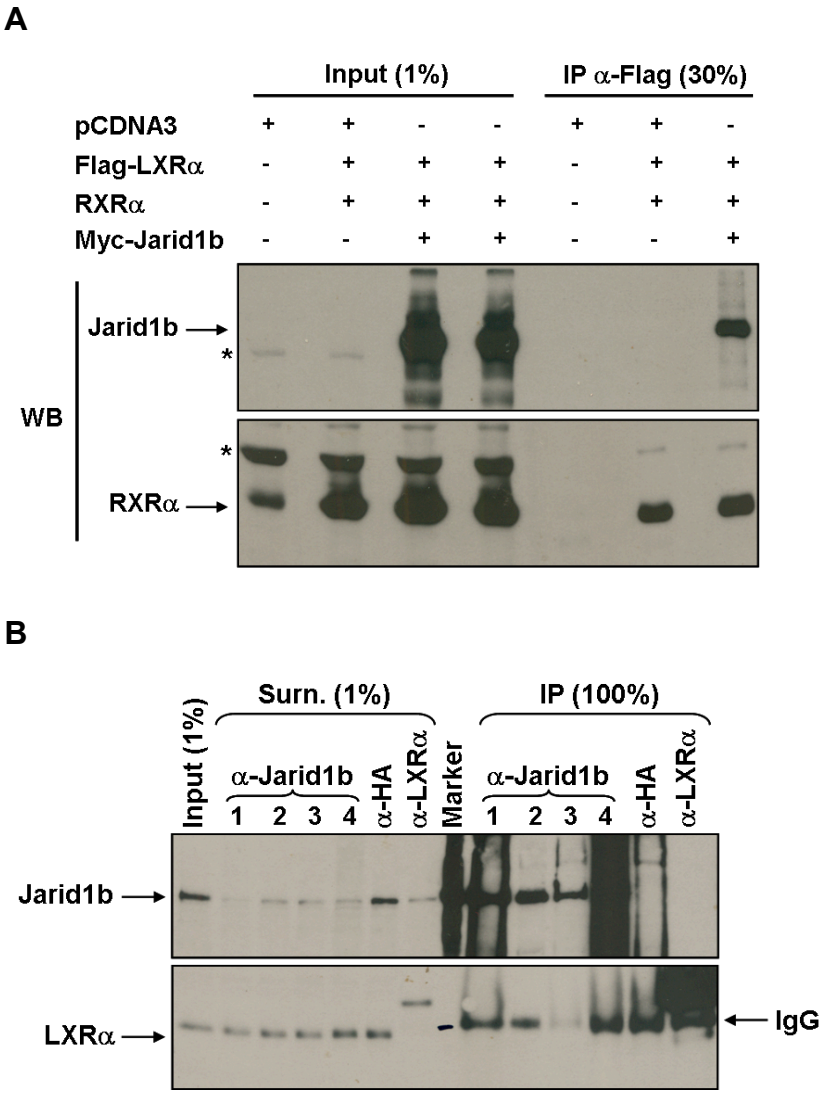

Figure 30 - Endogenous Jarid1b and LXRα do not interact directly.
A) 293T cells were transfected with expression vectors carrying Flag-LXRα, RXRα and myc-Jarid1b. As expected, RXRα is efficiently co-immunoprecipitated with LXRα; also Jarid1b co-immunoprecipitated with LXRα, when over-expressed. Negative control is represented by 293T cells transfected with empty vector. Asterisks (*) indicate non-specific bands. *B)* IP anti-Jarid1b in primary macrophages did not retrieve any LXRα signal; also the reciprocal IP anti-LXRα was not able to co-immunoprecipitate any detectable Jarid1b. Numbers (1, 2, 3, and 4) indicate different anti-Jarid1b IP protocols: 1 is IP with non-crosslinked Ab, 2 and 3 are IPs with crosslinked Ab + or - β-mercaptoethanol addition, and 4 is IP with a non-purified anti-Jarid1b serum (Abcam).

We further functionally characterized the possible LXRα transcriptional co-activating role of Jarid1b through a luciferase reporter assay. We first generated a LXRα responsive

luciferase reporter introducing a fragment of the human *ABCA1* promoter (from -919 to +239), containing the LXR-responsive element (LXRE), into a pGL vector (hABCA1-Luc). Luciferase was efficiently transcribed when this construct was delivered to 293T cells together with LXRα, alone or in combination with RXRα. However co-transfection of increasing amount of Jarid1b did not result in any evident transcriptional co-regulatory effect (Figure 31A).

On the contrary, Jarid1b acted as a transcriptional repressor in a different well-established luciferase reporter system, such as the MEKK1/AP-1 reporter, where the delivery of MEKK1 led to a strong activation of the luciferase gene under the control of an AP-1-responsive promoter, and the co-expression of Jarid1b caused a decrease of transcriptional activity proportional to the amount of expressed Jarid1b (Figure 31B), coherently to what published in literature (99).

Together these data suggest that Jarid1b is not a direct co-activator of LXR (scenario 2).

A

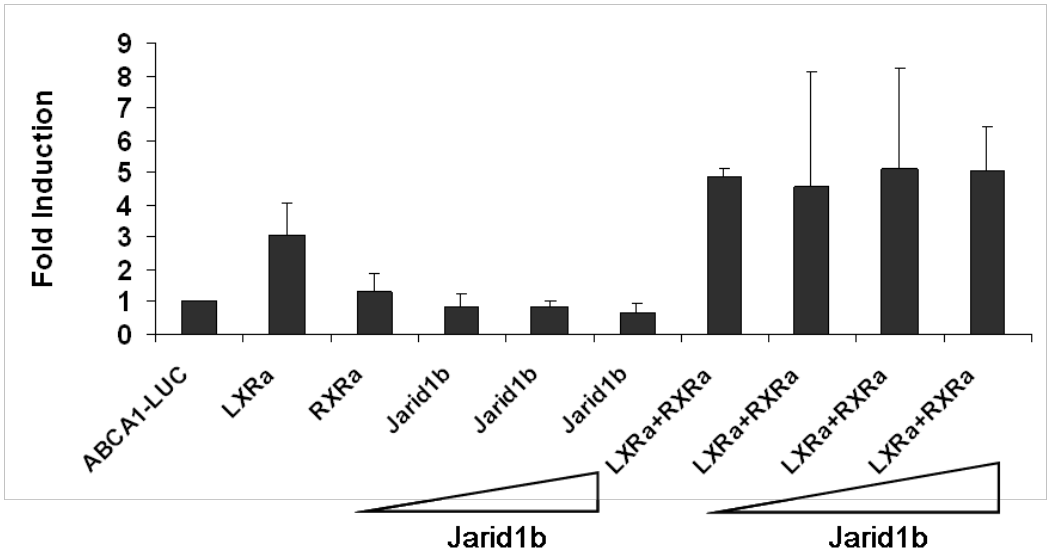

B

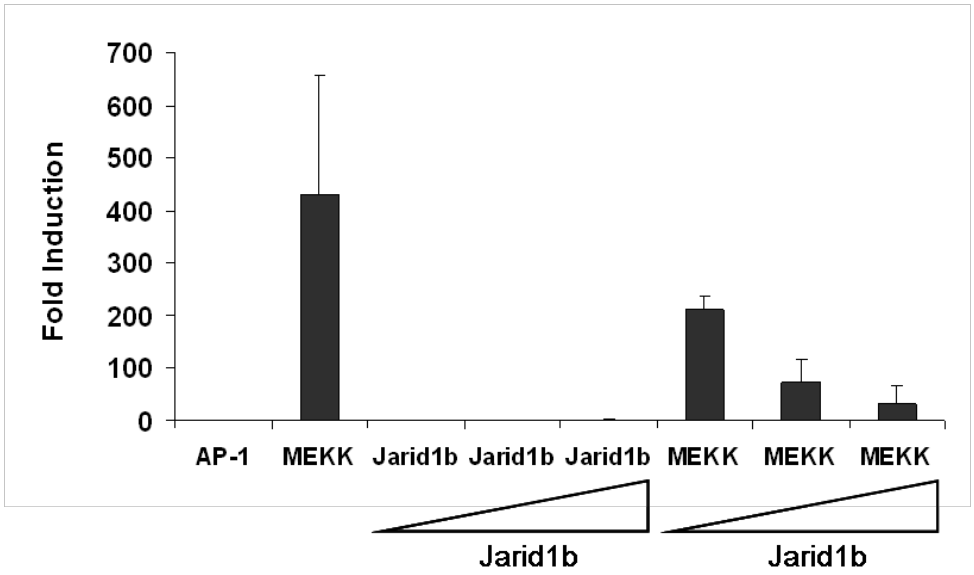

Figure 31 - Jarid1b is not a transcriptional co-activator of LXRα.
A) 293T cells were transfected with a luciferase reporter costruct under the control of the ABCA1 promoter, containing the LXR-responsive element (LXRE). The exogenous expression of LXRα induced the luciferase transcription and the effect was enforced by the co-expression of RXRα; the addition of increasing amount of Jarid1b did not result in any evident effect (either activation or repression) on LXRα/RXRα transcriptional activity. *B)* The functionality of the exogenously expressed Jarid1b was verified in a different well-established luciferase system, where an AP-1 luciferase reporter construct was co-transfected together with the activating MEKK1 kinase; in this system the co-expression of Jarid1b resulted in a reduced transcriptional activity, proportional to the amount of Jarid1b. Transfection efficiency and homogeneity were verified by western blot analyses of all the delivered proteins in each sample (data not shown).

So we hypothesized that Jarid1b could control the oxysterols pool of macrophages. Two are the main physiological LXR ligands in macrophages reported in literature: the 24,25-epoxycholesterol, a side product of the intracellular cholesterol synthesis pathway (81), and the 27-hydroxycholesterol, derived from the oxidation of the exogenous cholesterol (26). To understand which metabolite played a major role in our cellular system, we blocked the two ligands synthesis pathways and then tested the outcome on LXR activity by measuring the transcriptional effect on LXR target genes, in the absence of any alteration in LXRs expression levels. To block the two oxysterols synthesis pathways we took advantage of different inhibitors: the pravastatin, belonging to the family of statins, inhibits the Hmg-CoA reductase, the rate-limiting enzyme of cholesterol synthesis, competing with its substrate; Ro-48-8071, is a selective inhibitor of the 2,3-oxydosqualene:lanosterol cyclase (OSC), the enzyme that catalyze the cyclization of

monooxidosqualene to lanosterol in the cholesterol synthetic pathway; and cyclosporin A (CsA), an immunosuppressant drug, that inhibits the calcineurin-mediated signalling as well as the mitochondrial transition pore formation and that has been reported to inhibit the transcription of *Cyp27a1*, the enzyme catalyzing the 27-hydroxycholesterol synthesis (Figure 32A). We found that only the (partial) transcriptional inhibition of *Cyp27a1*, triggered by cyclosporin A, resulted in the impairment of LXR target genes expression (Figure 32B), suggesting that 27-hydroxycholesterol is the main LXR ligand active in the macrophage system we used.

A

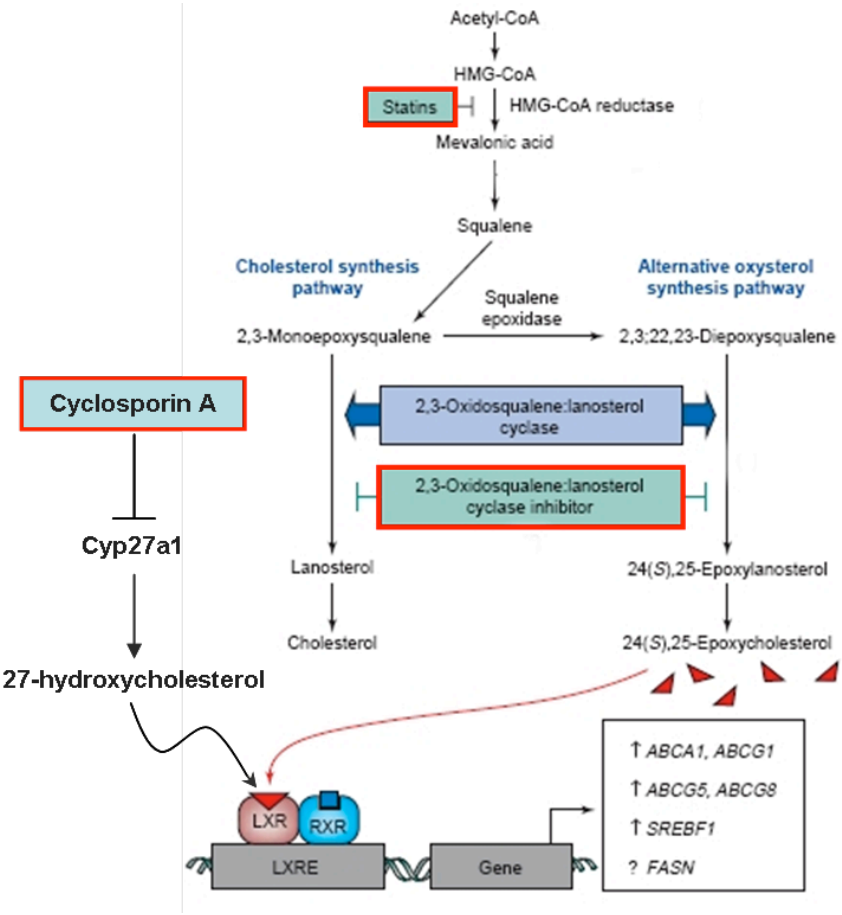

B

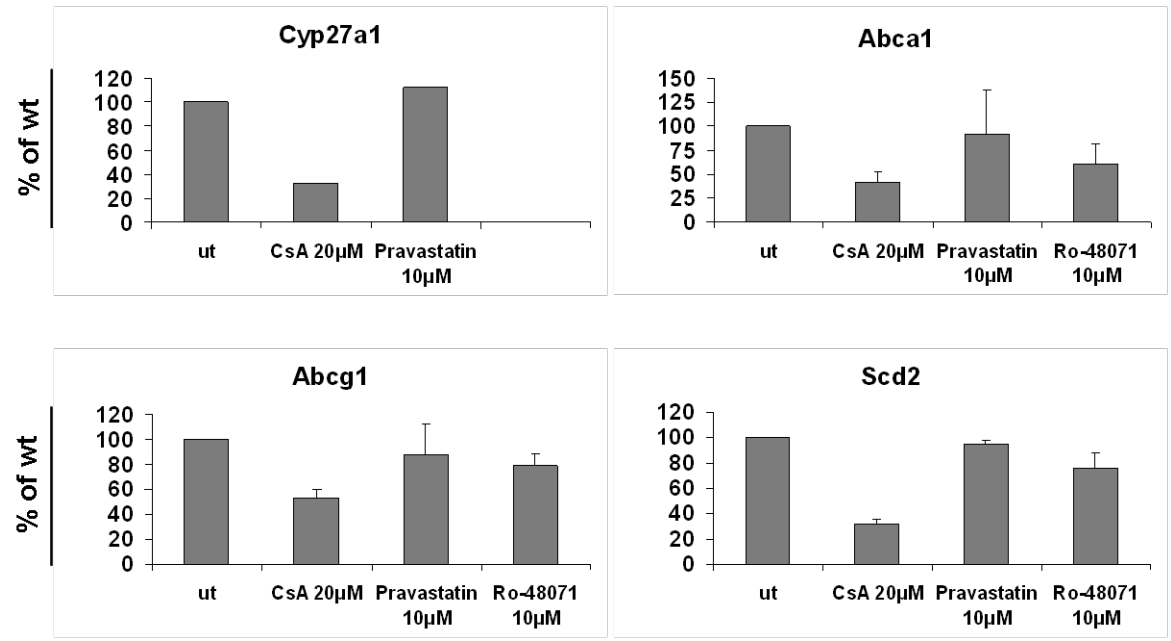

Figure 32 - Cyp27a1 is required for basal LXR activity in macrophages.
A) Schematic representation of endogenous and exogenous oxysterols synthesis pathways. In red are highlighted available inhibitors known to block the indicated pathways; adapted from (40). *B)* Primary macrophages were treated with cyclosporin A (20μM) and pravastatin (10μM) for 8 hours or with Ro-48-8071 (10μM) for 24 hours. Cyclosporin A (CsA) is a reported inhibitor of *Cyp27a1* expression, while pravastatin and Ro-48-8071 block the intracellular cholesterol biosynthesis, inhibiting the HMG-CoA reductase and the 2,3-oxydosqualene:lanosterol cyclase, respectively. Only the cyclosporin A treatment caused a significant reduction in the LXR target genes expression as shown by RT-QPCR analysis. Error bars, where present, represent the 95% confidence interval of two independent experiments.

Thus, we compared in wild-type and Jarid1b depleted cells the expression profile of the enzymes catalyzing the 27-hydroxycholesterol synthesis and degradation, Cyp27a1 and Sult2b1 respectively. While *Sult2b1* expression levels were not affected in Jarid1b knock-down macrophages, we found a two-fold reduction of *Cyp27a1* both at mRNA (Figure 33A) and protein (Figure 33B) levels, suggesting that Jarid1b regulates the 27-hydroxycholesterol synthesis pathway (scenario 3).

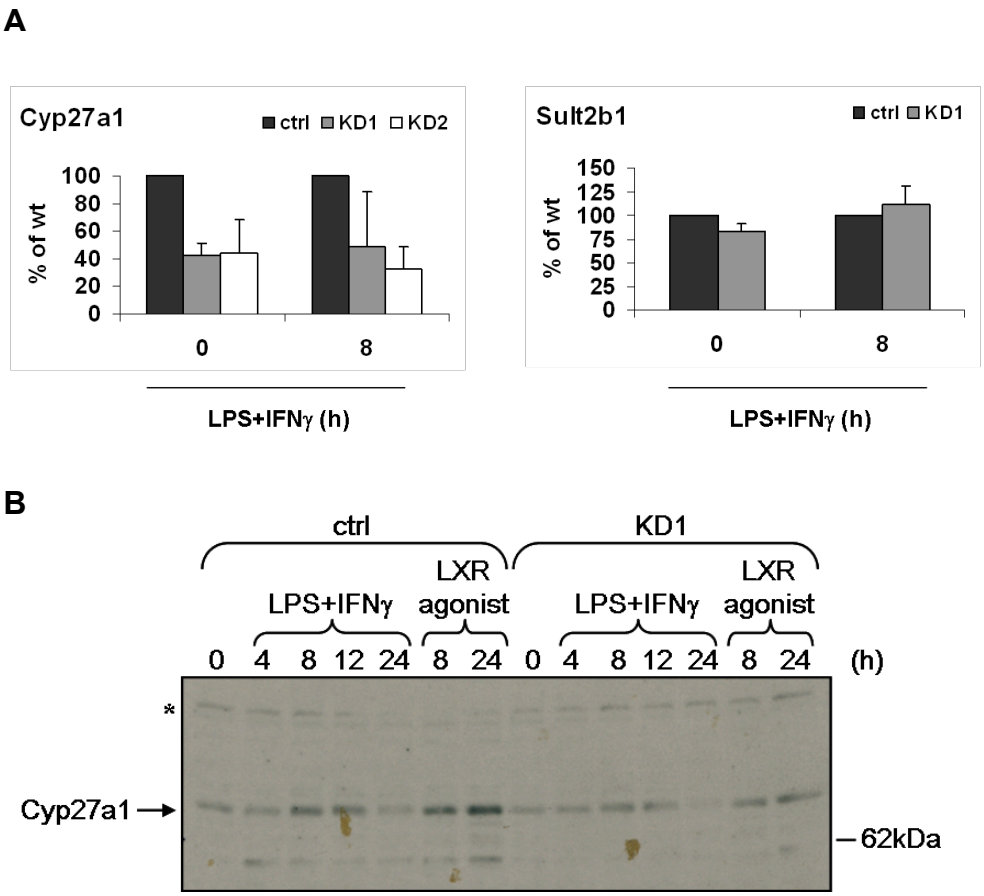

Figure 33 - Jarid1b depletion reduces the expression of Cyp27a1.
A) Expression profile (RT-QPCR) of the two enzymes that catalyze the production (*Cyp27a1*) and the degradation (*Sult2b1*) of 27-hydroxycholesterol in macrophages. Only *Cyp27a1* expression was impaired in Jarid1b-depleted cells. *B)* Western blot analysis on mitochondrial enriched protein extract confirmed a reduced Cyp27a1 expression in Jarid1b-depleted macrophages; LXR agonist is 24,25-epoxycholesterol. Asterisk (*) represents a non-specific band.

These data suggest that the mechanism linking Jarid1b depletion to LXR deficiency is likely represented by a reduced oxysterols content in Jarid1b-depleted cells, resulting in a decreased LXR activation.

5. Generation of Jarid1b knock-out mice[1]

To better understand the physiological role of Jarid1b we generated Jarid1b knock-out mice.

Mouse embryonic stem (ES) cell lines carrying a gene trap vector for *Jarid1b* gene were purchased. We chose two different ES cell lines (129P2/OlaHsd mouse strain), named

[1] This paragraph is mostly based on a collaboration with Dr. Liv Austenaa, PhD, who is the main responsible of this project.

RRO123 and RRR598, bearing the trap construct within *Jarid1b* second intron (Figure 34), allowing us to obtain two distinct Jarid1b-KO mouse strains. Once confirmed the gene trap insertion by PCR and X-Gal staining (Figure 35), the two ES cell lines were injected in C57BL/6 blastocysts to generate chimeras. Germ-line transmission was obtained and heterozygous offspring was mated to generate Jarid1b-KO mice.

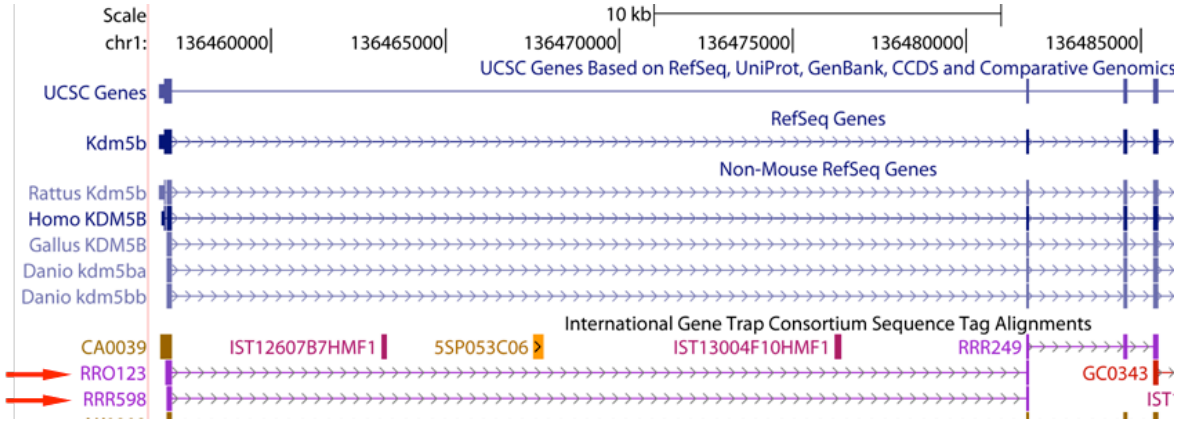

Figure 34 – *Jarid1b* "gene trapping" .
Genomic position of the two selected *Jarid1b* gene trap vectors, RRO123 and RRR598.

Must to say that this procedure led us to obtain (and use for the subsequent experiments) Jarid1b-KO mice in a C57BL/6-129P2 mixed genetic background.

ES cell lines were also injected in 129P2 blastocysts to obtain 129P2 pure Jarid1b-KO mice, but the very low breeding efficiency (typical of this strain) did not allow us to use these mice for experimental purposes.

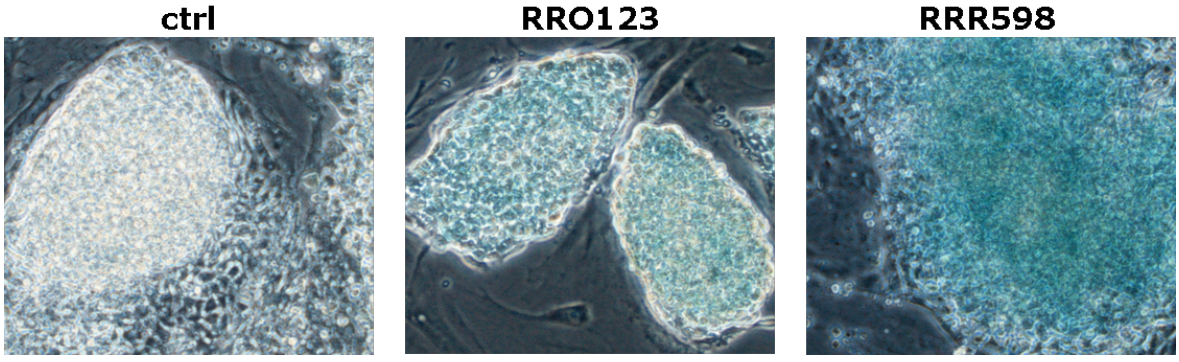

Figure 35 - *Jarid1b* gene trapping in ES cells.
X-Gal staining demonstrated the expression of the truncated fusion protein, indicating the successful insertion of the gene trap vector into *Jarid1b* gene. Cells electroporated with the Jarid1b knock-in construct, which does not bear the β-geo reporter cassette, were used as a negative control (ctrl).

Both Jarid1b-KO mouse strains are fully viable; nevertheless we observed that female KO mice are under-represented at weaning, and both male and female KO mice accumulated a small (~20-25%) but reproducible weight gap before weaning and maintained it afterwards (Figure 36). The underlying biological mechanism needs to be elucidated.

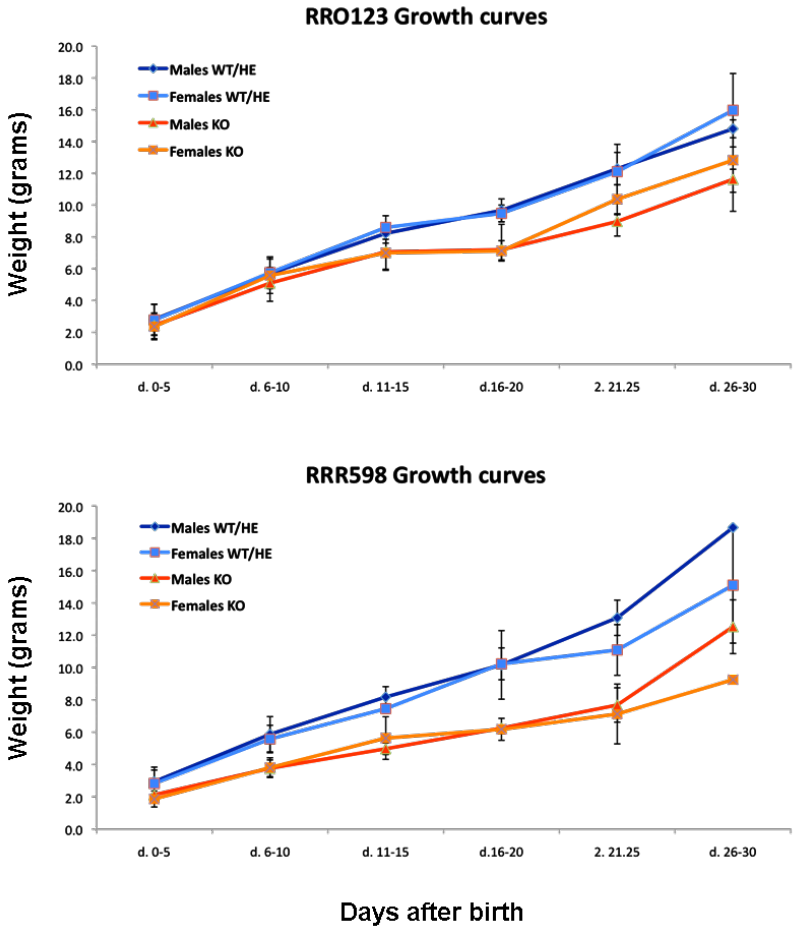

Figure 36 - Jarid1b-KO mice are smaller than their wild-type/heterozygous littermates.
Growth curves of both RRO123 and RRR598 knock-out mice highlithed that Jarid1b-ablated mice accumulate a weight gap compared to their wild-type/heterozygous siblings. Error bars represent standard deviation of either ≥ 25 mice (RRO123) or ≥ 9 mice (RRR598).

We also observed a slightly reduced number of bone marrow cells in KO mice (77,38% ± 13,1% respect to heterozygous mice) (Figure 37A). This observation prompted us to explore the possibility that the absence of Jarid1b might affect one of the bone marrow cellular sub-populations. Flow cytometry analyses (in collaboration with Dr. Isabella Pallavicini and Prof. Saverio Minucci, IFOM-IEO-Campus) revealed only a little increment in the number of more differentiated cells ($CD3^+$, $B220^+$ and $Ter\text{-}119^+$) in Jarid1b-ablated bone marrow, with a minimal non-significant decrease in the number of

long- and short-term hematopoietic stem cells (HSC) (Figure 37B). Although these data needs to be confirmed, they might be somehow linked to a possible role for Jarid1b in cellular proliferation, repeatedly hypothesized in literature, sometimes with opposite scenarios.

A

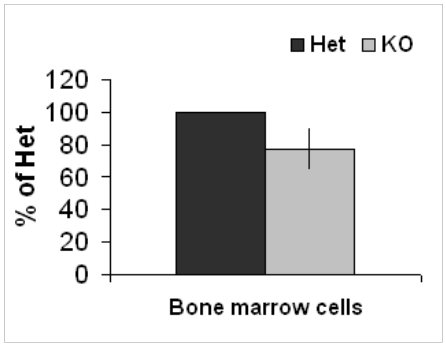

B

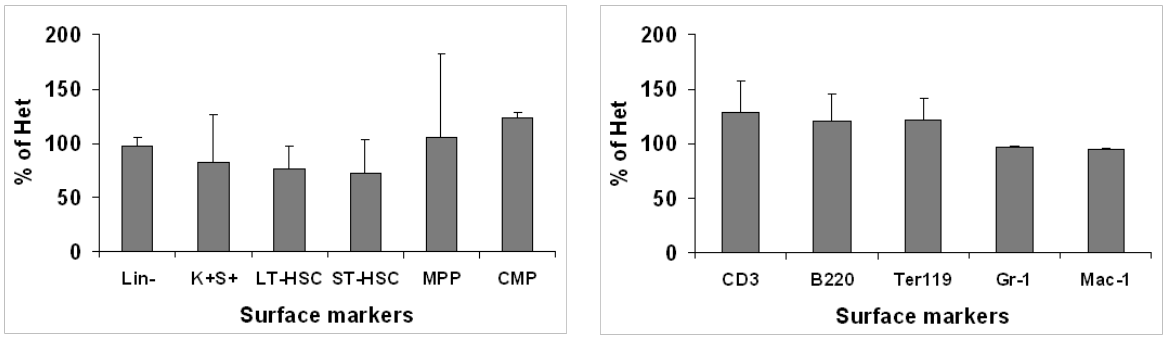

Figure 37 - Jarid1b-KO mice exhibit a little reduction in bone marrow cells number.
A) Cell count of bone marrow-extracted cells revealed a little reduction in the number of Jarid1b-ablated cell population. Cell number was normalized to mice body weight; represented is the average of 7 mice and error bar is standard deviation. *B)* Histograms summarize flow cytometry analyses of different bone marrow sub-populations. Represented is the relative cell number expressed as % of Het [(KO/Het)x100]. (Left panel) Total and fractionated lineage negative cells: hematopoietic stem cells (K+S+), long-term-HSC (LT), short-term-HSC (ST), multipotent progenitor cells (MPP) and common myeloid progenitor cells (CMP). (Right panel) Lineage positive cells: T-cells ($CD3^+$), B-cells ($B220^+$), erythroid cells ($Ter\text{-}119^+$) and myeloid cells ($Gr\text{-}1^+$ and $Mac\text{-}1^+$). Error bars represent standard deviation of 2 (Lin^-) or 3 (Lin^+) independent replicates.

6. Characterization of Jarid1b knock-out macrophages transcriptome

Once obtained Jarid1b knock-out mice, we first verified that Jarid1b-KO BMDM normally differentiated *in vitro* and did not show any evident morphologic abnormality if compared to their wild-type/heterozygous counterpart, also when challenged with inflammatory stimulation (Figure 38A). Indeed, expression analysis of macrophage differentiation

markers, such as lysozime M (*LysM*), colony stimulating factor 1 receptor (*Csf1r*) and the cell surface glycoprotein *F4/80*, did not reveal any significant difference between heterozygous and KO macrophages (Figure 38B).

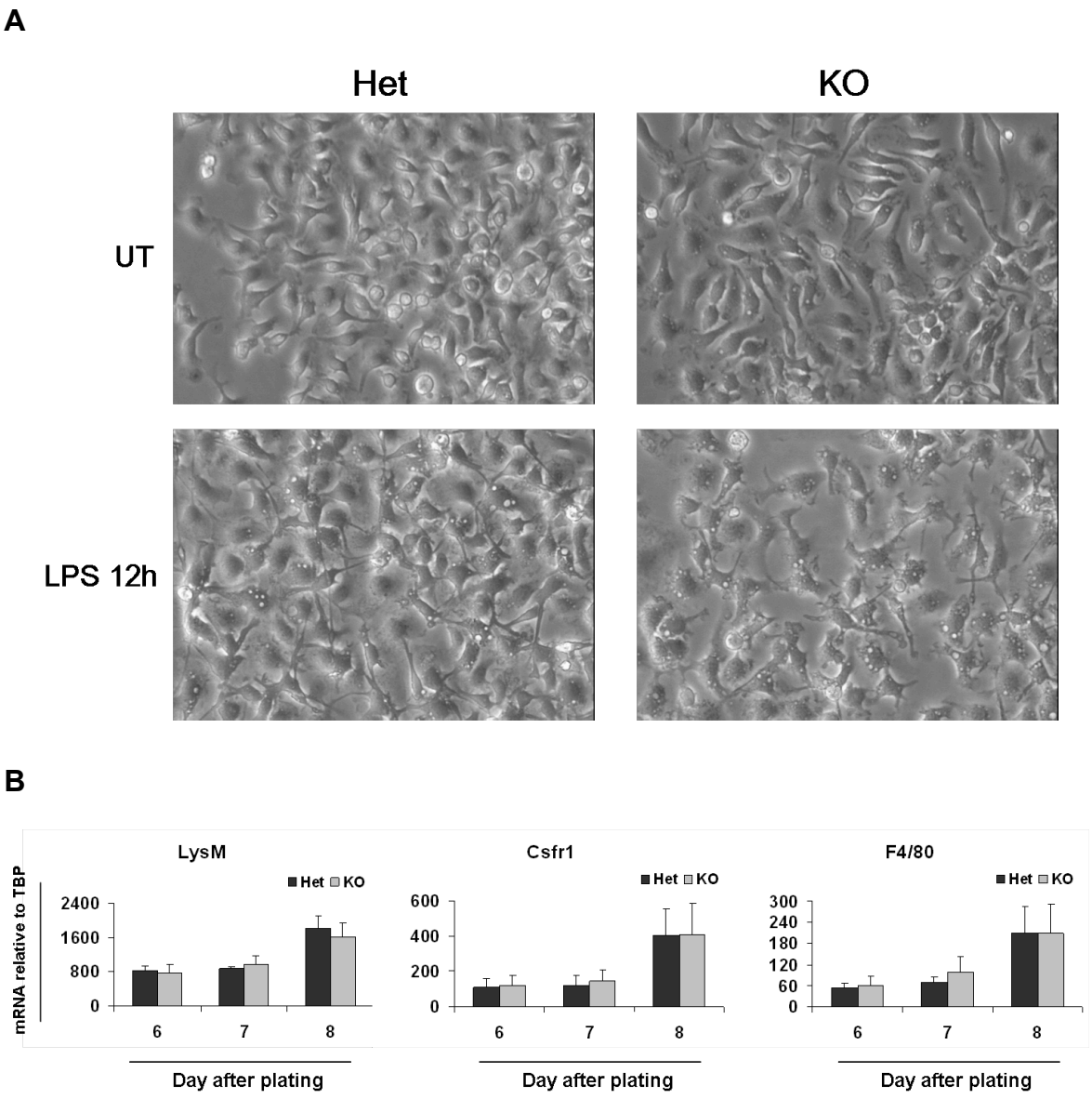

Figure 38 - Jarid1b-KO bone marrow-derived macrophages normally differentiate *in vitro*.
A) Bright-field microscope images (10x magnification) did not highlight evident morphological differences between Jarid1b Het and KO BMDM, before and after inflammatory stimulus. *B)* Macrophage differentiation markers are equally induced in Het and KO macrophages during differentiation (QPCR).

Once assessed that we could obtain normally differentiated macrophages, we confirmed that Jarid1b expression was completely abolished in these cells, both at mRNA and protein levels (Figure 39).

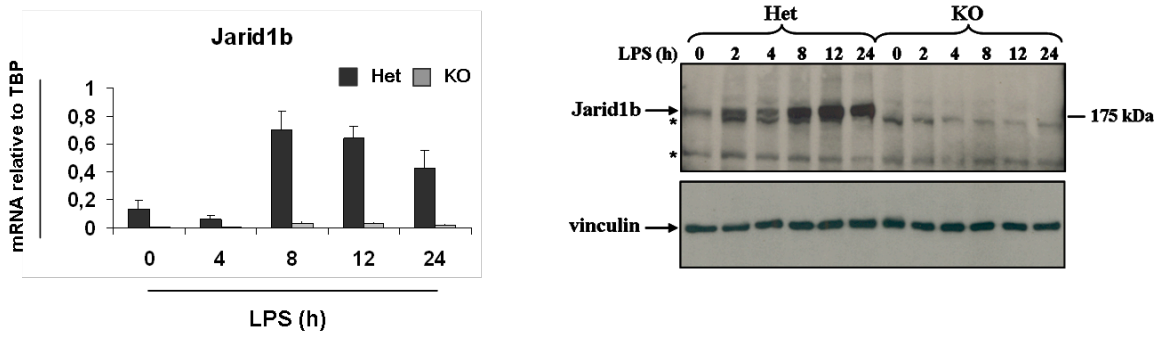

Figure 39 - Jarid1b expression is completely abrogated in Jari1b-KO macrophages.
QPCR (left) and western blot (right) demonstated the ablation of Jarid1b expression. Altough a residual of 1-4% was visible by QPCR, no signal could be detected by western blot, even when the film was over-exposed. Asterisks (*) indicate non-specific bands.

Since we have previously demonstrated that Jarid1b hypoxia- and LPS-triggered up-regulation is likely induced under the control of the transcription factor Hif1α, we wondered whether Jarid1b ablation might result in an altered hypoxic response. Thus, we analyzed the expression of some well-known Hif1α target genes, like *Vegfa* and *Nos2*, included two JmjC proteins (*Jmjd1a* and *Jmjd3*) that have been recently demonstrated to be Hif1α-dependent hypoxia-responsive genes (111). However, expression analysis did not highlight any significant alteration in the up-regulation of the genes we took in consideration (Figure 40), suggesting that Jarid1b ablation does not interfere with the hypoxia-induced activation of Hif1α target genes.

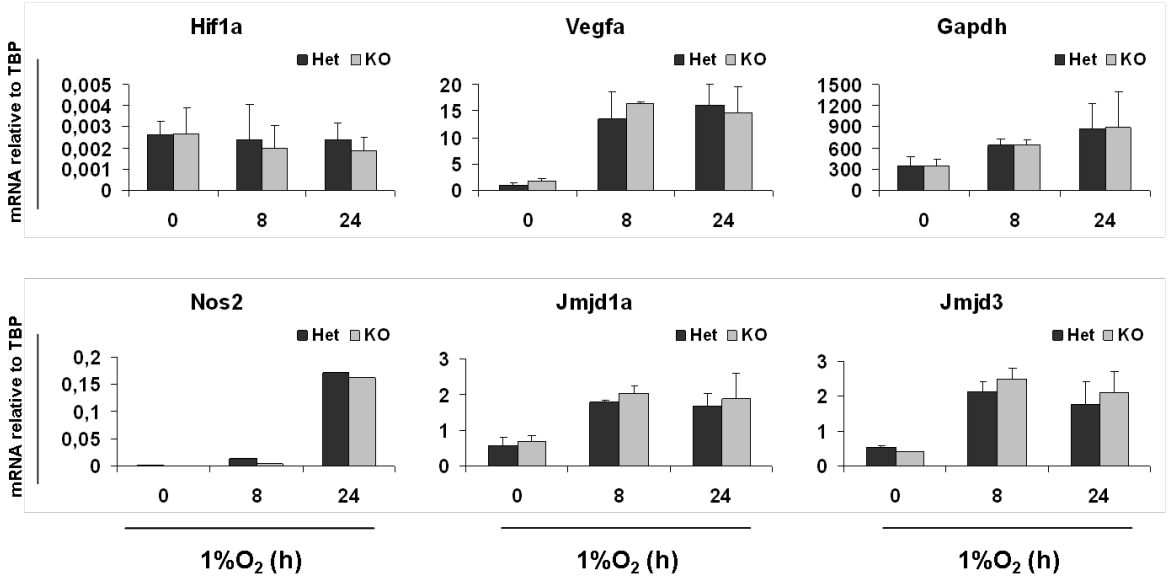

Figure 40 - Jarid1b ablation does not alter the hypoxic-dependent up-regulation of Hif1α target genes.

Well-known Hif1α target genes, such as *Vegfa* and *Nos2*, were normally induced in the absence of Jarid1b, when cells were exposed to low oxygen concentration. Also hypoxic-responsive JmjC proteins did not show significant expression alterations between heterozygous and KO macrophages.

We also explored the behaviour of LXR target genes in Jarid1b-KO cells to confirm the data previously obtained in Jarid1b-depleted macrophages. We confirmed that LXR target genes are induced during terminal differentiation (Figure 41A), so we analyzed their expression profile in a time-frame covering the differentiation-induced up-regulation. Although it was possible to observe, in some samples, an impairment in LXR target genes expression upon macrophage terminal differentiation, when multiple biological replicates were taken in consideration there was not any significant difference between heterozygous and Jarid1b-deprived macrophages (Figure 41B).

A

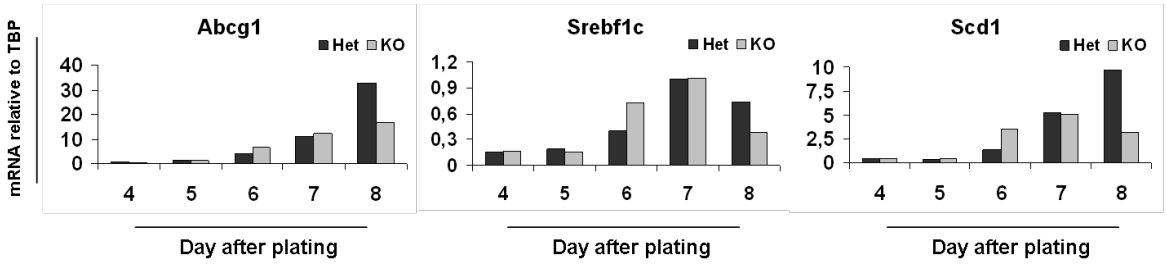

B

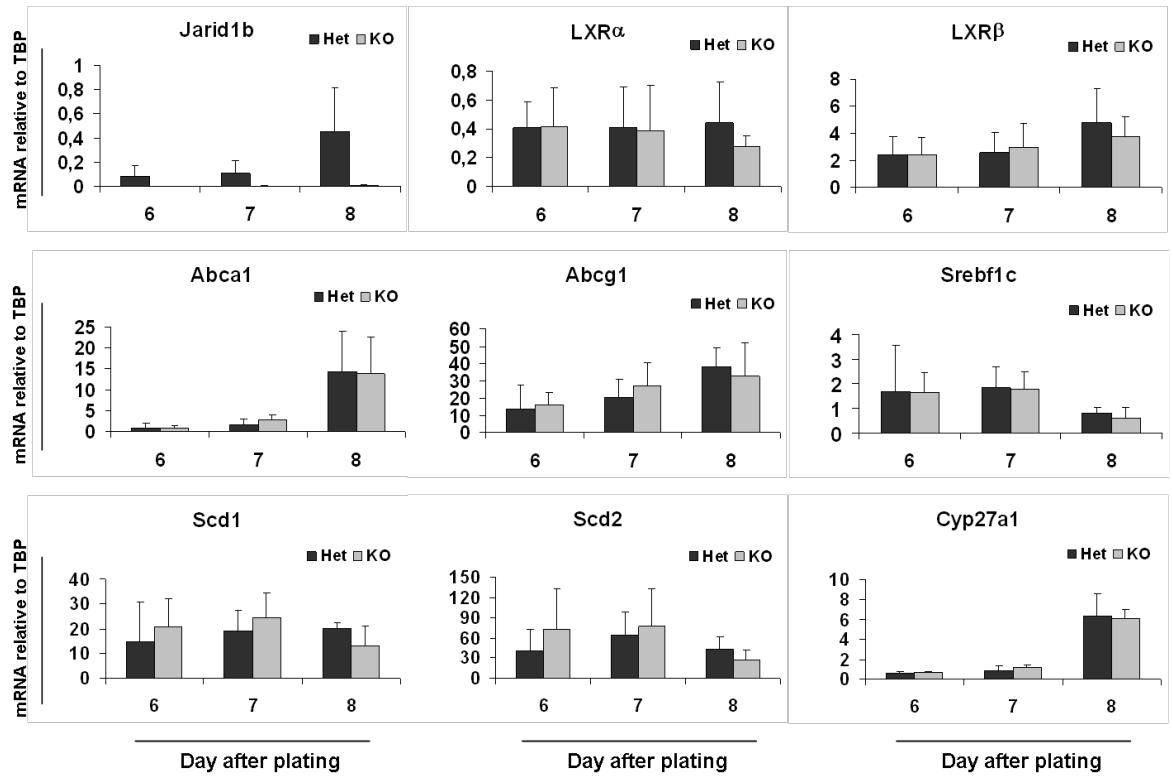

Figure 41 - LXR target genes expression is not always affected by Jarid1b ablation.
Macrophages were harvested starting from day 4 after plating in conditioned medium, every 24 hours. *A)* LXR target genes were induced during macrophage differentiation; sometime this induction was impaired in Jarid1b-KO cells. *B)* Statistical analysis of three independent replicates indicated that LXR target genes expression is not significantly affected in Jarid1b-ablated macrophages.

Looking for a possible mechanism that could explain the inconstant effect of Jarid1b-depletion/ablation on LXR target genes, we extended the expression analysis to an array of about 40 genes involved in: cholesterol uptake and efflux (membrane transporters), cholesterol storage and mobilization (enzymes catalyzing esterification and hydroxylation of cholesterol), intracellular cholesterol synthesis, fatty acid metabolism, and oxysterols synthesis and degradation, as well as oxysterols binding proteins. Unfortunately, we could not find any genes whose expression was significantly and constantly altered in the absence of Jarid1b (Supplementary table 1).

In order to understand whether the ablation of Jarid1b had any effect on macrophage cholesterol/oxysterols pools, and the transcriptional effect on LXR target genes was masked by other circumstances, we measured the amount of cholesterol and oxysterols in heterozygous and KO macrophages (in collaboration with Dr. Omar Maschi and Prof.

Donatella Caruso, Lab. of Biochemistry & Molecular Biology of Lipids, Dept. of Pharmacological Sciences at University of Milan). Concentration of oxysterols well correlated with the induction of LXR target genes during macrophage terminal differentiation, indicating that they are good predictors of LXR activity. However, we could not detect any difference in the amount of both intracellular and released cholesterol and oxysterols pools between heterozygous and Jarid1b-ablated macrophages (Figure 42).

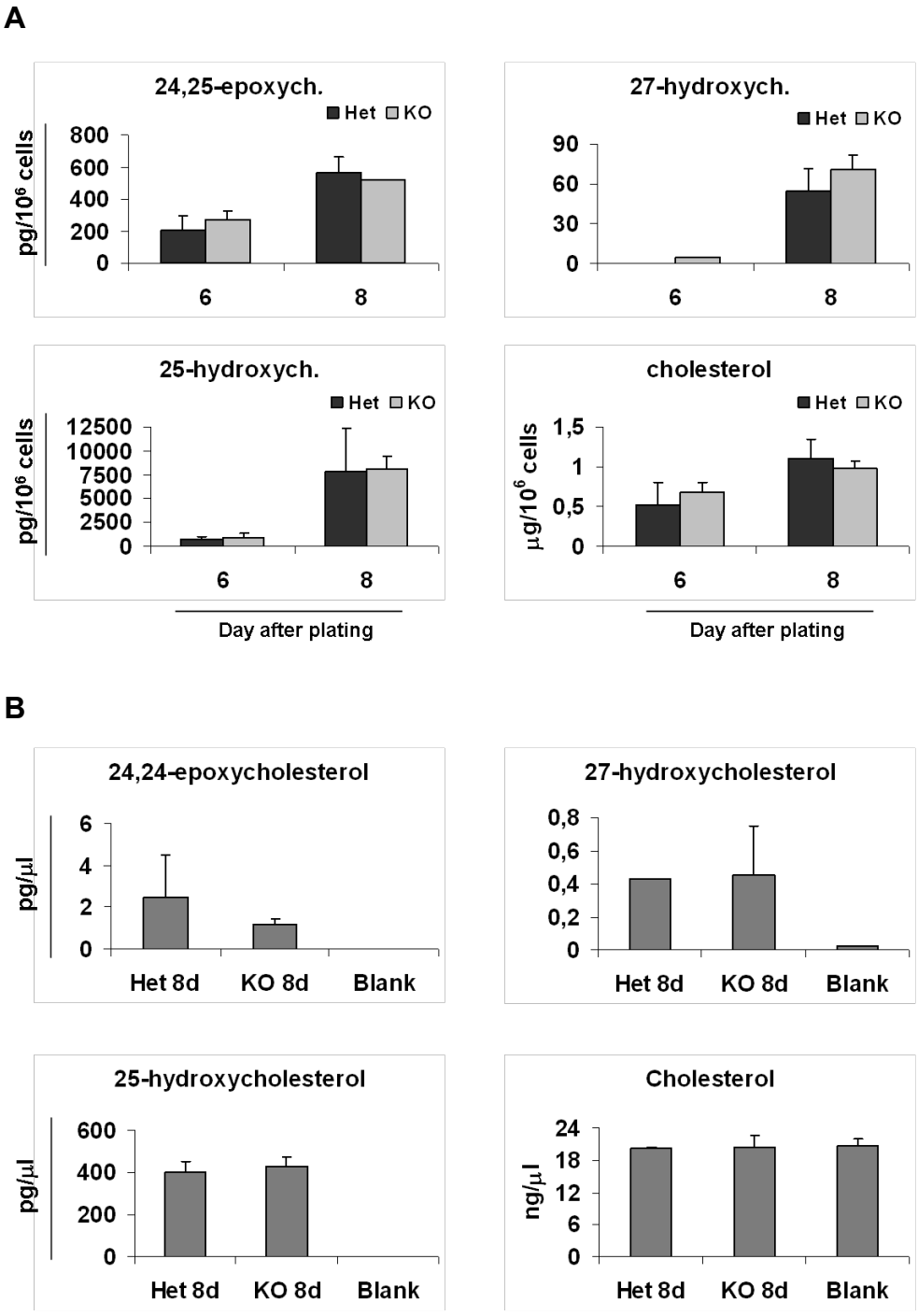

Figure 42 - Jarid1b deprivation does not alter cholesterol and oxysterols macrophages content.

A) Macrophages were harvested at day 6 and 8 of differentiation in conditioned medium, and fixed in ethanol 100% + butylhydroxytoluene (BHT - antioxidant agent). *B)* Cell culture medium was replaced with 10 ml/plate of fresh conditioned medium on day 6 after cell plating and then colleceted on day 8 to measure cholesterol and oxysterols relased by macrophages; the control (blank) is represented by the same medium plated for the same period in an empty petri dish. Cholesterol and oxysterols were first separated by HPLC and then identified and quantified by tandem mass spectrometry (done by Dr. Omar Maschi). Error bars represent standard deviation of two independent replicates.

Together these data would suggest that Jarid1b does not regulate the oxysterols cellular content and it is required neither for LXR activation nor for the transcriptional co-regulation of LXR target genes. Nevertheless, we think that the effect we repeatedly observed with two different shRNAs was not an artefact but rather was due to particular culture conditions difficult to control (see *Discussion*).

To obtain a global expression profile of Jarid1b-KO macrophages and more clearly identify those genes whose transcription is regulated by Jarid1b, we performed a cDNA microarray analysis in which gene expression of heterozygous macrophages stimulated with LPS for 0, 8 and 24 hours was compared to that of Jarid1b-ablated macrophages.

We chose heterozygous instead of wild-type cells to minimize the gene expression variability linked to the mixed genetic background. We also decided to analyze global gene expression in three biological independent replicates in order to get a robust dataset, which allowed us to run statistical analysis on the entire gene repertoire.

Microarray data showed a very limited number (similar to the one obtained with Jarid1b-depleted cells) of genes whose transcription was affected more than 1.5-fold (p-value ≤ 0.05) by Jarid1b ablation, and the transcriptional alteration was equally distributed between up- and down-regulation (Table 2).

Gene Symbol	F.C. (0h)	p-value	Gene Symbol	F.C. (8h)	p-value	Gene Symbol	F.C. (24h)	p-value
Kdm5b	-4,82736	3,98E-05	Kdm5b	-10,3893	7,29E-07	Kdm5b	-11,0896	5,44E-07
Gas5	-3,6273	0,000199	Gas5	-2,70046	0,001581	Gas5	-3,35025	0,000341
Gdf3	-2,60017	0,003362	Tm4sf1	-2,05234	0,015196	Stfa3	-2,48001	0,036467
Mcm6	-2,13539	0,014006	Mcm6	-2,02983	0,019992	Cxcl2	-1,78058	0,039308
Mamdc2	-1,93426	0,008618	Gda	-1,91793	0,023022	Adra1a	-1,76891	0,003243
Slc4a7	-1,80456	0,009386	St8sia4	-1,90355	0,010095	St8sia4	-1,67141	0,031538
1110032E23Rik	-1,7195	0,028285	Slpi	-1,65808	0,007014	Slc4a7	-1,60059	0,029981
2610318N02Rik	-1,61972	0,028463	EG432789	-1,63646	0,015317	E130112L23Rik	-1,56242	0,001653
Penk	-1,58557	0,02218	Mtss1	-1,58005	0,001222	Rpl34	-1,55107	0,025317
Etv5	-1,5418	0,029818	EG266459	-1,57105	0,001894	Rasal2	1,52297	0,016555
Adra1a	-1,524	0,019077	9030625A04Rik	1,50577	0,025686	9030625A04Rik	1,52516	0,022184
9030625A04Rik	1,67688	0,007428	Rcsd1	1,57929	0,038069	Cysltr2	1,53173	0,003802
Ralgps2	1,76455	0,012535	B3galnt1	1,58517	0,000296	C2	1,54249	0,027287
Sulf2	1,95284	0,000548	St3gal3	1,58742	0,022081	Steap3	1,55392	0,0447
Ctse	2,00813	0,029902	Pde10a	1,62304	0,021599	Rnase6	1,77678	0,032556
			Rtn1	1,64962	0,025403	Ctse	1,86149	0,048598
			Med29	1,65977	0,029973	Flnb	1,86319	0,048412
			Flnb	3,50125	0,00083	Morn4	1,92568	0,03766
						Slc13a3	3,34689	0,037253

Table 2 - Jarid1b ablation alters the expression of a limited number of genes in macrophages.
Microarray data (Affimetrix platform, GENE ST 1.0 Mouse) were obtained from three biological independent replicates and filtered for those genes showing a KO vs. Het fold change ≥ 1.5 with a p-value ≤ 0.05. In the table the selected genes (41 included *Jarid1b*) are ranked based on the fold change (F.C.) and divided in three separate columns representing the different time points of LPS stimulation.

We verified the expression alteration of about 20 of the selected genes by QPCR, obtaining a good validation (~70%) of microarray data (Figure 43). Looking at these genes it was impossible to identify a pathway whose transcriptional program was altered by the absence of Jarid1b.

A

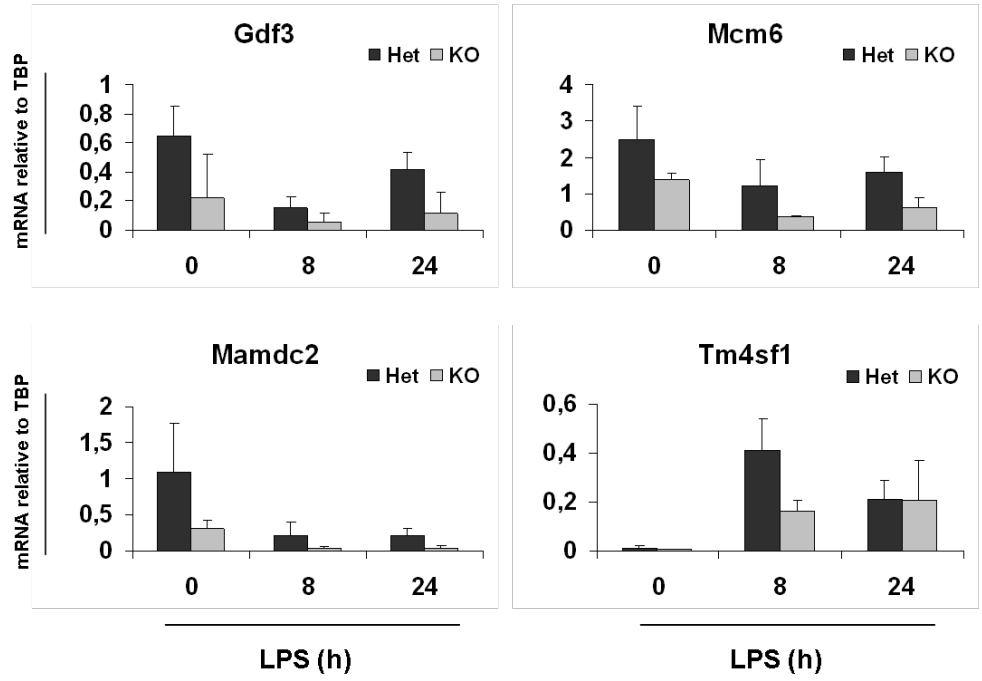

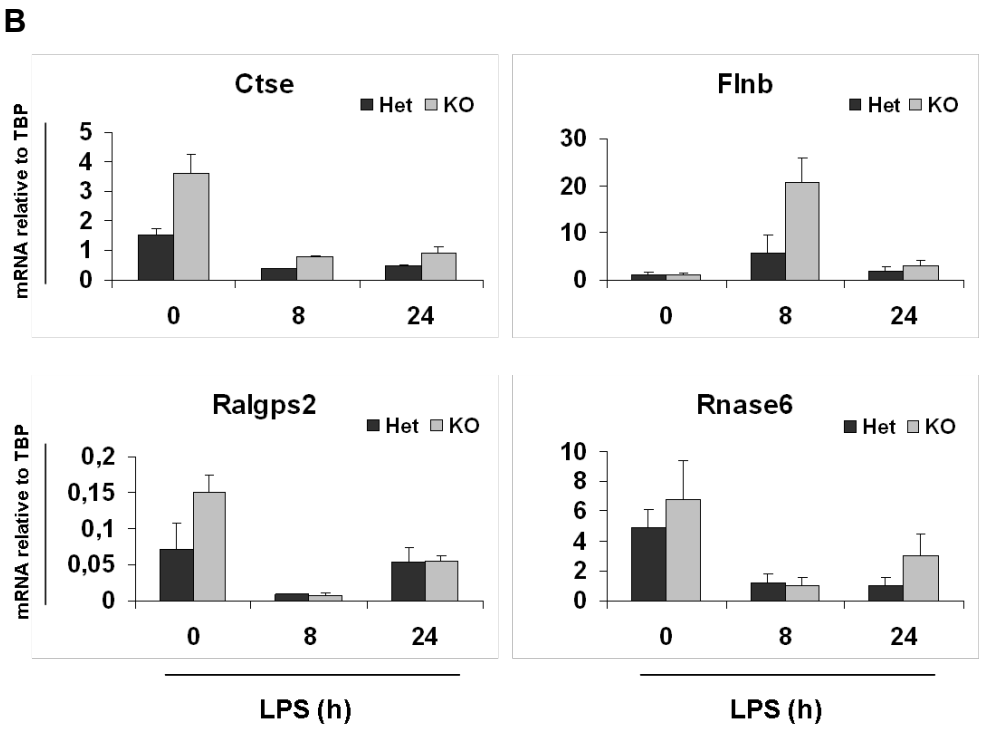

Figure 43 - Jarid1b-KO microarray data validation.
QPCR validation of Jarid1b Het vs. KO microarray data. Here reported are some examples of genes down-regulated *(A)* or up-regulated *(B)* in Jarid1b-KO macrophages.

Even though this extremely limited transcriptional outcome was surprising for a protein that is supposed to act as a transcriptional regulator, it was not totally unexpected for different reasons (see below and *Discussion*).

First, Seward and coll. showed that even though over-expression of Jarid1b in Hep3b cells resulted in a strong decrease of H3K4me3 and H3K4me2, it was not accompanied by a detectable reduction in RNA polymerase II C-terminal domain (CTD) phosphorylation (90), suggesting that Jarid1b misexpression may not have global effects on RNA PolII transcription.

Second, other JARID1 family members may compensate the absence of Jarid1b. To explore this possibility, we analyzed the expression profile of the other JARID1 family members in Jarid1b-deprived macrophages under the different conditions we had taken in consideration along the previous work: macrophage terminal differentiation, inflammatory stimulation and hypoxic stress. Neither *Jarid1a* nor *Jarid1c* or *Jarid1d* appeared to be up-

regulated in the absence of Jarid1b; only a small increase in *Jarid1c* expression could be envisioned after 4 and 8 hours of LPS stimulation (Figure 44).

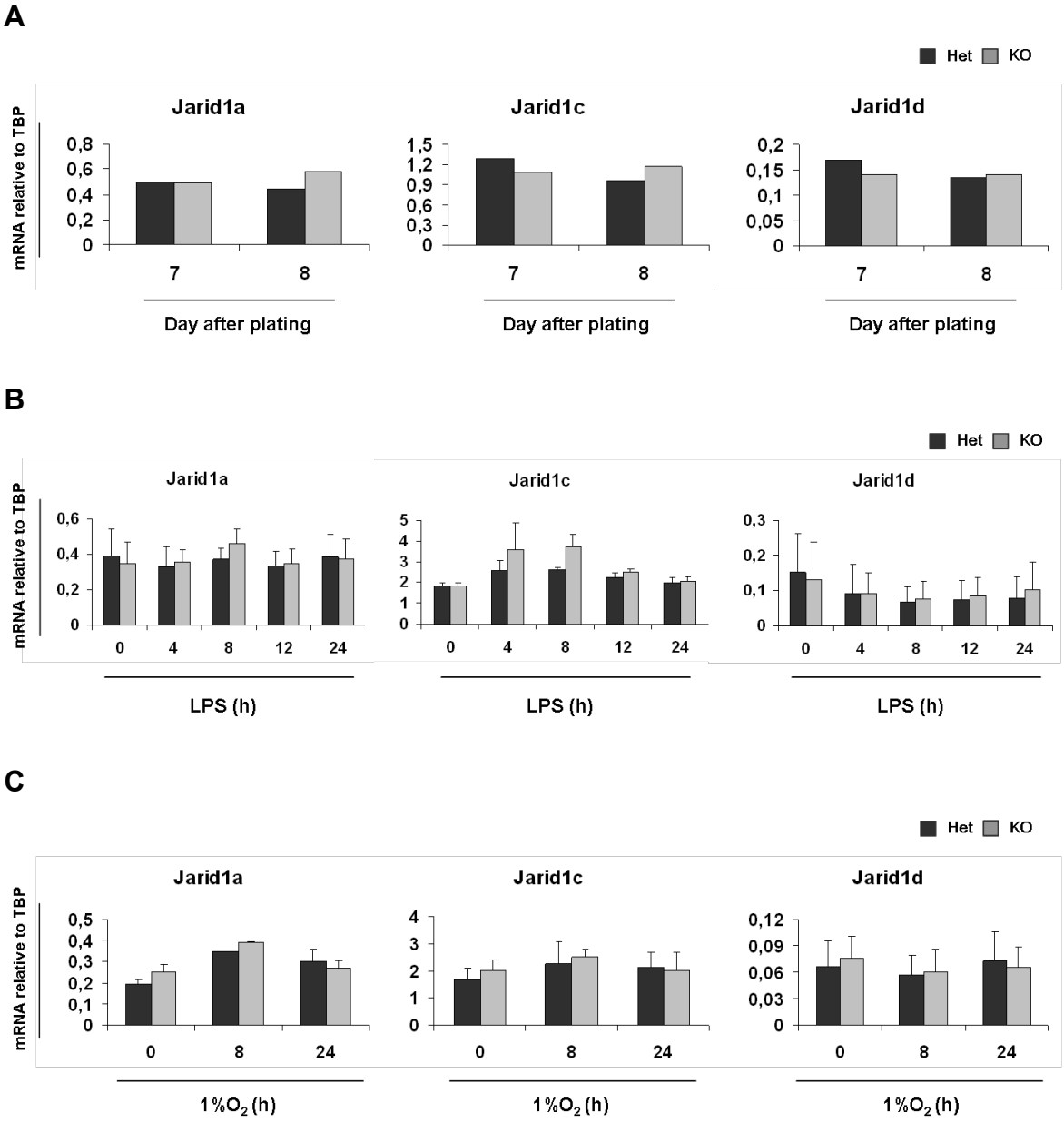

Figure 44 - JARID1 family members expression is not incremented in Jarid1b-KO macrophages.
QPCR analysis of *Jarid1a*, *Jarid1c* and *Jarid1d* did not highlight any clear up-regulation potentially aimed at compensate the absence of Jarid1b, neither during macrophage terminal differentiation *(A)* nor after LPS stimulation *(B)* or under hypoxic stress *(C)*.

Looking at the list of genes whose expression was altered by Jarid1b ablation, it was immediately evident that there was only one gene, except *Jarid1b* itself, consistently down-regulated in all the Jarid1b-KO microarray samples, that was *Gas5* (see 2nd row in Table 2).

Growth-arrest-specific transcript 5 (Gas5) is a non-protein-coding transcript, which accumulates during arrested cell growth. This accumulation can be explained by the classification of *Gas5* into the family of 5'-terminal oligopyrimidine (5'-TOP) genes: while the spliced *Gas5* RNA is normally associated with ribosomes and rapidly degraded, during arrested cell growth it accumulates in mRNP particles, as it has been reported for other 5'-TOP genes (95).

The real biological function of *Gas5* seems to be linked to its role as host gene for small nucleolar RNAs (snoRNAs); indeed it contains nine (ten in human) snoRNAs in its introns. Consistently with this function, the only evolutionary conserved *Gas5* regions are those corresponding to snoRNAs and the 5' sequences (Figure 45) needed to drive its transcription.

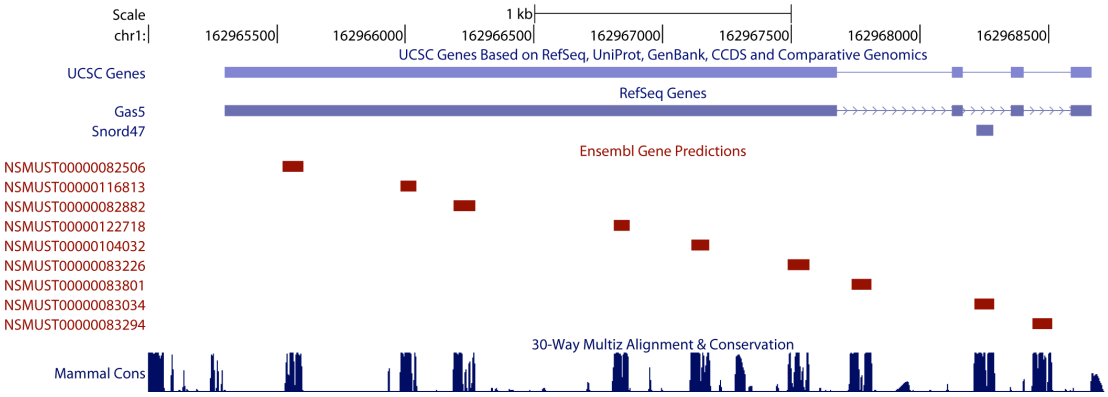

Figure 45 - *Gas5* is a snoRNA host gene.
Gas5 is a non-protein-coding transcript hosting nine snoRNAs inside its intronic regions. In this genome browser screenshot it is possible to appreciate that only the sequences corresponding to snoRNAs and the 5' region are conserved in mammals.

snoRNAs (small nucleolar RNA) represent one of the largest group of non-protein-coding RNAs and are divided into two major classes (C/D box and H/ACA box) on the basis of conserved sequence elements and characteristic secondary structures. In particular, snoRNAs act during post-transcriptional modifications of different RNAs (e.g. during ribosomes biogenesis), with H/ACA box and C/D box snoRNAs guiding pseudouridylation and methylation respectively (35). Most snoRNAs are encoded in the introns of protein-coding and non-coding genes in vertebrates, and many of them are clustered in different

introns of the same host gene, as in the case of *Gas5*, or in the introns of different host genes.

The nine snoRNAs encoded within *Gas5* belong to the C/D box family and have reported or predicted function in the 2'-O-methylation of rRNA.

When analyzed by QPCR, *Gas5* appeared to have very variable expression levels and the ablation of Jarid1b had only limited effects (and not always) on its expression (Figure 46), differently to what observed in microarray data. Thus, we decided to examine the expression of snoRNAs hosted within *Gas5* introns.

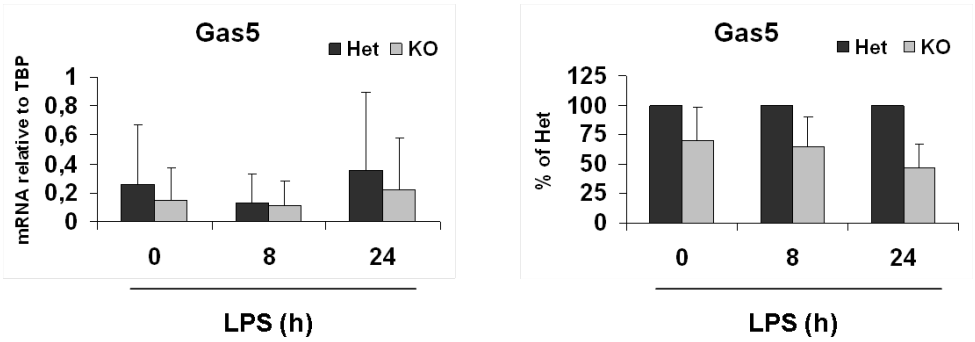

Figure 46 - *Gas5* expression is partially impaired in Jarid1b-KO macrophages.
QPCR analysis showed very variable *Gas5* mRNA levels (left panel), maybe due to the transcript instability. In Jarid1b-KO cells *Gas5* expression was partially impaired: the down-regulation became more consistent at late time points of LPS stimulation.

Preliminary results revealed that Jarid1b ablation impaired the expression of most of the *Gas5*-hosted snoRNAs (Figure 47A), also in a situation in which *Gas5* expression was completely unaffected (Figure 47B). Moreover, this down-regulation seemed to be directly attributable to Jarid1b as its re-expression in KO macrophages reverted the effect. Surprisingly, also the re-expression of a catalytically inactive mutant of Jarid1b was able to revert the snoRNA impaired expression, suggesting a possible role for Jarid1b independent of its enzymatic activity and highlighting the need of further studies.

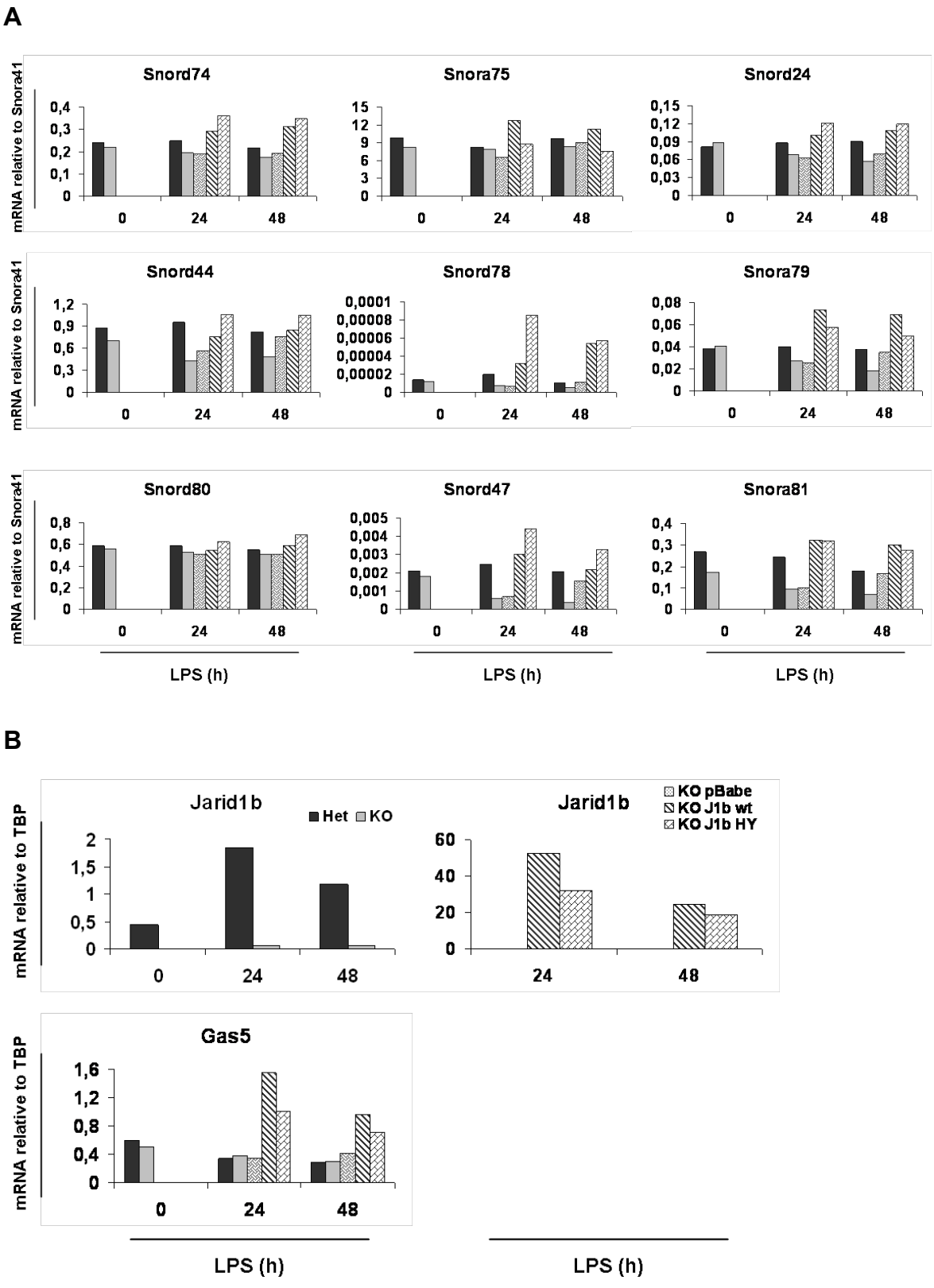

Figure 47 - *Gas5*-hosted snoRNAs expression is partially impaired by Jarid1b-ablation.
A) Jarid1b-deprivation impaired the expression of *Gas5*-hosted snoRNAs to different degree, also when *Gas5* transcript levels were not affected. Re-expression of Jarid1b in KO macrophages either restored snoRNAs expression to control levels or inverted the effect, resulting in an increased expression. *B) Jarid1b* and *Gas5* expression is shown; over-expression of *Jarid1b* in KO cells (only 24 and 48 hours samples) up-regulated *Gas5* transcript levels. Total RNA was extracted using the *mir*Vana kit (Ambion) in order to preserve the small RNAs fraction.

7. Characterization of Jarid1b enzymatic activity and genomic binding

As we could not identify a clear role for Jarid1b in transcriptional regulation, we proceeded to characterize its reported histone demethylase activity.

First of all, we confirmed that Jarid1b over-expression led to a strong reduction of trimethylation of lysine 4 on histone 3, and this effect was dependent on Jarid1b catalytic activity since a point mutation in the JmjC domain facial triad, reported to abolish Jarid1b enzymatic activity, restored H3K4me3 to control levels (Figure 48). Thus, Jarid1b is, at least, able to catalyze the demethylation of methylated H3K4. Moreover, Jarid1b acted as a transcriptional repressor in a luciferase reporter assay (Figure 31B), as expected for a H3K4me3 demethylase.

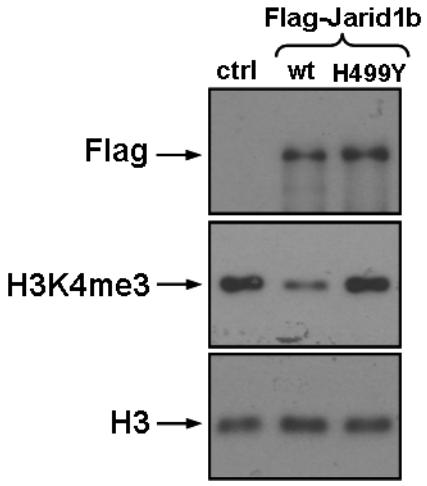

Figure 48 - H3K4me3 levels are reduced by Jarid1b over-expression.
Phoenix Eco were transfected with 10μg of an empty pCDNA3 vector (ctrl) or the same vector expressing the wild-type (Jarid1b wt) or the catalytically inactive (Jarid1b H499Y) Jarid1b. Cells were harvested 48 hours post-transfection and lysed in RIPA buffer (total protein extract). H3K4me3 levels were strongly reduced in cells ectopically expressing the wild type Jarid1b protein but restored to control levels in cells expressing the mutant form of Jarid1b, in which a point mutation (H499Y) kills its enzymatic activity.

However, either the depletion or the total ablation of Jarid1b did not cause a global detectable increase in methylation of H3K4 (Figure 49), indicating that Jarid1b is sufficient but not necessary for H3K4 demethylation.

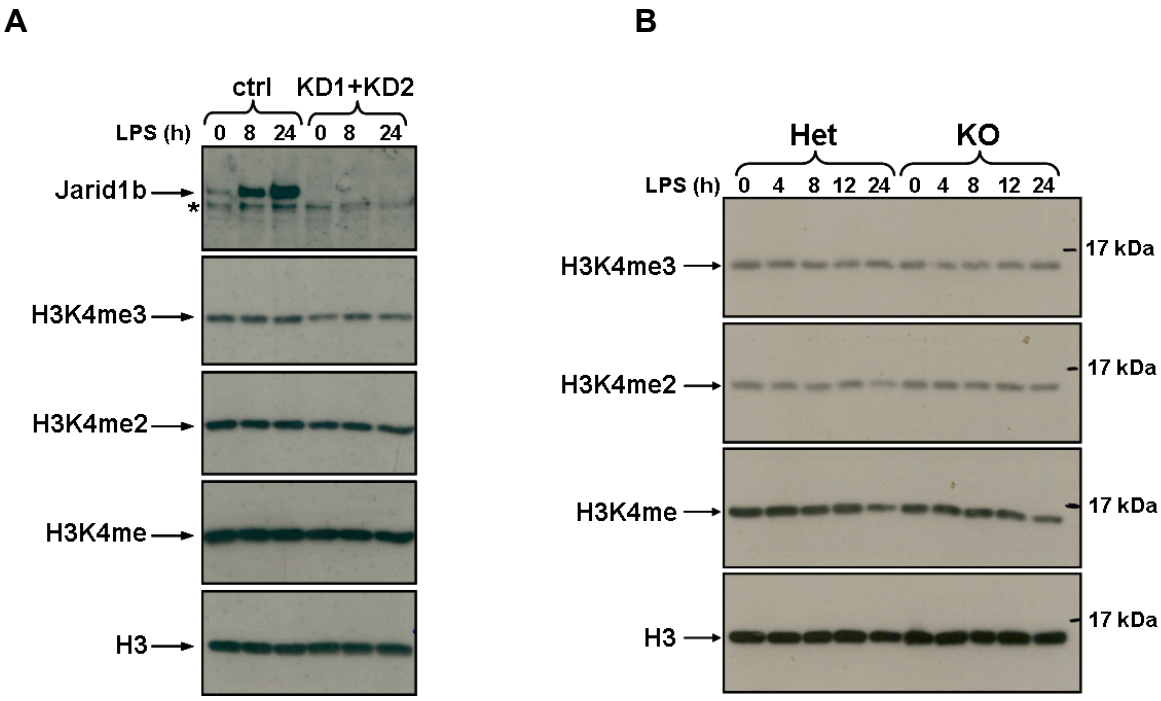

Figure 49 - Removal of Jarid1b does not produce global increase in H3K4 methylation.
A) BMDM were infected with a LMP empty vector (ctrl) or a mix of the two shRNAs (KD1+KD2); cells were stimulated with LPS for the indicated time points and harvested on day 8 post-infection. Nuclei were lysed in RIPA buffer. In a context of severe Jarid1b protein reduction *(A)*, or total ablation *(B)* methylation levels on H3K4 were not increased. Total H3 was used to normalize protein levels in *(A)* and *(B)*. Asterisk (*) indicates a non-specific band.

In order to determine whether Jarid1b deprivation had any direct or indirect effects on distinct lysine residues, we extended the analysis to the methylation levels of other lysines present on histone 3 tail and known to exert a role in chromatin architecture and transcriptional regulation. None of the chromatin marks analyzed showed evident alterations in Jarid1b-KO macrophages (Figure 50).

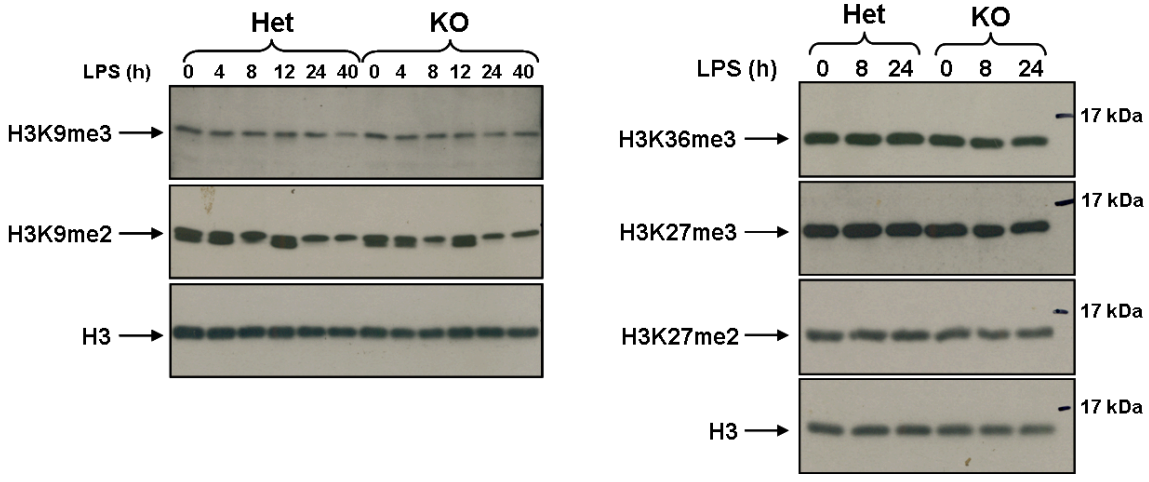

Figure 50 - Methylation of different lysine residues on H3 tail is not affected by Jarid1b ablation.
Jarid1b heterozygous and knock-out BMDM were stimulated with LPS for the specified time points and harvested on day 8 after plating in conditioned medium. Cells were lysed in RIPA buffer and total protein

extraxct was separated on a 15% PAGE. None of the considered lysines showed evident alteration in methylation levels.

We have previously shown that Jarid1b is entirely localized into the nucleus, but when we examined in deeper details the different sub-nuclear compartments we found only a very little amount of Jarid1b associated with histones, differently to what expected for a histone demethylase. The almost totality of Jarid1b was found in the DNAse released proteins fraction (Figure 51), suggesting a more dynamic DNA-mediated interaction between Jarid1b and chromatin.

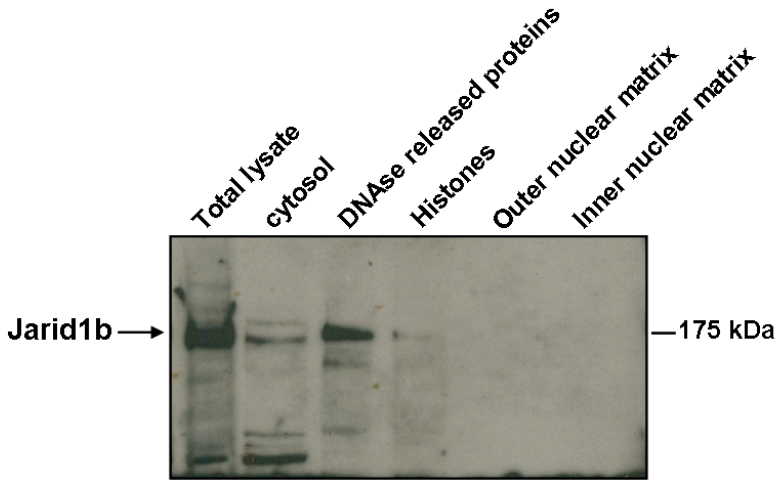

Figure 51 - Jarid1b is mainly localized in the DNAse released sub-nuclear protein fraction.
Differential sub-nuclear protein fractionation of J774 macrophages stimulated with LPS for 24 hours, revealed that Jarid1b was almost completely released from chromatin by DNAse treatment, suggesting that it interacts with DNA rather than with histone proteins. (Samples provided by Dr. Greta Caprara, PhD).

Aiming at defining the genomic binding of Jarid1b we took advantage of high-throughput ChIP analysis (ChIP-sequencing). We first performed chromatin immunoprecipitation on BMDM stimulated with LPS for 12 hours and then run three round of DNA-sequencing (in collaboration with Prof. Henk Stunnenberg, Radboud University Nijmegen Medical Centre).

Analyzing the data with restrictive parameters, namely a minimum threshold of 15 tags and a false discovery rate (FDR) of 0.0007, we retrieved a total of 95 peaks associated to 88 genes by proximity. These data were further scanned and compared with “input DNA”

sequencing data (non-immunoprecicpitated DNA), which allowed us to filter out false positive peaks due to sequencing biases (Figure 52A). Our final dataset comprised 72 peaks (associated with 71 genes), 48 of which were located close to TSS (±1.5 kb).

We verified the quality of this dataset analyzing by QPCR more than half of the peaks (38/72) and we obtained ~63% of validation, using an IP vs. mock fold enrichment ≥3 as validation parameter. When we considered the subset of peaks located close to the TSS and not associated with repeated sequences the validation rate was almost 100%, and 2/3 of these peaks had an IP vs. mock fold enrichment ≥5 (Figure 52B). Interestingly, some of these targets are genes involved in the inflammatory response, like the chemokines *Ccl2* and *Ccl5*, the nitric oxide synthase *Nos2*, the DNA fragmentation factor *Dffb*, the immuno-responsive gene *Irg1* and the prostaglandin receptor *Ptger4*. However, it was not possible to recognize a precise pathway, due to the little number of targets identified.

A

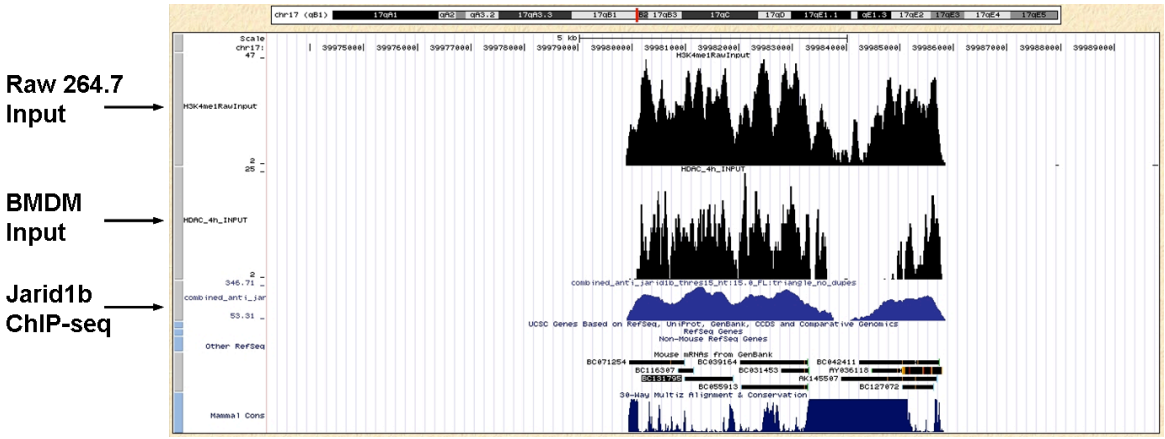

B

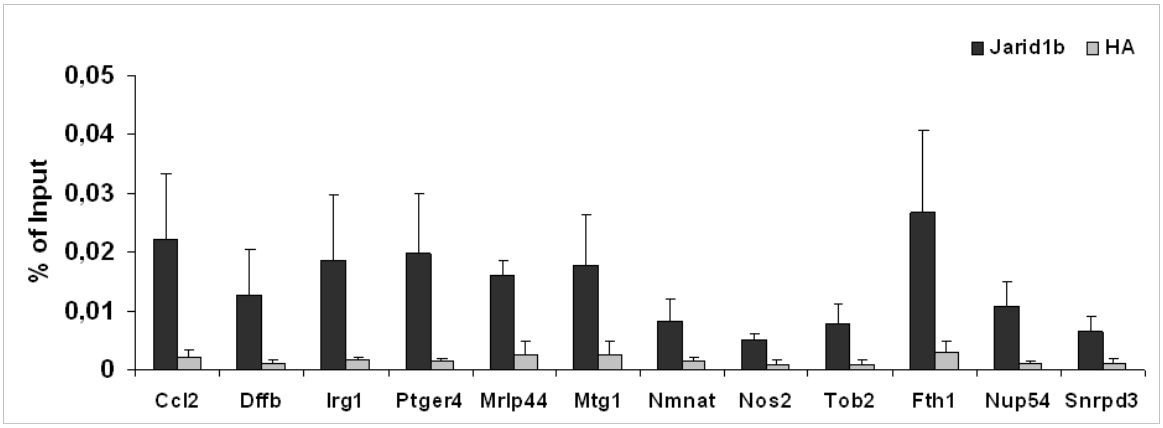

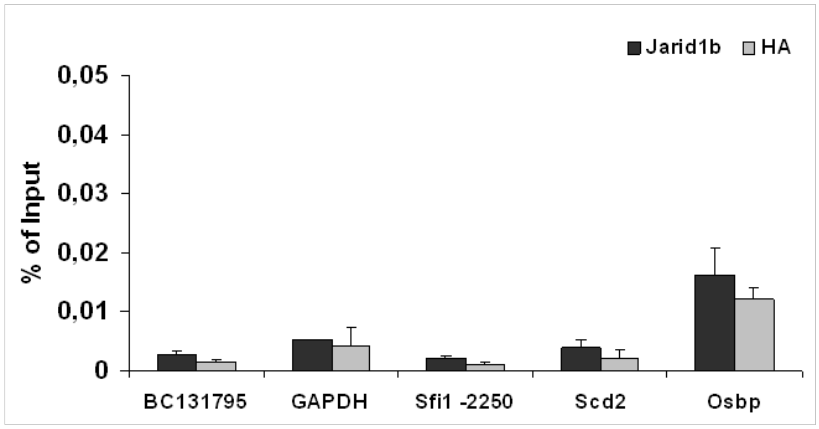

Figure 52 - Jarid1b binds to a limited number of genomic targets.
ChIP-sequencing analysis of Jarid1b revealed a limited number of bound targets. *A)* An example of ChIP-seq false positive target excluded by comparison with input DNA sequencing. *B)* Some examples of validated Jarid1b target genes; negative controls are represented by either excluded peaks or unrelated genes. Anti-HA ChIP was used as mock ChIP.

Moreover, crossing the dataset of the two genome-wide screenings, namely cDNA microarray and ChIP-sequencing, there was not any common genes. The little number of genes identified by these two approaches suggests that Jarid1b is not a general regulator of gene transcription, at least in the cellular system and conditions we examined.

SUPPLEMENTARY TABLE

Supplementary table 1 - Expression profile of "metabolic" genes in Jarid1b-KO macrophages.
Here are shown the expression profiles of 40 genes involved in cholesterol uptake and efflux, storage and mobilization, intracellular cholesterol synthesis, fatty acid metabolism, and oxysterols synthesis and degradation. Expression profiles are reported as expression levels relative to TBP (Relative expression), and as KO vs. Het ratio [(KO/Het)x100] (% of Het). % of Het representation of data allow to reduce the elevated expression variability among different biological preparations typical of these genes. Represented is the average of three (3x) or two (2x) independent replicates, with the respective standard deviations (St. Dev.) and 95% confidence interval (95% C.I.).

		Relative expression			% of Het		
Detector	**Sample Name**	**Average**	**St. Dev.**	**95% C.I.**	**Average**	**St. Dev.**	**95% C.I.**
3x							
Abca1	BM Het ut 6'd	0,9461	1,288611	1,458174			
	BM Het ut 7'd	1,7484	1,325384	1,499786			
	BM Het ut 8'd	14,4213	9,593357	10,85571			
	BM KO ut 6'd	0,954	0,484377	0,548114	254,631	200,2595	226,6108
	BM KO ut 7'd	2,90662	0,992292	1,122864	205,332	82,08342	92,88443
	BM KO ut 8'd	13,9186	8,791195	9,947991	97,634	7,452402	8,433032
Abcg1	BM Het ut 6'd	13,7931	13,69743	15,49982			
	BM Het ut 7'd	20,7023	10,26651	11,61744			
	BM Het ut 8'd	38,1407	11,23958	12,71855			
	BM KO ut 6'd	15,7754	7,844642	8,876885	162,922	95,42106	107,9771
	BM KO ut 7'd	26,9533	13,75294	15,56263	135,577	59,40694	67,22405
	BM KO ut 8'd	32,3794	19,34367	21,88902	80,9299	27,28965	30,88058
ApoE	BM Het ut 6'd	10,7363	1,937883	2,192881			
	BM Het ut 7'd	25,4243	16,06805	18,18237			
	BM Het ut 8'd	650,198	363,8216	411,6953			
	BM KO ut 6'd	10,7621	6,21565	7,03354	108,214	69,99182	79,20174
	BM KO ut 7'd	38,282	13,78849	15,60286	273,296	310,4433	351,2933
	BM KO ut 8'd	536,452	241,04	272,7574	118,795	116,0106	131,2759
Cd5l	BM Het ut 6'd	0,79437	0,949339	1,074258			
	BM Het ut 7'd	1,21033	1,37733	1,558567			
	BM Het ut 8'd	11,2207	11,36234	12,85746			
	BM KO ut 6'd	0,38229	0,314895	0,356331	130,44	117,8944	133,4076
	BM KO ut 7'd	1,52917	1,621259	1,834594	352,634	403,3577	456,4339
	BM KO ut 8'd	9,19636	9,195946	10,406	184,19	170,5445	192,9857
Cd36	BM Het ut 6'd	138,189	81,59751	92,33457			
	BM Het ut 7'd	157,603	114,1589	129,1806			
	BM Het ut 8'd	76,3775	35,8609	40,57968			
	BM KO ut 6'd	115,571	41,91409	47,42939	99,5481	47,61269	53,87784
	BM KO ut 7'd	163,936	75,15117	85,03999	121,708	41,61109	47,08651
	BM KO ut 8'd	65,9727	22,09539	25,00283	90,9254	17,6543	19,97735
Cyp27a1	BM Het ut 6'd	0,58552	0,243082	0,275069			
	BM Het ut 7'd	0,91637	0,48382	0,547484			
	BM Het ut 8'd	6,3392	2,329232	2,635726			
	BM KO ut 6'd	0,67348	0,090331	0,102217	126,143	40,1869	45,47492
	BM KO ut 7'd	1,13237	0,368264	0,416722	145,188	88,76407	100,4442
	BM KO ut 8'd	6,03138	1,044951	1,182451	99,5594	19,91928	22,54038
Fabp4	BM Het ut 6'd	3,15393	2,344444	2,652939			
	BM Het ut 7'd	1,49389	0,725703	0,821195			
	BM Het ut 8'd	0,93758	0,739424	0,836722			
	BM KO ut 6'd	2,63153	1,95252	2,209444	83,8101	63,28224	71,60927
	BM KO ut 7'd	1,18871	0,772555	0,874212	75,7947	42,07383	47,61014
	BM KO ut 8'd	0,4597	0,311391	0,352366	50,5672	23,608	26,71448
Fabp5	BM Het ut 6'd	69,9976	55,04355	62,28649			
	BM Het ut 7'd	45,4314	13,60611	15,39648			
	BM Het ut 8'd	73,8349	26,58441	30,08254			
	BM KO ut 6'd	71,8772	38,21567	43,2443	116,122	41,9602	47,48157
	BM KO ut 7'd	56,6338	25,7426	29,12996	119,851	27,30559	30,89862
	BM KO ut 8'd	51,0985	27,91137	31,58411	66,4983	25,2605	28,58442

Hmgcr	BM Het ut 6'd	26,641	9,090427	10,2866			
	BM Het ut 7'd	23,955	6,911456	7,820905			
	BM Het ut 8'd	15,562	7,481046	8,465445			
	BM KO ut 6'd	30,2264	13,94639	15,78153	110,292	28,49854	32,24854
	BM KO ut 7'd	22,2295	7,390216	8,362663	92,3059	15,31596	17,33132
	BM KO ut 8'd	12,7853	2,870839	3,2486	91,2023	32,28416	36,5323
Hsd17b7	BM Het ut 6'd	2,88038	1,231046	1,393034			
	BM Het ut 7'd	3,01421	1,91551	2,167564			
	BM Het ut 8'd	0,87856	0,577313	0,65328			
	BM KO ut 6'd	1,87499	0,1533	0,173472	73,4714	29,40058	33,26927
	BM KO ut 7'd	1,38456	0,400884	0,453634	61,7042	37,27955	42,18501
	BM KO ut 8'd	0,43675	0,134483	0,15218	66,7515	39,47956	44,6745
Insig1	BM Het ut 6'd	5,81048	4,926615	5,574887			
	BM Het ut 7'd	5,5664	3,074324	3,478861			
	BM Het ut 8'd	5,04085	3,132609	3,544816			
	BM KO ut 6'd	7,11886	5,266008	5,95894	122,688	51,79004	58,60487
	BM KO ut 7'd	4,83982	2,708044	3,064384	86,0558	5,069127	5,736152
	BM KO ut 8'd	3,90016	2,331717	2,638538	89,3404	36,89245	41,74697
Insig2	BM Het ut 6'd	2,86283	0,884048	1,000376			
	BM Het ut 7'd	2,71903	0,593445	0,671533			
	BM Het ut 8'd	3,08509	0,447787	0,50671			
	BM KO ut 6'd	2,52288	0,659537	0,746322	89,5048	14,95179	16,91924
	BM KO ut 7'd	2,27932	0,289168	0,327218	86,9327	22,95661	25,97737
	BM KO ut 8'd	2,79737	0,691863	0,782902	90,0992	11,59099	13,1162
Ldlr	BM Het ut 6'd	2,85681	1,292328	1,46238			
	BM Het ut 7'd	2,83413	0,756565	0,856118			
	BM Het ut 8'd	1,97605	0,581236	0,657718			
	BM KO ut 6'd	3,40477	1,189121	1,345592	125,011	32,58929	36,87758
	BM KO ut 7'd	2,26439	0,716313	0,81057	81,2776	19,28971	21,82796
	BM KO ut 8'd	1,32026	0,665959	0,75359	66,1799	32,02124	36,23478
LXRa	BM Het ut 6'd	0,40984	0,178767	0,20229			
	BM Het ut 7'd	0,40569	0,281366	0,31839			
	BM Het ut 8'd	0,44305	0,281042	0,318023			
	BM KO ut 6'd	0,4125	0,270783	0,306414	97,0224	32,46912	36,74159
	BM KO ut 7'd	0,38621	0,317402	0,359167	93,2691	21,69818	24,55335
	BM KO ut 8'd	0,2765	0,072109	0,081597	75,3287	36,61115	41,42865
LXRb	BM Het ut 6'd	2,42669	1,324538	1,498828			
	BM Het ut 7'd	2,55109	1,497325	1,694352			
	BM Het ut 8'd	4,74797	2,507202	2,837114			
	BM KO ut 6'd	2,39973	1,278876	1,447158	99,2587	1,534104	1,73597
	BM KO ut 7'd	2,95975	1,759689	1,991239	116,099	29,59856	33,4933
	BM KO ut 8'd	3,7361	1,504195	1,702126	82,8051	14,42935	16,32804
Msr1	BM Het ut 6'd	200,218	118,7052	134,3251			
	BM Het ut 7'd	180,691	110,2368	124,7424			
	BM Het ut 8'd	29,9806	14,26764	16,14506			
	BM KO ut 6'd	155,981	99,1288	112,1727	77,0469	23,24382	26,30238
	BM KO ut 7'd	145,359	131,9045	149,2612	72,3278	24,30356	27,50157
	BM KO ut 8'd	25,1428	16,36623	18,51979	79,8409	13,52593	15,30575
Osbp	BM Het ut 6'd	2,59448	0,933113	1,055897			
	BM Het ut 7'd	2,54522	0,685974	0,776238			
	BM Het ut 8'd	3,42816	1,125438	1,27353			
	BM KO ut 6'd	2,50083	0,664004	0,751377	100,43	20,62874	23,34319
	BM KO ut 7'd	2,46159	0,716381	0,810646	97,1521	16,20281	18,33487
	BM KO ut 8'd	2,64605	0,751763	0,850684	78,1278	6,975273	7,893119
Osbpl1a	BM Het ut 6'd	2,29711	1,503208	1,701009			
	BM Het ut 7'd	1,91437	1,49534	1,692105			
	BM Het ut 8'd	1,66154	1,410188	1,595748			
	BM KO ut 6'd	1,22792	1,893795	2,142992	34,6729	43,61156	49,35021
	BM KO ut 7'd	1,4213	2,216819	2,508521	45,3703	55,47448	62,77413
	BM KO ut 8'd	0,84247	1,258294	1,423867	32,4074	32,41471	36,68002
Pparg	BM Het ut 6'd	1,63358	1,134647	1,28395			
	BM Het ut 7'd	1,08757	0,633049	0,716349			
	BM Het ut 8'd	1,26986	0,626067	0,708448			
	BM KO ut 6'd	1,57835	1,146885	1,297799	94,4499	10,61358	12,01017
	BM KO ut 7'd	1,10472	0,432954	0,489925	108,887	25,69212	29,07284
	BM KO ut 8'd	1,40894	0,726428	0,822015	109,876	18,05669	20,43269

Scap	BM Het ut 6'd	1,0554	0,278121	0,314718			
	BM Het ut 7'd	1,11367	0,38668	0,437561			
	BM Het ut 8'd	1,16928	0,538915	0,609828			
	BM KO ut 6'd	1,18359	0,553889	0,626773	107,676	32,32124	36,57426
	BM KO ut 7'd	0,97855	0,37942	0,429346	88,6367	20,16439	22,81774
	BM KO ut 8'd	1,17343	0,506613	0,573275	102,101	10,88419	12,31639
Scarb1	BM Het ut 6'd	9,15573	4,235473	4,792801			
	BM Het ut 7'd	9,39143	4,178264	4,728064			
	BM Het ut 8'd	8,87355	2,450949	2,773459			
	BM KO ut 6'd	11,0777	5,65804	6,402557	121,119	49,45558	55,96323
	BM KO ut 7'd	10,8193	4,971034	5,625151	115,884	17,29606	19,57197
	BM KO ut 8'd	8,26069	0,936027	1,059195	97,943	27,58988	31,22032
Scd1	BM Het ut 6'd	14,5848	16,18596	18,3158			
	BM Het ut 7'd	19,0783	8,223991	9,306151			
	BM Het ut 8'd	20,1568	2,222471	2,514917			
	BM KO ut 6'd	20,792	11,18272	12,6542	245,387	164,6725	186,341
	BM KO ut 7'd	24,7035	9,781079	11,06813	134,887	40,43774	45,75877
	BM KO ut 8'd	12,9709	8,170954	9,246135	63,6357	36,5561	41,36636
Scd2	BM Het ut 6'd	40,241	32,64178	36,93698			
	BM Het ut 7'd	64,3793	34,71707	39,28535			
	BM Het ut 8'd	44,2885	16,16209	18,28879			
	BM KO ut 6'd	72,6323	59,29155	67,09348	219,858	137,3973	155,4768
	BM KO ut 7'd	77,8279	54,31891	61,46651	115,65	21,44445	24,26623
	BM KO ut 8'd	28,3548	13,17574	14,90948	65,5583	32,46485	36,73677
Srebf1a	BM Het ut 6'd	8,95856	4,003708	4,530538			
	BM Het ut 7'd	9,06911	3,561396	4,030025			
	BM Het ut 8'd	6,96089	3,215778	3,638928			
	BM KO ut 6'd	9,02267	4,52444	5,119792	97,9674	12,67671	14,34479
	BM KO ut 7'd	8,03457	2,518392	2,849776	91,113	10,00763	11,32449
	BM KO ut 8'd	5,76725	2,889673	3,269913	88,8517	31,78153	35,96353
Srebf1c	BM Het ut 6'd	1,69568	1,883763	2,131639			
	BM Het ut 7'd	1,82775	0,868239	0,982487			
	BM Het ut 8'd	0,81224	0,212638	0,240618			
	BM KO ut 6'd	1,63364	0,804585	0,910456	167,471	110,0916	124,5781
	BM KO ut 7'd	1,74343	0,728208	0,82403	97,1574	5,894667	6,670321
	BM KO ut 8'd	0,61385	0,427931	0,48424	70,4396	30,12978	34,09443
Srebf2	BM Het ut 6'd	15,7797	7,586886	8,585212			
	BM Het ut 7'd	16,4442	6,481176	7,334006			
	BM Het ut 8'd	13,183	3,096143	3,503551			
	BM KO ut 6'd	19,8511	8,194197	9,272437	128,591	8,713706	9,860305
	BM KO ut 7'd	17,7559	4,504258	5,096954	112,397	18,53504	20,97399
	BM KO ut 8'd	10,9298	4,878834	5,520818	81,8821	24,83066	28,09802
Star	BM Het ut 6'd	0,0559	0,021743	0,024604			
	BM Het ut 7'd	0,05305	0,017264	0,019535			
	BM Het ut 8'd	0,08668	0,04406	0,049857			
	BM KO ut 6'd	0,05861	0,022257	0,025185	105,324	20,91546	23,66764
	BM KO ut 7'd	0,04751	0,004387	0,004964	93,9814	20,59422	23,30412
	BM KO ut 8'd	0,05592	0,01076	0,012176	82,2503	54,62529	61,8132
2x							
Acat1	BM Het ut 6'd	7,74854	0,631441	0,714529			
	BM Het ut 7'd	6,95491	0,549778	0,622121			
	BM Het ut 8'd	5,54602	0,048249	0,054597			
	BM KO ut 6'd	7,15637	0,353067	0,399525	92,8517	12,12319	13,71843
	BM KO ut 7'd	7,07935	0,431548	0,488334	102,354	14,29593	16,17707
	BM KO ut 8'd	6,11686	0,083193	0,09414	110,291	0,540564	0,611694
Hdlbp	BM Het ut 6'd	13,2188	4,331857	4,901867			
	BM Het ut 7'd	14,0978	4,288188	4,852452			
	BM Het ut 8'd	19,9044	9,345179	10,57487			
	BM KO ut 6'd	14,4188	5,153464	5,831587	108,516	3,424668	3,875305
	BM KO ut 7'd	14,0301	5,173132	5,853842	98,4955	6,734826	7,621034
	BM KO ut 8'd	15,1804	4,993613	5,650701	79,0947	12,04718	13,63242
Lipa	BM Het ut 6'd	143,978	29,25752	33,10739			
	BM Het ut 7'd	140,663	71,98814	81,46075			
	BM Het ut 8'd	183	93,15456	105,4124			
	BM KO ut 6'd	140,266	55,60978	62,92723	95,4689	19,22375	21,75332

	BM KO ut 7'd	161,988	78,75716	89,12048	116,028	3,390511	3,836654
	BM KO ut 8'd	189,701	67,38086	76,24722	108,325	18,32171	20,73259
Lipe	BM Het ut 6'd	0,68285	0,443973	0,502393			
	BM Het ut 7'd	0,90065	0,638979	0,723059			
	BM Het ut 8'd	1,70787	1,203602	1,361979			
	BM KO ut 6'd	0,97157	0,677451	0,766594	139,52	8,496821	9,614881
	BM KO ut 7'd	1,26932	0,718069	0,812556	150,538	27,07341	30,63589
	BM KO ut 8'd	1,64092	0,561154	0,634993	112,418	46,36867	52,47013
Lss (Osc)	BM Het ut 6'd	1,82518	0,122063	0,138125			
	BM Het ut 7'd	2,34042	0,25638	0,290116			
	BM Het ut 8'd	1,6917	0,073274	0,082916			
	BM KO ut 6'd	2,48939	1,002225	1,134103	134,857	45,89213	51,93088
	BM KO ut 7'd	2,05992	0,464912	0,526087	87,4515	10,28464	11,63795
	BM KO ut 8'd	0,83963	0,206223	0,233359	49,4143	10,04991	11,37234
Msr2	BM Het ut 6'd	0,87183	0,566044	0,640527			
	BM Het ut 7'd	2,10133	0,757654	0,85735			
	BM Het ut 8'd	14,8908	1,848786	2,09206			
	BM KO ut 6'd	1,75439	1,380097	1,561698	189,86	35,03063	39,64017
	BM KO ut 7'd	6,68295	4,114591	4,656012	302,39	86,77948	98,19842
	BM KO ut 8'd	36,0879	1,556806	1,76166	244,887	40,85913	46,23561
Ppard	BM Het ut 6'd	0,8119	0,037184	0,042077			
	BM Het ut 7'd	0,98831	0,245332	0,277614			
	BM Het ut 8'd	2,50326	0,37672	0,426291			
	BM KO ut 6'd	0,78544	0,007302	0,008263	96,8629	5,335545	6,037626
	BM KO ut 7'd	1,14754	0,160615	0,18175	117,721	12,97082	14,6776
	BM KO ut 8'd	1,83272	0,398936	0,45143	75,2645	27,26331	30,85077
Ppargc1a	BM Het ut 6'd	0,00568	0,000578	0,000654			
	BM Het ut 7'd	0,00392	0,001728	0,001956			
	BM Het ut 8'd	0,00662	0,000799	0,000904			
	BM KO ut 6'd	0,00481	0,000581	0,000658	84,6061	1,629588	1,844019
	BM KO ut 7'd	0,0046	0,001486	0,001681	120,871	15,38496	17,4094
	BM KO ut 8'd	0,00609	0,00213	0,00241	90,6672	21,23103	24,02473
Ppargc1b	BM Het ut 6'd	1,276	0,696112	0,78771			
	BM Het ut 7'd	1,07507	0,42682	0,482983			
	BM Het ut 8'd	1,77874	1,125015	1,27305			
	BM KO ut 6'd	1,01406	0,626691	0,709155	77,6269	6,764964	7,655137
	BM KO ut 7'd	0,95697	0,547692	0,619761	85,6522	16,93953	19,16853
	BM KO ut 8'd	1,667	0,90065	1,019163	97,1336	10,80072	12,22194
Rxra	BM Het ut 6'd	0,09396	0,044386	0,050226			
	BM Het ut 7'd	0,07452	0,002496	0,002825			
	BM Het ut 8'd	0,21359	0,065362	0,073963			
	BM KO ut 6'd	0,08959	0,008099	0,009165	105,038	41,00027	46,39533
	BM KO ut 7'd	0,07461	0,012513	0,01416	99,8919	13,44519	15,21438
	BM KO ut 8'd	0,19511	0,072847	0,082432	90,3607	6,453968	7,303218
Shp	BM Het ut 6'd	0,07538	0,008586	0,009716			
	BM Het ut 7'd	0,08169	0,009049	0,01024			
	BM Het ut 8'd	0,08377	0,018564	0,021007			
	BM KO ut 6'd	0,08406	0,023047	0,02608	110,496	17,98911	20,35622
	BM KO ut 7'd	0,09899	0,024847	0,028116	120,237	17,09689	19,3466
	BM KO ut 8'd	0,0922	0,056253	0,063655	105,213	43,83708	49,60542
Sult2b1	BM Het ut 6'd	0,0135	0,010392	0,011759			
	BM Het ut 7'd	0,01171	0,007351	0,008319			
	BM Het ut 8'd	0,02114	0,008756	0,009908			
	BM KO ut 6'd	0,01487	0,008414	0,009521	122,482	31,96575	36,17198
	BM KO ut 7'd	0,0194	0,009353	0,010584	175,02	29,99584	33,94286
	BM KO ut 8'd	0,02746	0,020838	0,02358	119,728	48,97768	55,42244

DISCUSSION

1. Jarid1b expression is modulated by inflammatory stimuli and hypoxic stress

In this thesis, using a candidate approach, we demonstrated that the H3K4 demethylase Jarid1b, is strongly up-regulated in LPS-stimulated macrophages with a comparatively slow kinetics, raising the question of whether Jarid1b might be involved in the transcriptional regulation of the inflammatory response.

A very similar induction in Jarid1b expression levels was reached when macrophages were exposed to low oxygen concentration. Jarid1b has been recently shown in literature to be up-regulated by the hypoxia-inducible factor 1 alpha (Hif1α) in HepG2 cell line and mouse embryonic fibroblasts (MEFs) exposed to hypoxic conditions (46) (111); moreover Hif1α has been demonstrated to be transcriptionally up-regulated in response to inflammatory stimuli by NF-κB (76). In fact, we found that Hif1α binds to Jarid1b promoter in an LPS-dependent manner, strongly suggesting that also LPS-triggered Jarid1b up-regulation is controlled by this transcription factor. However, to formally prove that Hif1α drives the induction of Jarid1b also in an inflammatory context it would be necessary to determine if the LPS-dependent Jarid1b up-regulation is completely abolished in Hif1α null cells. This experiment would also answer another question, namely whether Hif1α is the main transcription factor controlling Jarid1b induction. In fact, the only partial impairment of Jarid1b up-regulation in absence of Hif1α would imply the existence of one or more other transcription factors involved in Jarid1b transcriptional control.

Interestingly, Jarid1b is the only member of the JARID1 family showing a modulated expression in response to both LPS stimulation and hypoxic stress.

The appearance of four different JARID1 proteins in higher eukaryotes is probably due to a functional specialization of the different members of the family, and Jarid1b is the most

divergent family member (see Figure 10). Therefore it is not unlikely that Jarid1b has evolved a completely distinct (or minimally overlapping) biological function, indeed its closest homolog Jarid1a has a completely uniform and flat expression profile in response to LPS stimulation.

More difficult it is to understand the biological meaning of Jarid1b up-regulation. In fact, although Jarid1b is the only JARID1 protein whose expression is induced by inflammatory stimuli and hypoxia, there are many other JmjC domain containing proteins that are modulated by the same environmental stresses (e.g. Jmjd1a, Jmjd3 and Jmjd2b).

Concerning the JmjC proteins hypoxia-induced up-regulation Xia and co-workers proposed that, because the hydroxylation and demethylation reactions catalyzed by 2-OG dioxygenases require molecular oxygen, the up-regulated expression of these enzymes under hypoxia may be a compensatory mechanism in response to decreasing oxygen tension (111). However, this hypothesis is counterintuitive: although an increased JmjC proteins production would give them an advantage in competing with other cellular oxygen-requiring processes for the limited oxygen availability, it would also result in an overload of inactive enzymes, just because of the oxygen deficiency. Moreover, Krieg and coll. have recently shown that Jmjd1a is enzymatically active in cells even under restrictive oxygen concentrations (46), suggesting that JmjC protein up-regulation is likely necessary for the realization of a specific functional program, rather than a simple adaptation to the oxygen scarceness.

Therefore, it would be intriguing to elucidate the role of Jarid1b in both inflammatory and hypoxia pathways, since the proposed function of Jarid1b in sustaining cellular proliferation hardly fits these two cellular contexts. In fact, LPS stimulation directs macrophages toward terminal differentiation; inflammation represents an energy costly endeavour for the cell; and during hypoxia, cellular metabolism is dampened by the limited oxygen availability; these are situations in which cells most unlikely will undergo cellular division.

Since LPS- and hypoxia-triggered Jarid1b up-regulation reaches almost identical levels and is, apparently, under the control of the same transcription factor (Hif1α), there is the possibility that it takes place to execute the same cellular program.

Different possible strategies may be applied to unravel the transcriptional network regulated by Jarid1b. One strategy may rely on a bioinformatic approach and would consist in the comparison of global gene expression profile of cells (macrophages) subjected to LPS or hypoxic stimulations; those genes whose expression is similarly altered in the two datasets and with a kinetics coherent with Jarid1b induction would be candidate genes. However, this kind of approach may retrieve a large amount of data difficult to be interpreted and, being based on simple correlations, might be misleading.

A distinct approach is the global gene expression profiling of cells in which physiological protein levels have been altered by over-expression or depletion.

2. Jarid1b depletion impairs LXR activation

We followed the second kind of approach, and cDNA microarray analysis showed that the depletion of Jarid1b in primary macrophages resulted in the down-regulation of a limited number of genes, all involved in the cholesterol metabolism and all controlled by the same transcription factor, the nuclear receptor LXR. Interestingly, LXR not only is a master regulator of cholesterol metabolism but is also involved in the negative regulation of some inflammatory genes (12). In addition, LXRα protein is induced by LPS stimulation with a kinetics compatible with Jarid1b up-regulation (see Figure 26B).

The treatment with oxysterols led to a normal expression of LXR target genes also in Jarid1b-depleted cells, indicating that LXR is functional even in the absence of Jarid1b. Moreover, we identified the 27-hydroxycholesterol as the main physiological LXR ligand in macrophages, and we found that the expression of Cyp27a1, the enzyme catalyzing its production, was impaired after Jarid1b knock-down. The collected data suggest that Jarid1b regulates the activation of LXR by controlling the oxysterols production.

Unluckily, the effect of Jarid1b depletion on LXR target gene expression was inconstant, possibly because of the high reactivity of LXRs to environmental cues, thus hindering a deeper understanding of the molecular mechanism linking Jarid1b to LXR activation. We could only envision the possibility that Jarid1b depletion affected LXR target genes expression only in particular macrophages sub-populations, as suggested by the expression analysis of the membrane receptors Ccr2 and Cx3cr1. These two cell-surface markers have been used, together with the granulocyte receptor 1 (Gr1), to define in mice two distinct macrophages populations that differ primarily on the amount of time they spend in the bloodstream before migrating into tissues. Inflammatory monocytes rapidly exit the blood and are defined as $Ccr2^{+}Cx3cr1^{low}Gr1^{+}$, whereas resident monocytes are characterized as $Ccr2^{-}Cx3cr1^{hi}Gr1^{-}$ (60).

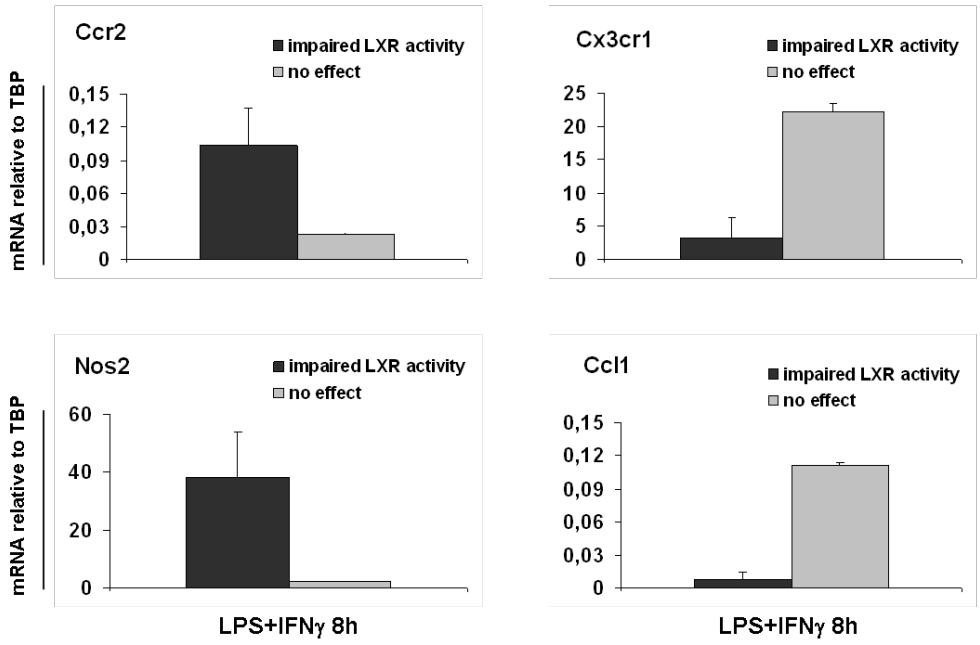

Figure 53 - Jarid1b depletion might affect LXR activity in specific macrophage sub-populations.
Wild-type macrophages (infected with the LMP empty vector) from different preparations were compared in the expression levels of some markers used for macrophage sub-populations classification. Those macrophages in which we detected a LXR target genes expression impairment following Jarid1b depletion, expressed high levels of *Ccr2* and *Nos2* and low levels of *Cx3cr1* and *Ccl1*, properties typically associated with inflammatory macrophages. Error bars represent standard deviation of 3 (impaired LXR activity) and 2 (no effect) independent replicates.

Although the significance of this classification remains elusive when applied to cultured macrophages, it appeared clear that the depletion of Jarid1b impaired LXR activity in "inflammatory" but not in "resident" macrophages (Figure 53). When we extended the

analysis to other macrophage classification criteria, like the balance between Il-12 and Il-10 production, we could not find any significant discrepancy among the different samples showing an opposite LXR activity outcome. Nevertheless, macrophage preparations in which we could not detect any Jarid1b-dependent reduced LXR target gene expression, showed an increased production of *Ccl1* accompanied by a strong reduction in *Nos2* expression levels, characteristic of regulatory macrophages (60).

A clean *in vivo* experiment to confirm the link between Jarid1b expression and LXR activity, irrespective of the underlying molecular mechanism, can be done in Jarid1b-KO mice. Indeed, a seminal work by Mangelsdorf and co-workers demonstrated that LXRα loss resulted in a rapid accumulation of hepatic cholesteryl esters when mice were fed with a high cholesterol diet (70). LXRα heterozygous mice showed an intermediate phenotype still with an important increase in hepatic cholesterol levels, indicating that LXRα needs to be fully active to exert its function. Hence, if Jarid1b deprivation dampens LXRα activity, even partially, this would produce a detectable outcome, that would be immediately visible in the case of a severe LXRα activity impairment (fat livers similar to LXRα null mice) or inferable from LXR target genes expression analysis and hepatic cholesterol measurement.

3. Jarid1b is not a general transcriptional regulator in macrophages

The generation of knock-out mice provided us a powerful tool for studying Jarid1b biological function. However, when we characterized the transcriptome of Jarid1b-ablated macrophages we found only a very little number of genes whose transcription was altered by Jarid1b absence and any affected pathway could not be identified.

This transcriptional outcome was, at least in part, surprising for a protein reported to be a H3K4 demethylase and a transcriptional repressor. Nonetheless, several are the possible explanations.

First of all there is the possibility of compensatory effects due to the presence of the other three JARID1 proteins. Although this is not likely to happen, because Jarid1b is the most

divergent member of the JARID1 family and the other JARID1 genes appeared to be unresponsive to the stimuli triggering Jarid1b up-regulation, this hypothesis can not be *a priori* excluded. Also the observation that neither *Jarid1a*, nor *Jarid1c* or *Jarid1d* are up-regulated in Jarid1b-KO cells is enough to exclude this hypothesis, because their physiological levels might be sufficient to compensate Jarid1b absence.

Another possibility is that Jarid1b acts as a H3K4 demethylase on its target genes, but the increased methylation levels deriving from Jarid1b deprivation are not sufficient to provoke an alteration in target genes transcription because of the presence of other layers of regulation. In fact, as mentioned before, it has been demonstrated that although Jarid1b over-expression in Hep3b cells led to a global decrease in H3K4me3 and me2 levels, it was not accompanied by a detectable reduction in PolII-CTD phosphorylation (90), suggesting that alterations in Jarid1b levels might not alter RNA PolII transcription.

A third hypothesis is that, even if Jarid1b is able to demethylate lysine 4 on histone 3 when over-expressed, this is not the (only) physiological target of Jarid1b enzymatic activity. Indeed, when we investigated Jarid1b chromatin binding by ChIP-sequencing we could retrieve only a limited number (72) of genomic targets. We also observed that, although a forced expression of Jarid1b led to a reduction of H3K4me3 global levels and this reduction was dependent on Jarid1b enzymatic activity, a modest ectopic expression as well as the ablation of Jarid1b did not result in any substantial alteration of this histone mark. Nevertheless, these data must be evaluated with caution because they could also find explanations associated to technical issues (such as a limited immunoprecipitation efficiency for the little number of targets identified in the ChIP-seq).

Above all, genome-wide analysis of H3K4me3 (and maybe H3K4me2) levels in Jarid1b-KO cells is needed to determine if the effects of Jarid1b deprivation on this chromatin mark can be appreciated at single genes level, thus confirming Jarid1b function as a H3K4 demethylase.

Together these observations at least raise the doubt that histones may be not the (only) physiological substrate of Jarid1b activity. This hypothesis is not completely naïve: for instance, the non-histone protein p53 have been shown to be demethylated on selected lysine residues by the H3K4me2/1 specific demethylase LSD1 (39). Moreover, in a previous work, we showed that the transcriptional effects of the H3K27 demethylase Jmjd3 in LPS-activated macrophages are largely independent of H3K27me3 demethylation (17).

Another hypothesis is that Jarid1b may exert an unreported non-enzymatic function, for instance plying structural roles in multi-molecular complexes. For example, Jarid2 has been demonstrated to interact with the Polycomb repressive complex 2 (PRC2) and to be required for the efficient binding of PRC2 to its target genes; moreover Jarid2 lacks the lysine demethylase activity and has been shown to inhibit the PRC2 methyltranferase activity *in vitro* through a non-enzymatic mechanism (68) (71) (91).

Intriguingly in this direction is our finding that Jarid1b ablation resulted in the impaired expression of some small nucleolar RNAs (snoRNAs) reported to be involved in 2'-O-methylation of ribosomal RNA (rRNA). Although this effect may simply result from a reduced transcription of the snoRNAs host gene (but this seems not to be the case as the snoRNAs expression impairment is evident even in situations in which *Gas5* expression is not altered), it might be a mechanism aimed at counterbalancing increased rRNA methylation levels. In this scenario Jarid1b might behave as a RNA demethylase and its absence would result in increased rRNA methylation levels triggering the reduction in snoRNAs expression.

4. Jarid1b and cell proliferation

One of the most consistently down-regulated genes in Jarid1b-ablated macrophages is the *Mcm6* gene, encoding for a helicase that separate DNA strands during DNA replication. *Mcm6* is expressed at low levels in early G1 phase and its subsequent accumulation through this phase of the cell cycle is important for the G1/S transition. This observation is

in agreement with the putative role of Jarid1b in facilitating the G1/S transition reported in literature, but would need to be further explored in a different cellular system (active cycling cells).

A recently published paper by Roesch and coll. showed that in melanoma Jarid1b was highly expressed only in a restricted population of slow-cycling cells with stem cell-like properties (78). They proposed a model in which Jarid1b has a dual role over time, immediately anti-proliferative but long-term tumour maintaining.

This work aroused a great interest about a possible function for Jarid1b in cell replication and self-renewal capacity. However, the observation that long-term culture of sorted Jarid1b-positive cells give rise to a heterogeneous daughter population, consisting of Jarid1b-positive and -negative cells (and vice versa), together with the finding that other JmjC proteins (e.g. JMJD1A) could be differentially regulated among slow- and normal-cycling cell sub-populations, raised the possibility that high Jarid1b expression levels in slow-cycling cell population might be merely correlative, and simply consequent to a hypoxic environment.

The availability of Jarid1b-KO cells would allow us to elucidate a possible role for Jarid1b in cellular proliferation and self-renewal through functional assays, like reconstitution of lethally irradiated recipient mice, and to investigate the influence of Jarid1b-deprivation on *in vivo* tumor growth by xenograft experiments.

Altogether our and published data suggest at least two distinct functions for Jarid1b: one linked to cell proliferation in active cycling cell populations, and one associated to inflammatory and hypoxic stresses response in macrophages. Nonetheless further studies are necessary to unravel the molecular mechanisms underlying both these two functions.

BIBLIOGRAPHY

1. **Allfrey, V. G., R. Faulkner, and A. E. Mirsky.** 1964. Acetylation and Methylation of Histones and Their Possible Role in the Regulation of Rna Synthesis. Proc Natl Acad Sci U S A **51:**786-94.
2. **Alon, U.** 2007. Network motifs: theory and experimental approaches. Nat Rev Genet **8:**450-61.
3. **Bannister, A. J., and T. Kouzarides.** 2004. Histone methylation: recognizing the methyl mark. Methods Enzymol **376:**269-88.
4. **Barrett, A., B. Madsen, J. Copier, P. J. Lu, L. Cooper, A. G. Scibetta, J. Burchell, and J. Taylor-Papadimitriou.** 2002. PLU-1 nuclear protein, which is upregulated in breast cancer, shows restricted expression in normal human adult tissues: a new cancer/testis antigen? Int J Cancer **101:**581-8.
5. **Bedford, M. T., and S. Richard.** 2005. Arginine methylation an emerging regulator of protein function. Mol Cell **18:**263-72.
6. **Benevolenskaya, E. V., H. L. Murray, P. Branton, R. A. Young, and W. G. Kaelin, Jr.** 2005. Binding of pRB to the PHD protein RBP2 promotes cellular differentiation. Mol Cell **18:**623-35.
7. **Bernstein, B. E., M. Kamal, K. Lindblad-Toh, S. Bekiranov, D. K. Bailey, D. J. Huebert, S. McMahon, E. K. Karlsson, E. J. Kulbokas, 3rd, T. R. Gingeras, S. L. Schreiber, and E. S. Lander.** 2005. Genomic maps and comparative analysis of histone modifications in human and mouse. Cell **120:**169-81.
8. **Bernstein, B. E., A. Meissner, and E. S. Lander.** 2007. The mammalian epigenome. Cell **128:**669-81.
9. **Borun, T. W., D. Pearson, and W. K. Paik.** 1972. Studies of histone methylation during the HeLa S-3 cell cycle. J Biol Chem **247:**4288-98.
10. **Briggs, S. D., M. Bryk, B. D. Strahl, W. L. Cheung, J. K. Davie, S. Y. Dent, F. Winston, and C. D. Allis.** 2001. Histone H3 lysine 4 methylation is mediated by Set1 and required for cell growth and rDNA silencing in Saccharomyces cerevisiae. Genes Dev **15:**3286-95.
11. **Byvoet, P., G. R. Shepherd, J. M. Hardin, and B. J. Noland.** 1972. The distribution and turnover of labeled methyl groups in histone fractions of cultured mammalian cells. Arch Biochem Biophys **148:**558-67.
12. **Castrillo, A., S. B. Joseph, S. A. Vaidya, M. Haberland, A. M. Fogelman, G. Cheng, and P. Tontonoz.** 2003. Crosstalk between LXR and toll-like receptor signaling mediates bacterial and viral antagonism of cholesterol metabolism. Mol Cell **12:**805-16.
13. **Castrillo, A., and P. Tontonoz.** 2004. Nuclear receptors in macrophage biology: at the crossroads of lipid metabolism and inflammation. Annu Rev Cell Dev Biol **20:**455-80.
14. **Charriere, G., B. Cousin, E. Arnaud, M. Andre, F. Bacou, L. Penicaud, and L. Casteilla.** 2003. Preadipocyte conversion to macrophage. Evidence of plasticity. J Biol Chem **278:**9850-5.
15. **Christensen, J., K. Agger, P. A. Cloos, D. Pasini, S. Rose, L. Sennels, J. Rappsilber, K. H. Hansen, A. E. Salcini, and K. Helin.** 2007. RBP2 belongs to a family of demethylases, specific for tri-and dimethylated lysine 4 on histone 3. Cell **128:**1063-76.
16. **D'Souza, B., F. Berdichevsky, N. Kyprianou, and J. Taylor-Papadimitriou.** 1993. Collagen-induced morphogenesis and expression of the alpha 2-integrin

subunit is inhibited in c-erbB2-transfected human mammary epithelial cells. Oncogene **8:**1797-806.

17. **De Santa, F., V. Narang, Z. H. Yap, B. K. Tusi, T. Burgold, L. Austenaa, G. Bucci, M. Caganova, S. Notarbartolo, S. Casola, G. Testa, W. K. Sung, C. L. Wei, and G. Natoli.** 2009. Jmjd3 contributes to the control of gene expression in LPS-activated macrophages. Embo J **28:**3341-52.
18. **De Santa, F., M. G. Totaro, E. Prosperini, S. Notarbartolo, G. Testa, and G. Natoli.** 2007. The histone H3 lysine-27 demethylase Jmjd3 links inflammation to inhibition of polycomb-mediated gene silencing. Cell **130:**1083-94.
19. **Demas, G. E., V. Chefer, M. I. Talan, and R. J. Nelson.** 1997. Metabolic costs of mounting an antigen-stimulated immune response in adult and aged C57BL/6J mice. Am J Physiol **273:**R1631-7.
20. **Dickins, R. A., M. T. Hemann, J. T. Zilfou, D. R. Simpson, I. Ibarra, G. J. Hannon, and S. W. Lowe.** 2005. Probing tumor phenotypes using stable and regulated synthetic microRNA precursors. Nat Genet **37:**1289-95.
21. **Dou, Y., T. A. Milne, A. J. Ruthenburg, S. Lee, J. W. Lee, G. L. Verdine, C. D. Allis, and R. G. Roeder.** 2006. Regulation of MLL1 H3K4 methyltransferase activity by its core components. Nat Struct Mol Biol **13:**713-9.
22. **Fodor, B. D., S. Kubicek, M. Yonezawa, R. J. O'Sullivan, R. Sengupta, L. Perez-Burgos, S. Opravil, K. Mechtler, G. Schotta, and T. Jenuwein.** 2006. Jmjd2b antagonizes H3K9 trimethylation at pericentric heterochromatin in mammalian cells. Genes Dev **20:**1557-62.
23. **Foster, S. L., D. C. Hargreaves, and R. Medzhitov.** 2007. Gene-specific control of inflammation by TLR-induced chromatin modifications. Nature **447:**972-8.
24. **Foster, S. L., and R. Medzhitov.** 2009. Gene-specific control of the TLR-induced inflammatory response. Clin Immunol **130:**7-15.
25. **Friedman, A. D.** 2007. Transcriptional control of granulocyte and monocyte development. Oncogene **26:**6816-28.
26. **Fu, X., J. G. Menke, Y. Chen, G. Zhou, K. L. MacNaul, S. D. Wright, C. P. Sparrow, and E. G. Lund.** 2001. 27-hydroxycholesterol is an endogenous ligand for liver X receptor in cholesterol-loaded cells. J Biol Chem **276:**38378-87.
27. **Gerken, T., C. A. Girard, Y. C. Tung, C. J. Webby, V. Saudek, K. S. Hewitson, G. S. Yeo, M. A. McDonough, S. Cunliffe, L. A. McNeill, J. Galvanovskis, P. Rorsman, P. Robins, X. Prieur, A. P. Coll, M. Ma, Z. Jovanovic, I. S. Farooqi, B. Sedgwick, I. Barroso, T. Lindahl, C. P. Ponting, F. M. Ashcroft, S. O'Rahilly, and C. J. Schofield.** 2007. The obesity-associated FTO gene encodes a 2-oxoglutarate-dependent nucleic acid demethylase. Science **318:**1469-72.
28. **Ghisletti, S., I. Barozzi, F. Mietton, S. Polletti, F. De Santa, E. Venturini, L. Gregory, L. Lonie, A. Chew, C. L. Wei, J. Ragoussis, and G. Natoli.** Identification and characterization of enhancers controlling the inflammatory gene expression program in macrophages. Immunity **32:**317-28.
29. **Ghisletti, S., W. Huang, K. Jepsen, C. Benner, G. Hardiman, M. G. Rosenfeld, and C. K. Glass.** 2009. Cooperative NCoR/SMRT interactions establish a corepressor-based strategy for integration of inflammatory and anti-inflammatory signaling pathways. Genes Dev **23:**681-93.
30. **Ghisletti, S., W. Huang, S. Ogawa, G. Pascual, M. E. Lin, T. M. Willson, M. G. Rosenfeld, and C. K. Glass.** 2007. Parallel SUMOylation-dependent pathways mediate gene- and signal-specific transrepression by LXRs and PPARgamma. Mol Cell **25:**57-70.
31. **Gildea, J. J., R. Lopez, and A. Shearn.** 2000. A screen for new trithorax group genes identified little imaginal discs, the Drosophila melanogaster homologue of human retinoblastoma binding protein 2. Genetics **156:**645-63.

32. **Glass, C. K., and S. Ogawa.** 2006. Combinatorial roles of nuclear receptors in inflammation and immunity. Nat Rev Immunol **6:**44-55.
33. **Glass, C. K., and M. G. Rosenfeld.** 2000. The coregulator exchange in transcriptional functions of nuclear receptors. Genes Dev **14:**121-41.
34. **Hayami, S., M. Yoshimatsu, A. Veerakumarasivam, M. Unoki, Y. Iwai, T. Tsunoda, H. I. Field, J. D. Kelly, D. E. Neal, H. Yamaue, B. A. Ponder, Y. Nakamura, and R. Hamamoto.** Overexpression of the JmjC histone demethylase KDM5B in human carcinogenesis: involvement in the proliferation of cancer cells through the E2F/RB pathway. Mol Cancer **9:**59.
35. **Henras, A. K., J. Soudet, M. Gerus, S. Lebaron, M. Caizergues-Ferrer, A. Mougin, and Y. Henry.** 2008. The post-transcriptional steps of eukaryotic ribosome biogenesis. Cell Mol Life Sci **65:**2334-59.
36. **Horton, J. D., J. L. Goldstein, and M. S. Brown.** 2002. SREBPs: activators of the complete program of cholesterol and fatty acid synthesis in the liver. J Clin Invest **109:**1125-31.
37. **Hotamisligil, G. S.** 2006. Inflammation and metabolic disorders. Nature **444:**860-7.
38. **Hotamisligil, G. S., and E. Erbay.** 2008. Nutrient sensing and inflammation in metabolic diseases. Nat Rev Immunol **8:**923-34.
39. **Huang, J., R. Sengupta, A. B. Espejo, M. G. Lee, J. A. Dorsey, M. Richter, S. Opravil, R. Shiekhattar, M. T. Bedford, T. Jenuwein, and S. L. Berger.** 2007. p53 is regulated by the lysine demethylase LSD1. Nature **449:**105-8.
40. **Huff, M. W., and D. E. Telford.** 2005. Lord of the rings--the mechanism for oxidosqualene:lanosterol cyclase becomes crystal clear. Trends Pharmacol Sci **26:**335-40.
41. **Iwase, S., F. Lan, P. Bayliss, L. de la Torre-Ubieta, M. Huarte, H. H. Qi, J. R. Whetstine, A. Bonni, T. M. Roberts, and Y. Shi.** 2007. The X-linked mental retardation gene SMCX/JARID1C defines a family of histone H3 lysine 4 demethylases. Cell **128:**1077-88.
42. **Joseph, S. B., M. N. Bradley, A. Castrillo, K. W. Bruhn, P. A. Mak, L. Pei, J. Hogenesch, M. O'Connell R, G. Cheng, E. Saez, J. F. Miller, and P. Tontonoz.** 2004. LXR-dependent gene expression is important for macrophage survival and the innate immune response. Cell **119:**299-309.
43. **Joseph, S. B., A. Castrillo, B. A. Laffitte, D. J. Mangelsdorf, and P. Tontonoz.** 2003. Reciprocal regulation of inflammation and lipid metabolism by liver X receptors. Nat Med **9:**213-9.
44. **Karin, M., and Y. Ben-Neriah.** 2000. Phosphorylation meets ubiquitination: the control of NF-[kappa]B activity. Annu Rev Immunol **18:**621-63.
45. **Klose, R. J., Q. Yan, Z. Tothova, K. Yamane, H. Erdjument-Bromage, P. Tempst, D. G. Gilliland, Y. Zhang, and W. G. Kaelin, Jr.** 2007. The retinoblastoma binding protein RBP2 is an H3K4 demethylase. Cell **128:**889-900.
46. **Krieg, A. J., E. B. Rankin, D. Chan, O. Razorenova, S. Fernandez, and A. J. Giaccia.** Regulation of the histone demethylase JMJD1A by hypoxia-inducible factor 1 alpha enhances hypoxic gene expression and tumor growth. Mol Cell Biol **30:**344-53.
47. **Leclerc, V., and J. M. Reichhart.** 2004. The immune response of Drosophila melanogaster. Immunol Rev **198:**59-71.
48. **Lee, C. H., A. Chawla, N. Urbiztondo, D. Liao, W. A. Boisvert, R. M. Evans, and L. K. Curtiss.** 2003. Transcriptional repression of atherogenic inflammation: modulation by PPARdelta. Science **302:**453-7.
49. **Lee, M. G., J. Norman, A. Shilatifard, and R. Shiekhattar.** 2007. Physical and functional association of a trimethyl H3K4 demethylase and Ring6a/MBLR, a polycomb-like protein. Cell **128:**877-87.

50. **Ley, K., C. Laudanna, M. I. Cybulsky, and S. Nourshargh.** 2007. Getting to the site of inflammation: the leukocyte adhesion cascade updated. Nat Rev Immunol **7:**678-89.
51. **Liang, G., R. J. Klose, K. E. Gardner, and Y. Zhang.** 2007. Yeast Jhd2p is a histone H3 Lys4 trimethyl demethylase. Nat Struct Mol Biol **14:**243-5.
52. **Litvak, V., S. A. Ramsey, A. G. Rust, D. E. Zak, K. A. Kennedy, A. E. Lampano, M. Nykter, I. Shmulevich, and A. Aderem.** 2009. Function of C/EBPdelta in a regulatory circuit that discriminates between transient and persistent TLR4-induced signals. Nat Immunol **10:**437-43.
53. **Loenarz, C., and C. J. Schofield.** 2008. Expanding chemical biology of 2-oxoglutarate oxygenases. Nat Chem Biol **4:**152-6.
54. **Lu, P. J., K. Sundquist, D. Baeckstrom, R. Poulsom, A. Hanby, S. Meier-Ewert, T. Jones, M. Mitchell, P. Pitha-Rowe, P. Freemont, and J. Taylor-Papadimitriou.** 1999. A novel gene (PLU-1) containing highly conserved putative DNA/chromatin binding motifs is specifically up-regulated in breast cancer. J Biol Chem **274:**15633-45.
55. **Madsen, B., M. Tarsounas, J. M. Burchell, D. Hall, R. Poulsom, and J. Taylor-Papadimitriou.** 2003. PLU-1, a transcriptional repressor and putative testis-cancer antigen, has a specific expression and localisation pattern during meiosis. Chromosoma **112:**124-32.
56. **Mangan, S., A. Zaslaver, and U. Alon.** 2003. The coherent feedforward loop serves as a sign-sensitive delay element in transcription networks. J Mol Biol **334:**197-204.
57. **Martin, C., and Y. Zhang.** 2005. The diverse functions of histone lysine methylation. Nat Rev Mol Cell Biol **6:**838-49.
58. **Medzhitov, R., and T. Horng.** 2009. Transcriptional control of the inflammatory response. Nat Rev Immunol **9:**692-703.
59. **Milo, R., S. Itzkovitz, N. Kashtan, R. Levitt, S. Shen-Orr, I. Ayzenshtat, M. Sheffer, and U. Alon.** 2004. Superfamilies of evolved and designed networks. Science **303:**1538-42.
60. **Mosser, D. M., and J. P. Edwards.** 2008. Exploring the full spectrum of macrophage activation. Nat Rev Immunol **8:**958-69.
61. **Murray, K.** 1964. The Occurrence of Epsilon-N-Methyl Lysine in Histones. Biochemistry **3:**10-5.
62. **Natoli, G.** Maintaining Cell Identity through Global Control of Genomic Organization. Immunity **33:**12-24.
63. **Ogawa, S., J. Lozach, C. Benner, G. Pascual, R. K. Tangirala, S. Westin, A. Hoffmann, S. Subramaniam, M. David, M. G. Rosenfeld, and C. K. Glass.** 2005. Molecular determinants of crosstalk between nuclear receptors and toll-like receptors. Cell **122:**707-21.
64. **Ozer, A., and R. K. Bruick.** 2007. Non-heme dioxygenases: cellular sensors and regulators jelly rolled into one? Nat Chem Biol **3:**144-53.
65. **Paik, W. K., and S. Kim.** 1973. Enzymatic demethylation of calf thymus histones. Biochem Biophys Res Commun **51:**781-8.
66. **Paik, W. K., and S. Kim.** 1969. Enzymatic methylation of histones. Arch Biochem Biophys **134:**632-7.
67. **Pascual, G., A. L. Fong, S. Ogawa, A. Gamliel, A. C. Li, V. Perissi, D. W. Rose, T. M. Willson, M. G. Rosenfeld, and C. K. Glass.** 2005. A SUMOylation-dependent pathway mediates transrepression of inflammatory response genes by PPAR-gamma. Nature **437:**759-63.
68. **Pasini, D., P. A. Cloos, J. Walfridsson, L. Olsson, J. P. Bukowski, J. V. Johansen, M. Bak, N. Tommerup, J. Rappsilber, and K. Helin.** JARID2

regulates binding of the Polycomb repressive complex 2 to target genes in ES cells. Nature **464:**306-10.

69. **Pasini, D., K. H. Hansen, J. Christensen, K. Agger, P. A. Cloos, and K. Helin.** 2008. Coordinated regulation of transcriptional repression by the RBP2 H3K4 demethylase and Polycomb-Repressive Complex 2. Genes Dev **22:**1345-55.
70. **Peet, D. J., S. D. Turley, W. Ma, B. A. Janowski, J. M. Lobaccaro, R. E. Hammer, and D. J. Mangelsdorf.** 1998. Cholesterol and bile acid metabolism are impaired in mice lacking the nuclear oxysterol receptor LXR alpha. Cell **93:**693-704.
71. **Peng, J. C., A. Valouev, T. Swigut, J. Zhang, Y. Zhao, A. Sidow, and J. Wysocka.** 2009. Jarid2/Jumonji coordinates control of PRC2 enzymatic activity and target gene occupancy in pluripotent cells. Cell **139:**1290-302.
72. **Pokholok, D. K., C. T. Harbison, S. Levine, M. Cole, N. M. Hannett, T. I. Lee, G. W. Bell, K. Walker, P. A. Rolfe, E. Herbolsheimer, J. Zeitlinger, F. Lewitter, D. K. Gifford, and R. A. Young.** 2005. Genome-wide map of nucleosome acetylation and methylation in yeast. Cell **122:**517-27.
73. **Ramsey, S. A., S. L. Klemm, D. E. Zak, K. A. Kennedy, V. Thorsson, B. Li, M. Gilchrist, E. S. Gold, C. D. Johnson, V. Litvak, G. Navarro, J. C. Roach, C. M. Rosenberger, A. G. Rust, N. Yudkovsky, A. Aderem, and I. Shmulevich.** 2008. Uncovering a macrophage transcriptional program by integrating evidence from motif scanning and expression dynamics. PLoS Comput Biol **4:**e1000021.
74. **Ravasi, T., C. A. Wells, and D. A. Hume.** 2007. Systems biology of transcription control in macrophages. Bioessays **29:**1215-26.
75. **Rea, S., F. Eisenhaber, D. O'Carroll, B. D. Strahl, Z. W. Sun, M. Schmid, S. Opravil, K. Mechtler, C. P. Ponting, C. D. Allis, and T. Jenuwein.** 2000. Regulation of chromatin structure by site-specific histone H3 methyltransferases. Nature **406:**593-9.
76. **Rius, J., M. Guma, C. Schachtrup, K. Akassoglou, A. S. Zinkernagel, V. Nizet, R. S. Johnson, G. G. Haddad, and M. Karin.** 2008. NF-kappaB links innate immunity to the hypoxic response through transcriptional regulation of HIF-1alpha. Nature **453:**807-11.
77. **Roesch, A., B. Becker, S. Meyer, P. Wild, C. Hafner, M. Landthaler, and T. Vogt.** 2005. Retinoblastoma-binding protein 2-homolog 1: a retinoblastoma-binding protein downregulated in malignant melanomas. Mod Pathol **18:**1249-57.
78. **Roesch, A., M. Fukunaga-Kalabis, E. C. Schmidt, S. E. Zabierowski, P. A. Brafford, A. Vultur, D. Basu, P. Gimotty, T. Vogt, and M. Herlyn.** A temporarily distinct subpopulation of slow-cycling melanoma cells is required for continuous tumor growth. Cell **141:**583-94.
79. **Roesch, A., A. M. Mueller, T. Stempfl, C. Moehle, M. Landthaler, and T. Vogt.** 2008. RBP2-H1/JARID1B is a transcriptional regulator with a tumor suppressive potential in melanoma cells. Int J Cancer **122:**1047-57.
80. **Romanyukha, A. A., S. G. Rudnev, and I. A. Sidorov.** 2006. Energy cost of infection burden: an approach to understanding the dynamics of host-pathogen interactions. J Theor Biol **241:**1-13.
81. **Rowe, A. H., C. A. Argmann, J. Y. Edwards, C. G. Sawyez, O. H. Morand, R. A. Hegele, and M. W. Huff.** 2003. Enhanced synthesis of the oxysterol 24(S),25-epoxycholesterol in macrophages by inhibitors of 2,3-oxidosqualene:lanosterol cyclase: a novel mechanism for the attenuation of foam cell formation. Circ Res **93:**717-25.
82. **Ruthenburg, A. J., C. D. Allis, and J. Wysocka.** 2007. Methylation of lysine 4 on histone H3: intricacy of writing and reading a single epigenetic mark. Mol Cell **25:**15-30.

83. **Saccani, S., S. Pantano, and G. Natoli.** 2002. p38-Dependent marking of inflammatory genes for increased NF-kappa B recruitment. Nat Immunol **3:**69-75.
84. **Sandelin, A., W. W. Wasserman, and B. Lenhard.** 2004. ConSite: web-based prediction of regulatory elements using cross-species comparison. Nucleic Acids Res **32:**W249-52.
85. **Santos-Rosa, H., R. Schneider, A. J. Bannister, J. Sherriff, B. E. Bernstein, N. C. Emre, S. L. Schreiber, J. Mellor, and T. Kouzarides.** 2002. Active genes are tri-methylated at K4 of histone H3. Nature **419:**407-11.
86. **Schneider, R., A. J. Bannister, F. A. Myers, A. W. Thorne, C. Crane-Robinson, and T. Kouzarides.** 2004. Histone H3 lysine 4 methylation patterns in higher eukaryotic genes. Nat Cell Biol **6:**73-7.
87. **Secombe, J., and R. N. Eisenman.** 2007. The function and regulation of the JARID1 family of histone H3 lysine 4 demethylases: the Myc connection. Cell Cycle **6:**1324-8.
88. **Secombe, J., L. Li, L. Carlos, and R. N. Eisenman.** 2007. The Trithorax group protein Lid is a trimethyl histone H3K4 demethylase required for dMyc-induced cell growth. Genes Dev **21:**537-51.
89. **Sedgwick, B., P. A. Bates, J. Paik, S. C. Jacobs, and T. Lindahl.** 2007. Repair of alkylated DNA: recent advances. DNA Repair (Amst) **6:**429-42.
90. **Seward, D. J., G. Cubberley, S. Kim, M. Schonewald, L. Zhang, B. Tripet, and D. L. Bentley.** 2007. Demethylation of trimethylated histone H3 Lys4 in vivo by JARID1 JmjC proteins. Nat Struct Mol Biol **14:**240-2.
91. **Shen, X., W. Kim, Y. Fujiwara, M. D. Simon, Y. Liu, M. R. Mysliwiec, G. C. Yuan, Y. Lee, and S. H. Orkin.** 2009. Jumonji modulates polycomb activity and self-renewal versus differentiation of stem cells. Cell **139:**1303-14.
92. **Shi, X., T. Hong, K. L. Walter, M. Ewalt, E. Michishita, T. Hung, D. Carney, P. Pena, F. Lan, M. R. Kaadige, N. Lacoste, C. Cayrou, F. Davrazou, A. Saha, B. R. Cairns, D. E. Ayer, T. G. Kutateladze, Y. Shi, J. Cote, K. F. Chua, and O. Gozani.** 2006. ING2 PHD domain links histone H3 lysine 4 methylation to active gene repression. Nature **442:**96-9.
93. **Shi, Y., F. Lan, C. Matson, P. Mulligan, J. R. Whetstine, P. A. Cole, and R. A. Casero.** 2004. Histone demethylation mediated by the nuclear amine oxidase homolog LSD1. Cell **119:**941-53.
94. **Shi, Y., and J. R. Whetstine.** 2007. Dynamic regulation of histone lysine methylation by demethylases. Mol Cell **25:**1-14.
95. **Smith, C. M., and J. A. Steitz.** 1998. Classification of gas5 as a multi-small-nucleolar-RNA (snoRNA) host gene and a member of the 5'-terminal oligopyrimidine gene family reveals common features of snoRNA host genes. Mol Cell Biol **18:**6897-909.
96. **Sosic, D., J. A. Richardson, K. Yu, D. M. Ornitz, and E. N. Olson.** 2003. Twist regulates cytokine gene expression through a negative feedback loop that represses NF-kappaB activity. Cell **112:**169-80.
97. **Tahiliani, M., P. Mei, R. Fang, T. Leonor, M. Rutenberg, F. Shimizu, J. Li, A. Rao, and Y. Shi.** 2007. The histone H3K4 demethylase SMCX links REST target genes to X-linked mental retardation. Nature **447:**601-5.
98. **Takeuchi, T., Y. Yamazaki, Y. Katoh-Fukui, R. Tsuchiya, S. Kondo, J. Motoyama, and T. Higashinakagawa.** 1995. Gene trap capture of a novel mouse gene, jumonji, required for neural tube formation. Genes Dev **9:**1211-22.
99. **Tan, K., A. L. Shaw, B. Madsen, K. Jensen, J. Taylor-Papadimitriou, and P. S. Freemont.** 2003. Human PLU-1 Has transcriptional repression properties and interacts with the developmental transcription factors BF-1 and PAX9. J Biol Chem **278:**20507-13.

100. **Taverna, S. D., S. Ilin, R. S. Rogers, J. C. Tanny, H. Lavender, H. Li, L. Baker, J. Boyle, L. P. Blair, B. T. Chait, D. J. Patel, J. D. Aitchison, A. J. Tackett, and C. D. Allis.** 2006. Yng1 PHD finger binding to H3 trimethylated at K4 promotes NuA3 HAT activity at K14 of H3 and transcription at a subset of targeted ORFs. Mol Cell **24:**785-96.
101. **Tester, A. M., J. H. Cox, A. R. Connor, A. E. Starr, R. A. Dean, X. S. Puente, C. Lopez-Otin, and C. M. Overall.** 2007. LPS responsiveness and neutrophil chemotaxis in vivo require PMN MMP-8 activity. PLoS One **2:**e312.
102. **Thanos, D., and T. Maniatis.** 1995. Identification of the rel family members required for virus induction of the human beta interferon gene. Mol Cell Biol **15:**152-64.
103. **Thomas, G., H. W. Lange, and K. Hempel.** 1972. [Relative stability of lysine-bound methyl groups in arginie-rich histones and their subfrations in Ehrlich ascites tumor cells in vitro]. Hoppe Seylers Z Physiol Chem **353:**1423-8.
104. **Thomson, J. P., P. J. Skene, J. Selfridge, T. Clouaire, J. Guy, S. Webb, A. R. Kerr, A. Deaton, R. Andrews, K. D. James, D. J. Turner, R. Illingworth, and A. Bird.** CpG islands influence chromatin structure via the CpG-binding protein Cfp1. Nature **464:**1082-6.
105. **Tian, J., A. M. Avalos, S. Y. Mao, B. Chen, K. Senthil, H. Wu, P. Parroche, S. Drabic, D. Golenbock, C. Sirois, J. Hua, L. L. An, L. Audoly, G. La Rosa, A. Bierhaus, P. Naworth, A. Marshak-Rothstein, M. K. Crow, K. A. Fitzgerald, E. Latz, P. A. Kiener, and A. J. Coyle.** 2007. Toll-like receptor 9-dependent activation by DNA-containing immune complexes is mediated by HMGB1 and RAGE. Nat Immunol **8:**487-96.
106. **Tsukada, Y., J. Fang, H. Erdjument-Bromage, M. E. Warren, C. H. Borchers, P. Tempst, and Y. Zhang.** 2006. Histone demethylation by a family of JmjC domain-containing proteins. Nature **439:**811-6.
107. **Vallabhapurapu, S., and M. Karin.** 2009. Regulation and function of NF-kappaB transcription factors in the immune system. Annu Rev Immunol **27:**693-733.
108. **Valledor, A. F., F. E. Borras, M. Cullell-Young, and A. Celada.** 1998. Transcription factors that regulate monocyte/macrophage differentiation. J Leukoc Biol **63:**405-17.
109. **Whetstine, J. R., A. Nottke, F. Lan, M. Huarte, S. Smolikov, Z. Chen, E. Spooner, E. Li, G. Zhang, M. Colaiacovo, and Y. Shi.** 2006. Reversal of histone lysine trimethylation by the JMJD2 family of histone demethylases. Cell **125:**467-81.
110. **Wysocka, J., T. Swigut, H. Xiao, T. A. Milne, S. Y. Kwon, J. Landry, M. Kauer, A. J. Tackett, B. T. Chait, P. Badenhorst, C. Wu, and C. D. Allis.** 2006. A PHD finger of NURF couples histone H3 lysine 4 trimethylation with chromatin remodelling. Nature **442:**86-90.
111. **Xia, X., M. E. Lemieux, W. Li, J. S. Carroll, M. Brown, X. S. Liu, and A. L. Kung.** 2009. Integrative analysis of HIF binding and transactivation reveals its role in maintaining histone methylation homeostasis. Proc Natl Acad Sci U S A **106:**4260-5.
112. **Xiang, Y., Z. Zhu, G. Han, X. Ye, B. Xu, Z. Peng, Y. Ma, Y. Yu, H. Lin, A. P. Chen, and C. D. Chen.** 2007. JARID1B is a histone H3 lysine 4 demethylase up-regulated in prostate cancer. Proc Natl Acad Sci U S A **104:**19226-31.
113. **Yamamoto, M., S. Yamazaki, S. Uematsu, S. Sato, H. Hemmi, K. Hoshino, T. Kaisho, H. Kuwata, O. Takeuchi, K. Takeshige, T. Saitoh, S. Yamaoka, N. Yamamoto, S. Yamamoto, T. Muta, K. Takeda, and S. Akira.** 2004. Regulation of Toll/IL-1-receptor-mediated gene expression by the inducible nuclear protein IkappaBzeta. Nature **430:**218-22.

114. **Yamamoto, Y., U. N. Verma, S. Prajapati, Y. T. Kwak, and R. B. Gaynor.** 2003. Histone H3 phosphorylation by IKK-alpha is critical for cytokine-induced gene expression. Nature **423:**655-9.
115. **Yamane, K., K. Tateishi, R. J. Klose, J. Fang, L. A. Fabrizio, H. Erdjument-Bromage, J. Taylor-Papadimitriou, P. Tempst, and Y. Zhang.** 2007. PLU-1 is an H3K4 demethylase involved in transcriptional repression and breast cancer cell proliferation. Mol Cell **25:**801-12.
116. **Yamasaki, S., E. Ishikawa, M. Sakuma, H. Hara, K. Ogata, and T. Saito.** 2008. Mincle is an ITAM-coupled activating receptor that senses damaged cells. Nat Immunol **9:**1179-88.
117. **Zelcer, N., and P. Tontonoz.** 2006. Liver X receptors as integrators of metabolic and inflammatory signaling. J Clin Invest **116:**607-14.
118. **Zhou, W., P. Zhu, J. Wang, G. Pascual, K. A. Ohgi, J. Lozach, C. K. Glass, and M. G. Rosenfeld.** 2008. Histone H2A monoubiquitination represses transcription by inhibiting RNA polymerase II transcriptional elongation. Mol Cell **29:**69-80.

ACKNOWLEDGMENTS

This thesis is the result of four years of life at IFOM-IEO Campus and there are many people I should, must and, most of all, would like to thank, as they contributed in making these years unforgettable.

First of all I would like to thank my supervisor Dr. Gioacchino Natoli who transfused to me a bit of his tremendous passion for science. He first very carefully followed my initiation to the research world and then he allowed me to find my independence. He is definitely a great leader.

I would like to thank all the Natoli's group members, in particular Francesca who supervised my work during the first years of my PhD and taught me most of what I am able to do now, and Liv who shared with me joys and sorrows of the Jarid1b project; but also Isabel, Betsabeh, Flore, Greta, Elena, Luca, Sara, Serena, Agnese and Iros for their help, suggestions and friendship.

I thank my co-supervisors Dr. Giuseppe Testa and Dr. Valerio Orlando who "lost" their time giving me suggestions and helping my scientific growth.

I would like to thank all the people who collaborated in this study: Prof. Donatella Caruso and Dr. Omar Maschi at University of Milan, Prof. Henk Stunnenberg at Radboud University Nijmegen, Prof. Saverio Minucci and Dr. Isabella Pallavicini here at IFOM-IEO Campus, for their precious contribution to the project.

I thank all the IFOM-IEO Campus facilities which made my research easier and faster, I am sure I will miss how they make the research life "facile".

I would like to thank all the friends I met during these years in the campus who made me feeling in this place like at home: in particular, Francesca, Federica, Elisa, Paola, Elena, Gianluca, Silvia, Daniele, Stefano, Ilaria, Andrea, Chiara, Maria Grazia and Elisa. I apologize for all those I'm not mentioning, but you are all in my heart.

Last but not least I would like to thank a lot my family who supported me everyday, even from 1000 km of distance.